Design and Analysis of a Hybrid Power System for Remote Natural Gas Pipeline Control Stations

By

©Muhammad Waqas (B.Sc.)

A Thesis submitted to the School of Graduate Studies in partial fulfillment of the requirements for the degree of

Master of Engineering

Faculty of Engineering and Applied Science

Memorial University of Newfoundland

October 2024

St. John's Newfoundland and Labrador Canada

Abstract

The most efficient way to transport natural gas from its source to its destination is through a pipeline network. The efficient operation of natural gas pipeline control stations relies on electrical equipment such as data loggers, control systems, surveillance and communication devices, etc. These stations are strategically located in remote areas, making it challenging to maintain a reliable and continuous power supply. As a result, non-renewable energy sources like natural gas and diesel are typically used for power generation due to the lack of reliable electrical infrastructure. This thesis offers a comprehensive solution to replace high-cost energy sources with a cost-effective and environmentally friendly alternative for remotely located natural gas pipeline control stations. The first step involves designing a hybrid power system (HPS) using HOMER Pro software to address the unique needs of a remote natural gas pipeline control station in Pakistan as a case study. A detailed analysis of capital and energy costs shows that the proposed system is cost-effective compared to the existing setup. The design is validated through dynamic modeling in MATLAB/Simulink R2022 and experimental validation is conducted using hardware in the loop (HIL) and OPAL-RT Technologies' real-time OP5707XG simulator. The second step involves assessing the output power quality of the designed hybrid power system. Since inverters play a critical role in hybrid power systems, their impact on output power is significant. Various multilevel inverter topologies are analyzed and compared with a conventional two-level inverter. Simulations are performed in MATLAB/Simulink, showing that increasing output voltage levels approximates a sinusoidal waveform, reducing Total Harmonic Distortion (THD) and improving power quality. The experimental validation of the nine-level cascaded H-bridge Multilevel Inverter (MLI) is conducted using Hardware-in-the-Loop (HIL) with OPAL-RT Technologies' real-time OP5707XG simulator. Finally, in the third and last step, an Internet of Things (IoT)-based, open-

source SCADA architecture is designed to monitor the designed hybrid power system, addressing the limitations of existing proprietary and non-configurable SCADA architectures. The proposed system includes voltage and current sensors for data collection, an ESP32-WROOM-32E microcontroller as the Remote Terminal Unit (RTU) for processing, a Blynk IoT-based cloud server serving as the Master Terminal Unit (MTU) for data storage and human-machine interaction (HMI), and a GSM SIM800L module with a local Wi-Fi router for communication between the RTU and MTU. The proposed system exhibited a low power consumption of 3.9 W and incurred an overall cost of 40.1 CAD making it an extremely cost-effective solution for remote natural gas pipeline control stations.

Acknowledgments

First and foremost, I thank Allah Almighty for His grace and favors throughout this master's program.

Next, my heartfelt gratitude goes to my thesis supervisor, Prof. Dr. Mohsin Jamil, and my co-supervisor Dr. Ashraf Ali Khan, for their patience and guidance in this thesis. I have benefited immensely from your wealth of knowledge and expertise in the fields of instrumentation and control, renewable energy systems, hybrid power systems, and power electronics. To you, I say a very big thank you for always making yourself available to answer my questions and to steer me in the right direction.

I want to thank my friend Ahmed Talal, whose invaluable support made it possible for me to come to this country and embark on my studies. Thank you!

I would also like to extend my gratitude to the School of Graduate Studies, Faculty of Engineering and Applied Science, Memorial University, and my parent organization Sui Northern Gas Pipelines Limited for their support and conducive environment for this research.

Finally, I would like to acknowledge the technical, moral, and emotional support of my family, friends, and colleagues throughout the period of carrying out this research work. Thank you all!!!

Table of Contents

List of Tables

List of Figures

List of Abbreviations

ADC	Analog-to-Digital Converter
FIDs	Field Instrument Devices
GSM	Global System for Mobile Communications
HPS	Hybrid Power System
HOMER	Hybrid Optimization of Multiple Energy Resources
HTTP	Hypertext Transfer Protocol
IoT	Internet of Things
LCD	Liquid Crystal Display
MATLAB	Matrix Laboratory
MPPT	Maximum Power Point Tracking
MTU	Master Terminal Units
MLI	Multilevel Inverter
PV	Photo Voltaic
PLCs	Programmable Logic Controllers
PWM	Pulse Width Modulation
RLNG	Re-Gasified Liquified Natural Gas
RTU	Remote Terminal Unit
RESs	Renewable energy sources
SCADA	Supervisory Control and Data Acquisition
TCF	Trillion Cubic Feet
UI	User Interface
VSI	Voltage Source Inverter

Nomenclature

$\Delta I/\Delta V$	Incremental Conductance
I/V	Array Conductivity
V_i	Input Voltage
V_0	Output Voltage
L	Inductance
ΔI_L	Inductor Ripple Current
f_s	Minimum Switching Frequency
C	Capacitance
V_{dc}	DC Voltage
L_g	DG side Inductor
C_f	Filter Capacitance
D	Duty Cycle
I_o	Diode's leakage or saturation current
K	Boltzmann Constant

Chapter 1: Introduction

1.1 Introduction

1.1.1 Background

Energy has become a fundamental element of modern life, playing a crucial role in enhancing living standards and fostering economic growth. The pursuit of civilizations, urbanization, population expansion, and industrialization have all contributed to a constant increase in the need for energy throughout human history (UN population prediction). Currently, energy is used globally in the transportation, power generation, industrial, commercial, and residential sector [1]**.** Reliable energy resources are essential for modern existence and ensuring an adequate energy supply is pivotal for economic development. The use of fossil fuels as the primary energy source is essential for sustainable progress in sectors such as industry, agriculture, infrastructure, information technology, household applications, transportation, and more. However, with ongoing economic advancement, the exploration and utilization of oil and gas reserves are intensifying, alongside the growing consumption of these conventional resources. Addressing the depletion of traditional energy sources remains a key challenge, necessitating innovative solutions [2].

The availability of energy at an affordable cost is another critical factor in driving a nation's prosperity. It ensures that industries can operate efficiently, businesses can thrive, and households can maintain a high quality of life, thereby supporting overall economic growth and development [3]. Furthermore, energy has attained the status of a strategic asset globally. Recognizing its vital role, the World Summit on Sustainable Development (WSSD) has highlighted how energy contributes to fostering stable and socially inclusive development.

Energy can be derived from a variety of sources which are primarily categorized into renewable

and non-renewable types. Among these, non-renewable sources, particularly fossil fuels, are the most widely utilized. Fossil fuels, including coal, natural gas, oil, and peat, are extensively used across various sectors [4]. Fossil fuels are the dominant source of energy globally, accounting for 67.9% of the world's energy consumption. This is followed by nuclear energy at 10.9%, and hydropower at 16.2%. Renewable energy sources make up the smallest portion of the energy mix [5]. Natural gas is preferred over other fossil fuels, such as coal and oil because it has a lower carbon intensity and produces less environmental harm during extraction and use [6]. The global consumption of natural gas increased from 5353 trillion cubic feet (Tcf) in 1980 to 113 Tcf in 2010. This rapid increase was observed across various regions of the world. For example, in the Middle East, the demand for natural gas increased from 3.1 Tcf in the 1980s to 51.7 Tcf in 2017, reflecting the region's rapid economic growth. A similar pattern of growing consumption of natural gas in North America was recorded from 58.5 Tcf in 1980 to 91.2 Tcf in 2017 [7]. Therefore, the production and use of natural gas are crucial for driving economic prosperity in nations.

Natural gas significantly meets Pakistan's energy needs and plays a crucial role in the country's electricity production. It is a major source of energy, contributing extensively to the generation of electricity in Pakistan [8]. The year 1952 marked the discovery of extensive natural gas reserves, approximately 12 trillion cubic feet in Sui, Balochistan province of Pakistan. In the wake of this discovery, a vast gas infrastructure was established to generate electricity and meet domestic, commercial, and industrial needs. Over time, the consumption of natural gas as a primary energy source in Pakistan gradually increased. By 2005, natural gas use had reached a high, accounting for about 50% of Pakistan's total energy consumption. However natural gas supplies began to rapidly deplete in 2006 due to excessive usage, poor management, and a lack of exploration for new gas reserves. Consequently, the production of natural gas has remained relatively stagnant in

comparison to the rising demand, resulting in a shortage. The rapid depletion of fossil fuel reserves caused by the demand-supply gap and lack of exploration of new reserves has led to Pakistan importing a significant portion of its petroleum products to meet roughly one-third of its energy needs. To bridge this gap, Pakistan has turned to importing liquefied natural gas (LNG) mainly from Qatar, following a similar pattern to fossil fuels such as petrol and diesel, rather than harnessing domestic alternative energy sources [9]. Figure 1.1 shows the natural gas imports for Pakistan from year 1975 to year 2022.

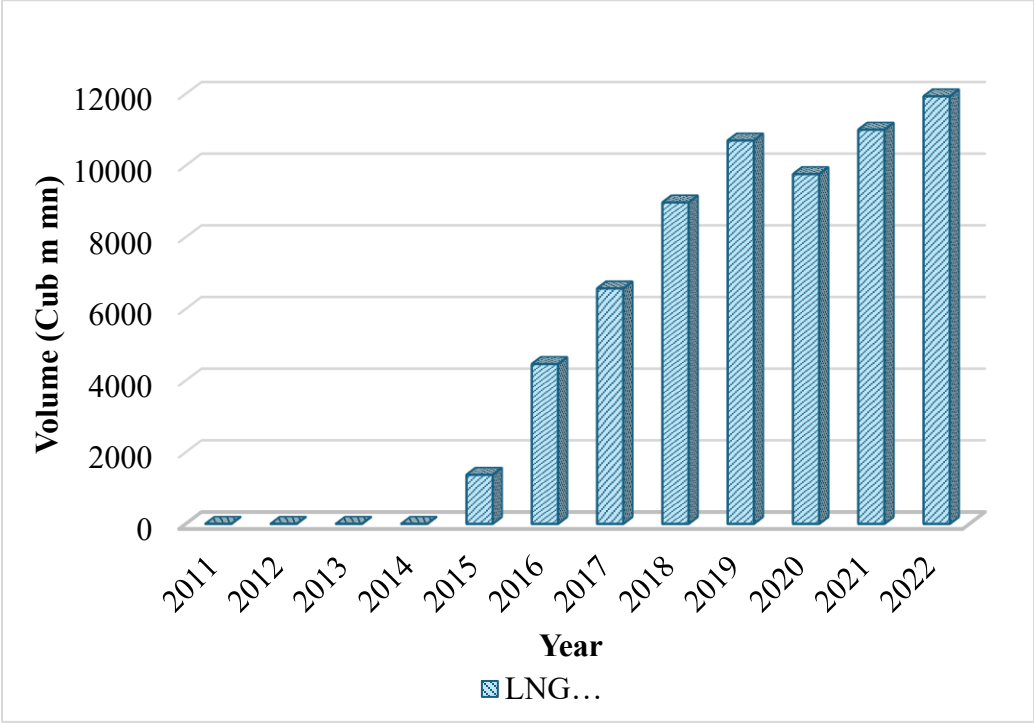

Figure 1.1. Pakistan's liquified natural gas (LNG) imports [10]

The price of LNG is influenced by the international market and several global factors. By the end of 2021, the cost of LNG delivered to Pakistan had increased to almost US$16 per MMBtu, which was over four times higher than the average domestic gas price. Figure 1.2 shows a comparison between the weighted average prices of RLNG (Re-Gasified Liquified Natural Gas) and the current average wellhead prices in Pakistan.

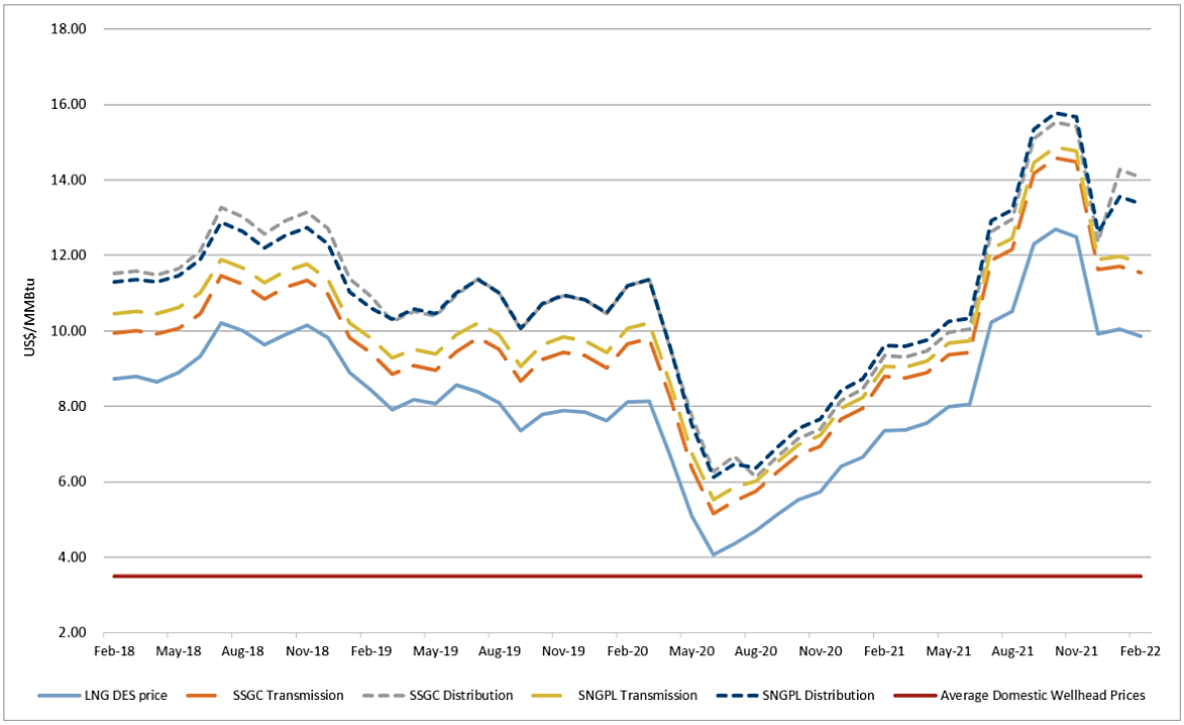

Figure 1.2. Weighted avg. RLNG prices vs. current avg. domestic wellhead prices [11]

Moreover, conventional energy sources, mainly derived from fossil fuels, not only have a significant impact on the environment and contribute to environmental pollution but are also facing an impending crisis of depletion. Therefore, depending exclusively on fossil fuels for electricity generation not only imposes a strain on the economy but can also have adverse effects on the environment and the natural ecosystem. Other than hydro, electricity generation in Pakistan is mostly based on natural gas, coal, or furnace oil, all of which are nonrenewable sources of energy and imported from other nations.

Due to storage constraints, natural gas must be quickly transported to its destination after extraction. There are several methods for transmitting natural gas from its source to its destination [12]. There are two common methods for transporting natural gas: as Liquefied Natural Gas (LNG) and Compressed Natural Gas (CNG). LNG is natural gas cooled to -162 degrees Celsius (-260 degrees Fahrenheit) to convert it into a liquid, significantly reducing its volume for economical

transport and storage, typically by ships. CNG, on the other hand, is natural gas compressed to high pressure (around 3,600 psi or more) to decrease its volume, making it suitable for transport via pipeline networks. Pipeline transport is mainly used for local distribution, while ships are used for international transport [13].

Efficient management of natural gas transportation to various regions within Pakistan is carried out by two leading companies namely Sui Northern Gas Pipelines Limited (SNGPL) and Sui Southern Gas Company Limited (SSGCL). Numerous natural gas pipeline control stations manage the operation and maintenance of high-pressure pipeline networks. These control stations are strategically located in geographically remote and sparsely populated areas. Operation and maintenance of these high-pressure natural gas pipeline control stations in such remote locations pose substantial challenges, mainly due to the inconsistent electricity supply from nearby grid stations, one of the reasons for the ongoing energy crisis while such sensitive control stations require an uninterrupted and continuous power supply. The effective transportation of natural gas through a pipeline network depends upon a variety of electrical equipment which includes gas turbines, gas discharge cooling system, gas compressors, and various other electrically powered equipment which is installed within such control stations. For this reason, fossil fuels like natural gas and diesel continue to be the primary source of electrical power at control stations situated in remote areas.

When SNGPL began operations after the discovery of significant natural gas reserves in Pakistan, control stations were initially designed to operate on natural gas gen-sets by consuming natural gas internally from the pipeline network for power generation, as alternative power sources were either unavailable or unreliable. For this reason, fossil fuels like natural gas and diesel continue to be the primary source of electrical power at control stations situated in remote areas. However,

future scenarios of natural gas depletion were not considered at their inception. Now, with diminishing local natural gas reserves and increased dependence on costly imported LNG, using natural gas for power generation at these stations is economically unfeasible. This reliance on natural gas for electric power, despite resource depletion, is both wasteful and inefficient. Thus, a consistent supply of electricity from conventional fossil fuels is threatened by rising fuel prices, which are driven by ongoing global conflicts and increasing demands to reduce environmental pollution. These factors make it challenging to rely solely on fossil fuels for power generation, highlighting the need for alternative energy solutions. Therefore, it is crucial to shift to renewable energy sources, particularly solar and wind power, due to their sustainability, environmental benefits, and decreasing costs.

Due to the intermittent nature of renewable energy sources, hybrid power systems that combine both conventional and renewable energy sources are preferred and employed for electricity generation [14]. These systems are reliable and environmentally friendly, reducing dependence on a single resource, which is essential in areas with limited natural resources [15].

Pakistan has significant potential for solar energy due to its geographic location and abundant sunlight. Pakistan experiences some of the highest insolation levels globally, averaging 8.5 hours of daylight per day. Balochistan has the highest solar PV potential at 5.8 kWh/day, followed by Sindh and Southern Punjab with potentials of 4.5 to 5.4 kWh/day. Northern Punjab, Khyber Pakhtunkhwa, and Gilgit Baltistan have a potential between 3.4 and 4.4 kWh/day. Studies indicate that Pakistan's monthly mean daily Global Horizontal Irradiance (GHI) ranges from 4.44 to 5.83 kWh/m², with an annual average of 5.27 kWh/m². The lowest annual mean daily GHI is 4.44 kWh/m², still higher than the global annual mean of 3.61 kWh/m². Therefore, the solar energy potential for power generation across various regions in Pakistan ranges from 2 to 8.5 kWh/m²/day

[16]. Given these facts, it is advisable to encourage the use of solar energy for power generation, especially in rural and remote areas where these control stations are situated. Solar energy offers a reliable and sustainable power source that can address the unique challenges of remote locations, such as limited access to traditional power grids and the need for uninterrupted energy supply. Promoting solar energy in these areas not only supports energy independence but also contributes to environmental conservation by reducing reliance on fossil fuels.

1.1.2 Site Selection

Site selection is a crucial step when establishing, expanding, or relocating any project, especially for large-scale solar photovoltaic systems. Given the significant long-term investment required, the success of the system heavily depends on site selection. The goal is to find the best location with optimal conditions for installation. Key factors to consider include solar irradiance, economic metrics like internal rate of return (IRR), net present value (NPV), return on investment (ROI), as well as carbon emission reductions and policy support.

Sui Northern Gas Pipelines Limited (SNGPL) is the leading integrated natural gas provider in North Central Pakistan, serving over 7.22 million customers in Punjab, Khyber Pakhtunkhwa, and Azad Jammu & Kashmir. Its transmission network comprises 9,239 kilometers of high-pressure pipelines, while its distribution network includes 142,998 kilometers of low-pressure pipelines. The company operates eleven compressor stations along the transmission network, which are strategically located at remote and unpopulated locations and essential for the smooth operation of the pipeline network. The selected site for this research is a natural gas compressor station owned by Sui Northern Gas Pipelines Limited (SNGPL) in Pakistan. The site is located in the remote and sparsely populated area of Gali Jagir, Fateh Jhang (33.427522, 72.625862). Figure 1.3 shows an aerial view of the selected site along with its coordinates on Google Maps.

Figure 1.3. Aerial view of the selected site on Google Maps.

1.2 Hybrid Power System

A hybrid power system (HPS) combines various energy sources, both conventional and renewable, to optimize energy production. The energy sources can be solar photovoltaic, wind, fuel cells (FCs), internal combustion engines (ICEs), batteries, and supercapacitors (SCs) [17]. The output from an HPS can be heat, electricity, or both (co-generation). Renewable energy resources (RERs) are intermittent and can be unreliable on their own. By integrating different power sources, HPS compensates for the variability of renewable energy outputs, resulting in more reliable energy production. Additionally, HPS helps reduce the variability issues associated with renewable energy and decreases emissions compared to solely using fossil-fuel generators.

Hybrid power systems combine various energy sources, including Solar photovoltaic and wind turbines are widely used and researched renewable energy sources for electricity generation. Their efficiency has improved over time, making them suitable for both modular and large-scale

applications where resources are abundant. Among the two, solar photovoltaic is most commonly used for off-grid household applications due to its modular nature [18]. Hybrid power systems (HPS) provide a reliable and continuous power supply to end users by combining multiple energy sources. Some of these systems also incorporate battery storage to ensure a steady power supply even when the primary energy sources are not available [14].

1.2.1 Solar Photovoltaic System

A solar photovoltaic (PV) system converts sunlight directly into electricity using solar cells. A photovoltaic cell, also known as a solar cell, is used to convert solar energy into electrical energy. These cells are made of semiconductor materials, such as silicon, which generate electric current when exposed to sunlight and multiple solar cells are combined to form a PV solar panel. Solar PV systems are a clean and renewable source of energy, widely used for both residential and commercial electricity generation. They can be installed on rooftops, integrated into building materials, or set up as large solar farms. There are various types of solar photovoltaic systems as described below [19].

- **Grid-Tied (On-Grid) Systems:** Connected to the utility grid, this type of system does not have a battery bank. However, it supplies electricity to the property and can feed excess power back to the grid. They are cost-effective but do not function during grid outages when there is no solar irradiance unless battery storage is available.
- **Off-Grid Systems:** Independent from the grid, these systems use batteries to store energy for continuous power supply. They are ideal for remote areas but have higher initial costs and require battery maintenance.
- **Hybrid Systems:** Combining solar PV with other energy sources like wind turbines or natural gas/diesel generators, often with battery storage, these systems provide reliable

power even during low sunlight and grid outages but are more complex.

1.2.2 Types of Photovoltaic Modules

A photovoltaic (PV) module, or solar panel, comprises multiple solar cells that convert sunlight into electrical energy. Common configurations include 60-cell modules for residential use, 72-cell modules for commercial and industrial applications, and 96-cell modules for high-power needs. These cells are arranged in series and parallel within the module to optimize power output, with each cell made from semiconductor materials like silicon. The number of cells in a module affects its size and power capacity, allowing for various applications and energy demands. PV modules come in several structural types, each suited to different applications as described below.

- **Monocrystalline Silicon Modules:** These modules are made from a single crystal structure, characterized by their dark color and rounded edges. They offer high efficiency and are space-efficient, making them ideal for situations where space is limited. However, they are more expensive to produce compared to other types.
- **Polycrystalline Silicon Modules:** Composed of multiple silicon crystals, these modules have a bluish tint and are less expensive than monocrystalline modules. They provide good efficiency but are slightly less efficient and space-efficient, making them a cost-effective choice for many applications.
- **Thin-Film Modules:** These modules use layers of photovoltaic material deposited onto a substrate. They are lightweight, flexible, and perform well in low light and high temperatures. While they are versatile and can be integrated into various surfaces, they generally have lower efficiency and require more space compared to crystalline silicon modules.
- **Bifacial Modules:** Capable of capturing sunlight on both the front and rear sides, bifacial

modules utilize reflected light to enhance overall energy yield. They offer higher energy production but come with higher costs and require specific installation to optimize reflected sunlight.

1.2.3 Main Components of Photovoltaic System

The output power of a solar photovoltaic (PV) system primarily depends on solar irradiance and temperature, both of which can fluctuate throughout the day and year. Solar irradiance, or the intensity of sunlight, directly influences how much electricity the panels can generate. At the same time, temperature affects the efficiency of the photovoltaic cells, with higher temperatures typically reducing their performance. To achieve maximum output and efficiency, it is crucial to have well-designed solar PV components, including high-quality panels, Maximum Power Point Tracking (MPPT) or charge controller, DC-DC converters, and efficient inverters. These components help optimize energy capture and conversion, ensuring the system performs efficiently despite varying environmental conditions. Two of the main power electronics components involved in photovoltaic system circuitry are the DC-DC converter along the Maximum Power Point Tracking (MPPT) algorithm and the DC-AC inverter controlled by various Pulse Width Modulation (PWM) techniques.

- **DC-DC Converter:** A DC-DC converter is an electronic device that converts direct current (DC) from one voltage level to another. A DC-DC converter with an MPPT (Maximum Power Point Tracking) controller is a critical component in solar power systems, designed to optimize energy harvest from photovoltaic panels. The DC-DC converter adjusts the voltage level between the solar panel and the load or battery to ensure efficient power transfer. The MPPT controller dynamically tracks the Maximum Power Point of the solar panel, compensating for variations in sunlight and temperature to maximize power output.

This synergy enhances the overall efficiency of the solar energy system, ensuring that the panels produce the highest possible power at all times, thereby increasing the system's reliability and energy yield. There are several types of DC-DC converters, each with specific functions and applications. A buck converter, also known as a step-down converter, reduces the input voltage to a lower output voltage. It is widely used in applications where a stable and lower voltage is needed. The buck converter operates by switching on and off a transistor to control the energy transferred to the output. A boost converter, or step-up converter, increases the input voltage to a higher output voltage. This type of converter is used when a higher voltage is required from a lower voltage source. The boost converter works by storing energy in an inductor and releasing it at a higher voltage. A buck-boost converter can either increase or decrease the input voltage, providing an output voltage that can be either greater or less than the input voltage. This versatility makes it suitable for applications where the input voltage can vary widely but a stable output voltage is required. It combines the principles of both buck and boost converters.

- **DC-AC Inverter:** The inverter is a crucial component in solar PV systems, ensuring that the DC electricity generated by the panels is converted to AC electricity, compatible with the grid and household appliances. Inverters typically employ transistors, MOSFETs, or IGBTs to create a series of on-off pulses that mimic an AC waveform. The resulting square wave or modified sine wave is then processed through filters to produce a smooth sine wave output, which closely matches the characteristics of standard AC power. They utilize various modulation techniques to shape the AC output and ensure efficient power conversion. Pulse Width Modulation (PWM) and Sinusoidal Pulse Width Modulation (SPWM) are commonly used to create waveforms that approximate a sine wave, balancing

efficiency and waveform quality. High-quality filtering, such as LC or LCL filters, smooths the output reduces harmonic distortion, and optimizes performance and efficiency.

The use of multilevel inverters in photovoltaic (PV) systems enhances their performance by improving power quality, efficiency, and reliability. By generating a near-sinusoidal AC output with multiple voltage levels, multilevel inverters reduce harmonic distortion, leading to better energy transfer and minimizing losses. They also operate at lower switching frequencies, which reduces switching losses and increases overall system efficiency. Additionally, the modular nature of these inverters allows for scalability and easier maintenance in larger PV systems. The reduced voltage stress on components, coupled with lower electromagnetic interference, further improves system longevity and stability. Multilevel inverters also enable higher utilization of the DC output from solar panels and offer better fault tolerance, ensuring continued operation even during component failures. Altogether, these benefits make multilevel inverters an ideal choice for optimizing energy conversion in modern photovoltaic systems and these combined techniques result in more stable, high-quality AC power suitable for a range of applications [20].

1.3 SCADA for Photovoltaic Systems

Supervisory Control and Data Acquisition (SCADA) systems are used for monitoring and controlling industrial processes and infrastructure. They gather real-time data from sensors and other devices, process this data, and provide operators with insights to manage and control operations efficiently. SCADA systems are commonly used in various industries, including energy, water treatment, manufacturing, and transportation, to oversee and manage operations effectively [21].

1.3.1 Generations of SCADA Systems

- **First Generation (1970s-1980s) - Basic SCADA:** The first generation of SCADA systems, developed in the 1960s and 1970s, was primarily based on analog technology and focused on centralizing control for large-scale industrial processes. These systems utilized analog signals to monitor and control operations, with operators using physical controls such as dials and gauges. Communication was often limited to point-to-point connections, and data acquisition was mostly manual. The primary goal was to improve efficiency by automating control tasks and providing a centralized view of operations.
- **Second Generation (1980s-1990s) - Distributed SCADA:** In the 1980s and 1990s, the second generation of SCADA systems emerged with the introduction of digital technology and computer-based control. These systems incorporated digital data acquisition and processing, allowing for more sophisticated data handling and visualization. They utilized personal computers and graphical user interfaces (GUIs) to provide operators with a more intuitive and interactive experience. Communication protocols became more standardized, enabling better integration with various field devices and systems. The focus of this generation was on enhancing system reliability, flexibility, and the ability to handle larger and more complex processes.
- **Third Generation (1990s-2000s) - Networked SCADA**: The third generation of SCADA systems, which began in the 2000s, integrated advanced networking technologies, including Ethernet and the Internet, to enhance connectivity and remote access. These systems adopted modern software architectures and embraced distributed control strategies, allowing for greater scalability and modularity. The incorporation of database management systems and real-time data analytics improved decision-making and

operational efficiency. Enhanced security features were introduced to protect against emerging cyber threats, and systems became more user-friendly with improved graphical displays and customizable dashboards.

- **Fourth Generation (2000s-Present) - Web-Based and Cloud SCADA**: The fourth generation of SCADA systems, emerging in the 2010s and beyond, utilizes the Internet of Things (IoT), cloud computing, and advanced analytics to revolutionize process management. These systems provide exceptional connectivity for real-time data collection from numerous smart sensors and devices. Cloud-based platforms offer scalable data storage and processing, while advanced analytics and machine learning deliver predictive insights and automated decision-making. The integration of mobile and remote access technologies allows operators to monitor and control systems from anywhere.

SCADA systems and IoT are complementary technologies that, when integrated, provide powerful solutions for monitoring and controlling industrial processes. IoT enhances SCADA systems with advanced data collection, connectivity, analytics, and remote capabilities, leading to more efficient and intelligent management of operations.

1.4 Research Objectives

Energy is crucial to modern life, driving economic growth, enhancing quality of life, and enabling technological advancements. Reliable energy is essential for powering industrial activities, improving household comfort, supporting healthcare, and facilitating the digital economy. Historically, fossil fuels like coal, oil, and natural gas have been the main energy sources. However, fossil fuel depletion, rising prices, and environmental impacts have become major concerns. Hence the transition to renewable energy sources necessitates investments in new technologies and infrastructure.

Natural gas is widely used as a cleaner alternative to other fossil fuels due to its lower carbon emissions. It is a crucial source of energy for electricity generation, heating, and as a raw material in various industries. The transportation of natural gas typically involves extensive pipeline networks, which are managed and monitored by control stations. These control stations ensure the safe and efficient operation of the pipelines and are strategically located in remote areas where the availability of reliable and consistent power is a challenge. Consequently, these stations primarily rely on internal consumption of natural gas and diesel for electricity generation. This reliance is both wasteful and inefficient, considering the critical need to conserve natural gas and reduce environmental impact.

This research aims to design a hybrid power system for these remote control stations, integrating solar photovoltaics, battery storage, and backup natural gas and diesel generators. The goal is to provide a reliable, cost-effective, and sustainable energy solution that reduces dependence on fossil fuels, conserves natural gas reserves, mitigates environmental impact, and ensures continuous power supply for the control stations.

The key contributions of the proposed work are outlined as follows:

- Examine the potential of renewable energy in developing countries to lower per-unit energy costs and address the global impact of climate change
- Design and size a hybrid power system using HOMER Pro, focusing on optimizing the capacity and configuration of components to meet the energy needs of a specific remote natural gas pipeline control station as a case study.
- Conduct dynamic modeling of the proposed hybrid power system using MATLAB Simulink to evaluate the system's response, voltage fluctuations, load effects, and power quality under varying conditions.

- The experimental validation of the designed hybrid power system using hardware in the loop (HIL) to confirm the systems' robustness and overall performance.
- Analysis and improvement of power quality of PV system by examining various inverter topologies.
- Design of an IOT-based SCADA system for monitoring the proposed hybrid power system for a remote natural gas pipeline control station.

1.5 Thesis Structure

The thesis consists of five separate chapters, each described as follows.

Chapter 1 begins with an overview of energy demand, discussing the historical reliance on fossil fuels for power generation, rising costs, and environmental impact. It also covers using natural gas as a cleaner energy source and transportation. The chapter underscores the need for hybrid power systems incorporating renewable energy sources, describing photovoltaic (PV) systems and their main components. Additionally, it introduces SCADA systems and their various generations. The chapter includes a comprehensive literature review, identifies gaps in existing research, and explains the motivation behind this study.

Chapter 2 describes the comprehensive design of a photovoltaic system for a remote natural gas pipeline control station, accounting for monthly electricity usage and available solar resources. It also covers the design of a power storage system that uses a natural gas generator for backup power. The design and optimization analysis are performed using HOMERPRO software, and the system's economic viability is evaluated. A version of this chapter has been accepted and presented at the 2023 IEEE 32nd Annual Newfoundland Electrical and Computer Engineering Conference (NECEC), and the paper is available in the MUN research repository.

Chapter 3 provides an overview of the photovoltaic system designed for a natural gas control

station pipeline located in a remote area of Pakistan, serving as a case study. It comprehensively analyzes the site's electrical load and available solar energy resources. The chapter also evaluates the system's real-time response by performing dynamic modeling of the designed photovoltaic system in MATLAB Simulink under varying conditions. The proposed system is experimentally validated using hardware-in-the-loop (HIL) testing with the OPAL-RT Technologies OP5707XG simulator to ensure its robustness and overall performance. A version of this chapter has been peer-reviewed and published in "Energies - An Open Access Journal from MDPI" in April 2024. (*Energies* **2024**, *17*, 1763. https://doi.org/10.3390/en17071763).

Chapter 4 focuses on a key component of photovoltaic systems: the DC-AC inverter. It explains how the output power quality of photovoltaic systems can be enhanced using multilevel inverters, describing various topologies. The chapter includes the design of different multilevel inverters and compares them to conventional two-level inverters through THD analysis with resistive and resistive-inductive loads. A version of this chapter has been accepted and presented at the 12th International Conference on Smart Grid (icSmartGrid 2024) and is available on IEEE Xplore data base. (DOI: 10.1109/icSmartGrid61824.2024.10578256)

Chapter 5 covers the design of an IoT-based, open-source SCADA system to monitor a hybrid power system at a remote natural gas pipeline control station, addressing the shortcomings of existing proprietary and non-configurable SCADA systems. A version of this chapter has been peer-reviewed and published in "Electronics - An Open Access Journal from MDPI" in August 2024. (*Electronics* **2024**, *13*, 3235. https://doi.org/ 10.3390/electronics13163235).

Chapter 6 of the thesis summarizes the conclusions from the preceding chapters and suggests potential areas for future research that could build on this study.

References

[1] "Total Energy Monthly Data - U.S. Energy Information Administration (EIA)". Accessed: Dec. 19, 2023. [Online]. Available: https://www.eia.gov/totalenergy/data/monthly/index.php

[2] S. Ali *et al.*, "Evaluating Green Technology Strategies for the Sustainable Development of Solar Power Projects: Evidence from Pakistan", *Sustainability*, vol. 13, no. 23, Art. no. 23, Jan. 2021, doi: 10.3390/su132312997.

[3] J. Anwar, "Analysis of energy security, environmental emission and fuel import costs under energy import reduction targets: A case of Pakistan", *Renewable and Sustainable Energy Reviews*, vol. 65, pp. 1065–1078, Nov. 2016, doi: 10.1016/j.rser.2016.07.037.

[4] H. Yaqoob *et al.*, "Energy evaluation and environmental impact assessment of transportation fuels in Pakistan", *Case Studies in Chemical and Environmental Engineering*, vol. 3, p. 100081, Jun. 2021, doi: 10.1016/j.cscee.2021.100081.

[5] A. A. Mahesar *et al.*, "Effect of Cryogenic Liquid Nitrogen on the Morphological and Petrophysical Characteristics of Tight Gas Sandstone Rocks from Kirthar Fold Belt, Indus Basin, Pakistan", *Energy Fuels*, vol. 34, no. 11, pp. 14548–14559, Nov. 2020, doi: 10.1021/acs.energyfuels.0c02553.

[6] J. W. Tester, E. M. Drake, M. J. Driscoll, M. W. Golay, and W. A. Peters, "*Sustainable Energy, second edition: Choosing Among Options"*. MIT Press, 2012.

[7] "Energy economics | Home", bp global. Accessed: Jul. 25, 2024. [Online]. Available: https://www.bp.com/en/global/corporate/energy-economics.html

[8] A. M. Shar, "Natural Gas Potential of Pakistan an Important Parameter in Mitigating Greenhouse Gas Emissions", *Pak J Anal Environ Chem*, vol. 21, no. 2, pp. 209–218, Dec. 2020, doi: 10.21743/pjaec/2020.12.23.

[9] S. Kanwal, M. T. Mehran, M. Hassan, M. Anwar, S. R. Naqvi, and A. H. Khoja, "An integrated future approach for the energy security of Pakistan: Replacement of fossil fuels with syngas for better environment and socio-economic development", *Renewable and Sustainable Energy Reviews*, vol. 156, p. 111978, Mar. 2022, doi: 10.1016/j.rser.2021.111978.

[10] "Pakistan Natural Gas: Imports, 1975 – 2024 | CEIC Data". Accessed: Jul. 25, 2024. [Online]. Available: https://www.ceicdata.com/en/indicator/pakistan/natural-gas-imports

[11] "Rising LNG dependence in Pakistan is a recipe for high costs, financial instability, and energy insecurity". Accessed: Jul. 25, 2024. [Online]. Available: https://ieefa.org/resources/rising-lng-dependence-pakistan-recipe-high-costs-financial-instability-and-energy

[12] B. Guo and A. Ghalambor, "Natural Gas Engineering Handbook".

[13] N. Khan, S. Dilshad, R. Khalid, A. R. Kalair, and N. Abas, "Review of energy storage and transportation of energy", *Energy Storage*, vol. 1, no. 3, p. e49, 2019, doi: 10.1002/est2.49.

[14] S. Rehman, "Hybrid power systems – Sizes, efficiencies, and economics", *Energy Exploration & Exploitation*, vol. 39, no. 1, pp. 3–43, Jan. 2021, doi: 10.1177/0144598720965022.

[15] A. Panda, A. K. Dauda, H. Chua, R. R. Tan, and K. B. Aviso, "Recent advances in the integration of renewable energy sources and storage facilities with hybrid power systems", *Cleaner Engineering and Technology*, vol. 12, p. 100598, Feb. 2023, doi: 10.1016/j.clet.2023.100598.

[16] S. A. Khatri, K. Harijan, M. A. Uqaili, S. F. Shah, N. H. Mirjat, and L. Kumar, "Solar photovoltaic potential and diffusion assessment for Pakistan", *Energy Science & Engineering*, vol. 10, no. 7, pp. 2452–2474, 2022, doi: 10.1002/ese3.1149.

[17] E. Saif and İ. Emınoğlu, "Hybrid Power Systems in Multi-Rotor UAVs: A Scientific Research and Industrial Production Perspective", *IEEE Access*, vol. 11, pp. 438–458, 2023, doi: 10.1109/ACCESS.2022.3232958.

[18] A. K. Onaolapo, G. Sharma, P. N. Bokoro, T. Adefarati, and R. C. Bansal, "A comprehensive review of the design and operations of a sustainable hybrid power system", *Computers and Electrical Engineering*, vol. 111, p. 108954, Oct. 2023, doi: 10.1016/j.compeleceng.2023.108954.

[19] A. Awasthi *et al.*, "Review on sun tracking technology in solar PV system", *Energy Reports*, vol. 6, pp. 392–405, Nov. 2020, doi: 10.1016/j.egyr.2020.02.004.

[20] Y. Cai, Y. He, H. Zhou, and J. Liu, "Design Method of LCL Filter for Grid-Connected Inverter Based on Particle Swarm Optimization and Screening Method", *IEEE Transactions on Power Electronics*, vol. 36, no. 9, pp. 10097–10113, Sep. 2021, doi: 10.1109/TPEL.2021.3064701.

[21] L. O. Aghenta, M. T. Iqbal, L. O. Aghenta, and M. T. Iqbal, "Design and implementation of a low-cost, open source IoT-based SCADA system using ESP32 with OLED, ThingsBoard and MQTT protocol", *ELECTRENG*, vol. 4, no. 1, pp. 57–86, 2020, doi: 10.3934/ElectrEng.2020.1.57.

Chapter 2: Design and Analysis of a Hybrid Power System for a Remote Natural Gas Pipeline Control Station

Preface

A version of this manuscript has been accepted and presented at the 2023 IEEE 32nd Annual Newfoundland Electrical and Computer Engineering Conference (NECEC), and the full paper is available in the MUN research repository. As the primary author, I led the research efforts, including literature reviews, system design, modeling, and results analysis. I drafted the initial manuscript and revised it based on feedback from the co-authors and the peer review process. Dr. Mohsin Jamil, my research supervisor, and Mirza Jabbar Aziz Baig, my senior, provided research supervision and guidance, reviewed and corrected the manuscript, and contributed valuable research ideas throughout its development.

Abstract

The efficient operation of natural gas pipeline control stations relies on electrical equipment such as data loggers, control systems, surveillance and communication devices, etc. These control stations are often located in remote areas, where maintaining a reliable, uninterrupted, and continuous power supply poses a significant challenge. In this paper, a hybrid power system (HPS) is proposed to meet the unique requirements of a specific remote natural gas pipeline control station as a case study. Based on the collected site data and load profile for a connected load of 275KW, the proposed system is designed using HOMER Pro software. To ensure continuous and sustainable power supply to the control station, the proposed system combines solar photovoltaic (PV) panels with conventional natural gas generators. The detailed analysis of the capital and energy costs associated with the proposed system reveals that the system is suitable for selected site and can reduce costs substantially.

2.1 Introduction

The sustained development of every country relies on energy, and the utilization of fossil fuels to provide primary energy is indispensable for achieving sustainable development across a range of sectors, including industry, transportation, infrastructure, information technology, agriculture, household applications, and more [1]. Natural gas accounts for a significant portion of Pakistan's energy needs, and is also a major source of electricity generation. In 1952, Pakistan witnessed the discovery of extensive natural gas reserves, approximately amounting to 12 trillion cubic feet, in Sui, Baluchistan province of Pakistan. Following this discovery, an extensive gas infrastructure was established to cater to domestic needs, electricity generation, and industrial applications. The transportation of gas to different regions across the country has been efficiently managed by two key entities, namely Sui Northern Gas Pipelines Limited (SNGPL) and Sui Southern Gas Company Limited (SSGCL). Over time, the consumption of natural gas as a primary energy source in Pakistan exhibited a gradual increase [2].

The transmission and distribution of natural gas via pipeline network rely on a range of electrical equipment, including gas turbines, gas compressors, and various other electrically powered equipment situated within control stations. These control stations are strategically located in geographically remote and sparsely populated areas. Operation and maintenance of these high-pressure natural gas pipeline control stations in such remote locations pose substantial challenges, mainly due to the unreliable electricity supply from nearby grid stations, one the reason for ongoing energy crisis. Metropolitan areas have an uninterrupted supply of electricity throughout the year in contrast to many rural and remote areas. According to 2021 data from the World Bank, approximately 15.5% of the world's rural population and remote areas did not have access to

electrical power [3]. Thus, fossil fuels such as diesel and natural gas remain the predominant source of electrical power at such control stations in remote areas.

In today's world, there is growing apprehension regarding environmental issues and society's heavy reliance on fossil fuels [4]. Conventional energy sources, primarily based on fossil fuels, not only contribute substantially to environmental pollution as well as in the midst of an impending depletion crisis. Though, relying solely on fossil fuels for energy generation can have detrimental effects on the environment and the natural world. In Pakistan, other than hydro, electricity production predominantly relies on natural gas, coal, or furnace oil, all of which are non-renewable sources and are imported from various countries. Approximately one-third of Pakistan's energy demand is met through these imports. The heavy reliance on imported energy resources not only burdens end-user with additional costs but also poses a significant challenge to Pakistan's economy, which has consistently faced current account deficits for more than two decades, with only rare exceptions. To cover these deficits, the country has mostly resorted to borrowing funds from friendly nations, issuing international sovereign bonds, and seeking financial assistance from multilateral banks. This approach has been necessary due to the limited flow of foreign direct investments into Pakistan, primarily hindered by bureaucratic inefficiencies and the absence of a conducive political and regulatory environment [5]. To confront these issues, it is imperative to transition toward renewable energy sources, with solar and wind power taking center stage due to their inexhaustible, environmentally friendly nature, and decreasing costs.

Given the intermittent nature of renewable energy sources, hybrid power systems that combine renewable energy sources and conventional energy sources are used to generate electricity [6]. Solar energy is regarded as the most suitable renewable energy source for Pakistan. Pakistan's solar energy potential stands at approximately 5500 terawatt-hours per year, surpassing its present

electricity consumption by more than fivefold. With an average daily solar insolation of 5.30 kWh/m^2 and the potential for a solar energy output of up to 10,000 GW, Pakistan boasts substantial solar energy prospects. Figure 2.1 illustrates the distribution of solar insolation across Pakistan, providing clear evidence of the abundant solar resources available for utilization [7]. Hence the use of solar energy to generate electricity particularly in remote areas is encouraged after consideration of these facts.

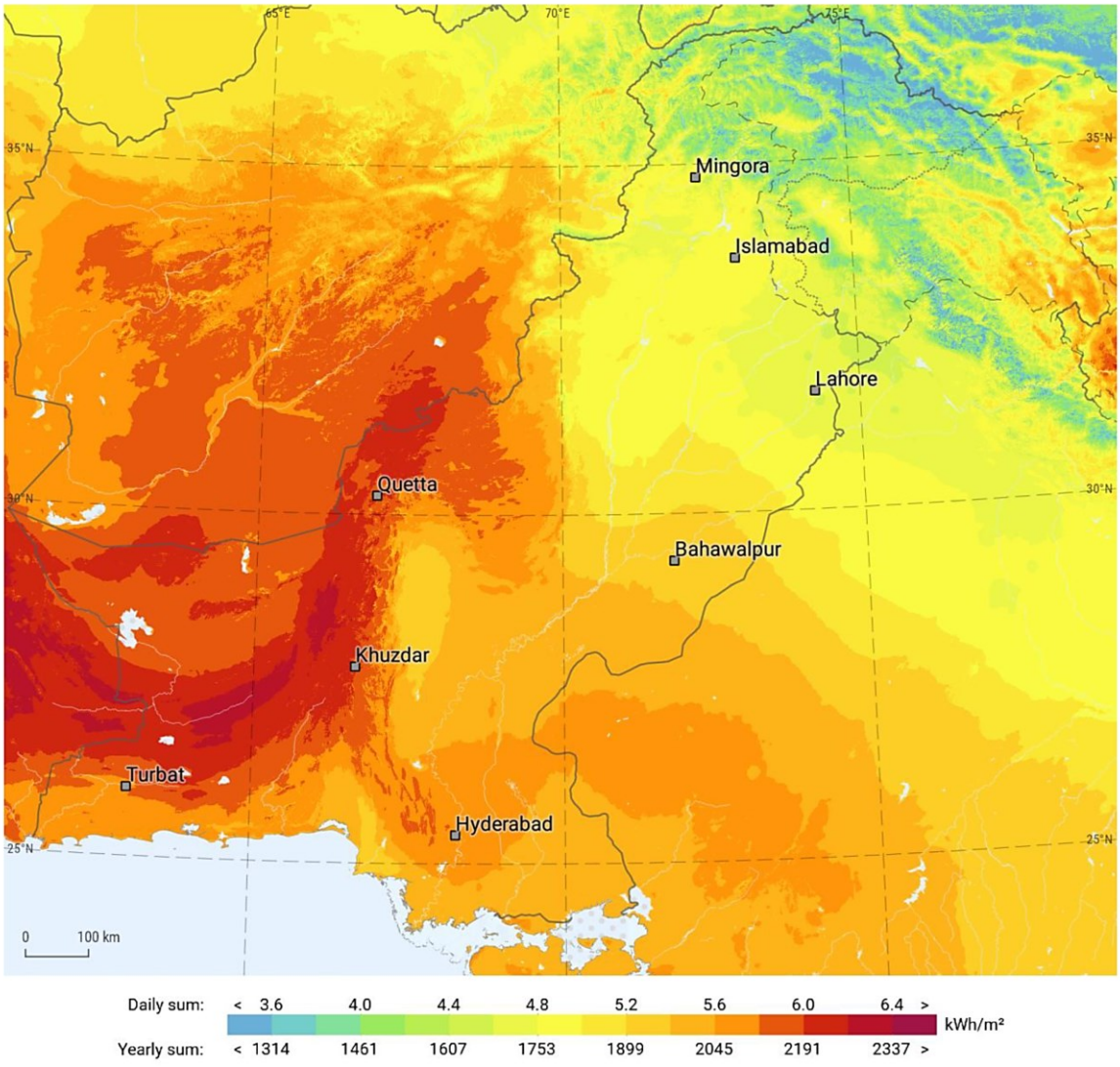

Figure 2.1. Solar insolation levels in Pakistan [7]

2.2 Selected Site Details and Load Analysis

2.2.1 Site Selection

Sui Northern Gas Pipelines Limited (SNGPL) stands as the largest integrated natural gas company providing natural gas to more than 7.22 million consumers in North Central Pakistan through an extensive network that spans in Punjab, Khyber Pakhtunkhwa and Azad Jammu & Kashmir. SNGPL transmission network comprises of 9,239 KM high-pressure gas pipelines. The distribution network of company consists of 142,998 KM low pressure gas pipeline. The transportation of natural gas from gas wells to end consumers involves compression and pressure enhancement of natural gas at compressors stations, also known as control stations. These control stations are strategically located at different remote locations along with the transmission network. SNGPL operates 11 compressor stations to facilitate compression of natural gas so that it could be delivered to doorsteps of end consumers.

The site selected as a part of this study is one of natural gas compressor stations of SNGPL located in unpopulated and remote area of Pakistan known as Gali Jagir, Fateh Jhang (33.427522,72.625862). As shown in chapter 1 of thesis, Figure 1.3 depicts the aerial view along with the coordinates of selected site on google map.

Figure 2.2 shows the actual view of selected site which is a control station for high pressure natural gas pipeline network in remote area of Pakistan. This site has a total area of 11 acre which consists of 6-acre compressor station area and 5-acre residential block area. There is sufficient space available at selected site (both rooftop and ground space) which can be utilized for installation of solar PV panels.

Figure 2.2. Actual view of selected site

2.2.2 Solar Global Horizontal Irradiance

Solar Global Horizontal Irradiance (GHI) is an important factor in assessing site feasibility. It represents the amount of sunlight energy measured at a specific location. As shown in Figure 2.3, it is evident that solar radiation is consistently available at the selected location throughout the year, with values ranging from 3.19 kWh/m^2/day to 7.43 kWh/m^2/day. Likewise, clearness index is another important factor taken into account while evaluating site feasibility. It is measure of clearness of atmosphere and it is an arbitrary, dimensionless number that ranges from 0 to 1 with higher values occurring during clear and sunny conditions, and lower values during dusty or cloudy conditions. For selected site its value varies between 0.552 to 0.689 as shown in Figure 2.3. Homer Pro software is used to get solar GHI and clearness index data for selected site.

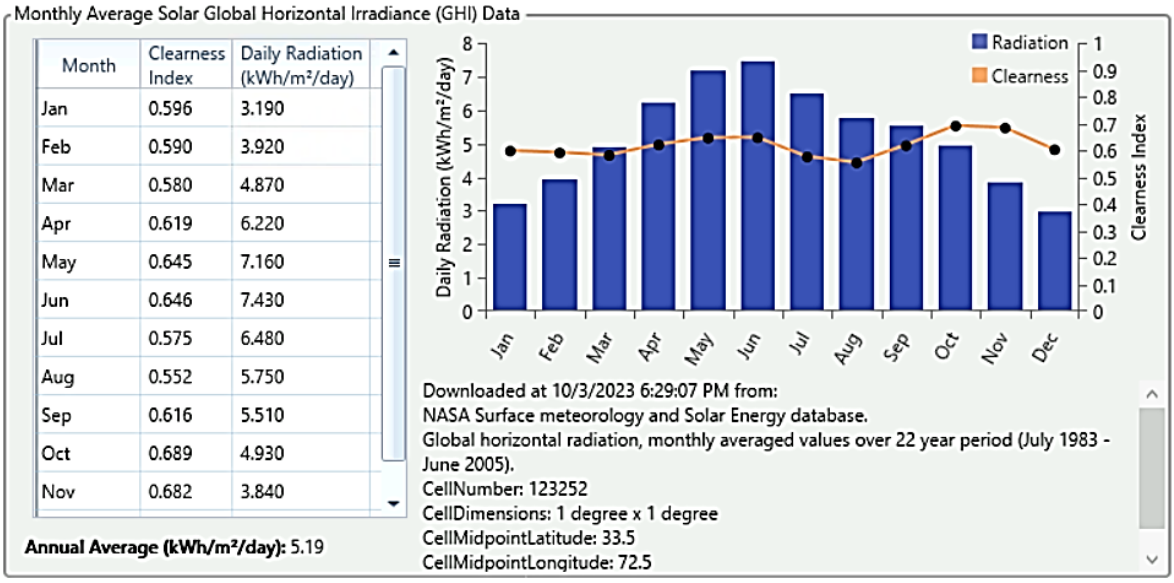

Figure 2.3. Solar GHI and clearness index of selected site

2.2.3 Electrical Load Analysis

The electrical load at the selected site is categorized into two major groups. First one is gas compressor station load and second one is residential load (staff colony load). Station load mainly consists of control equipment for natural gas turbines, air compressors, gas discharge cooling system, fire suppression system, metering equipment and other related equipment. The residential load consists of domestic load for approximately 30 quarters for staff which is operating the gas compressor station. The hourly load data for year 2022 and corresponding load profile has been shown in Figure 2.4.

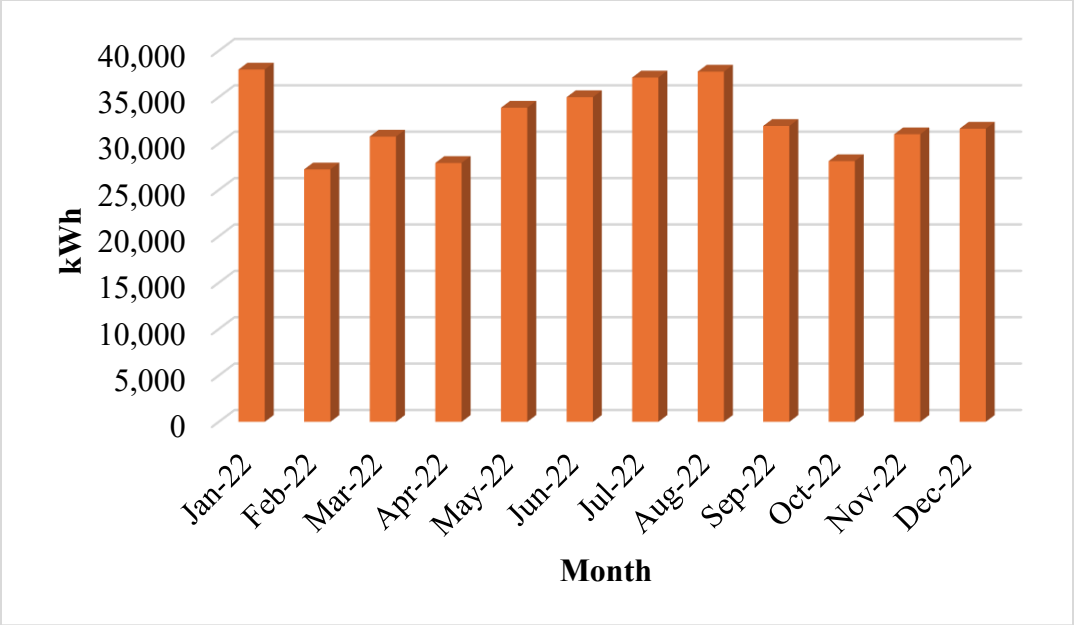

Figure 2.4. Monthly electrical consumption (Year 2022)

2.3 Proposed Hybrid Power System

The proposed hybrid system for selected site includes a DC power source which consists of PV panels and battery bank and alongside an AC power source which is natural gas genset. Hence it comprises of both AC bus and DC bus, while the bus configuration is designed for operational and maintenance flexibility while ensuring uninterrupted power supply. Since a constant power supply is required for the reliable operation of natural gas compressor stations, the proposed hybrid system is effectively built with backup resources to deliver uninterrupted power. The block diagram of proposed hybrid system is shown in Figure 2.5.

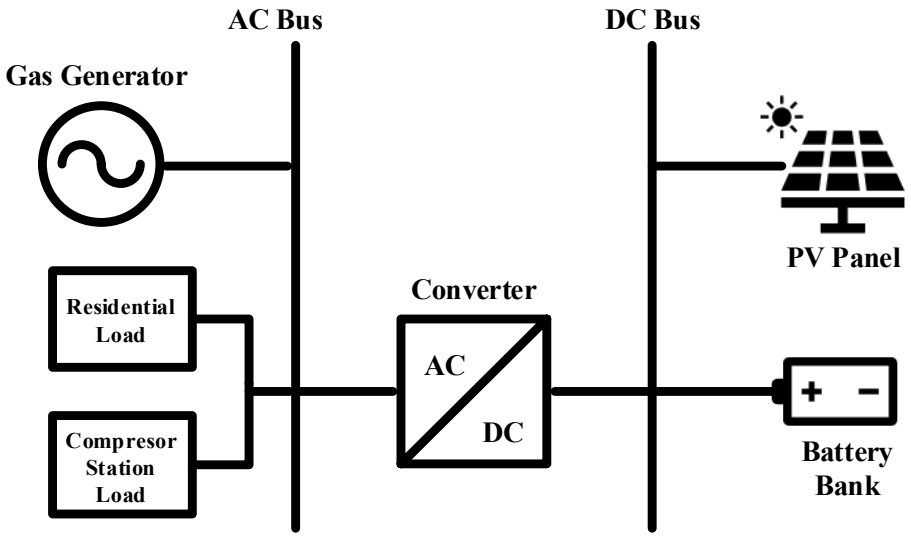

Figure 2.5. Proposed hybrid power system

The current power generation source at the selected site relies solely on natural gas generators, primarily due to the consistent availability of natural gas, regardless of the energy cost per kWh. However, in the proposed hybrid power system PV panels and battery bank are incorporated which will be optimally utilized at maximum and natural gas generator will be mainly utilized during peak load demand, otherwise it will act as backup. The detailed structure for proposed hybrid power system is discussed below:

2.3.1 Gas Generator

A natural gas generator is a device that generates electricity by burning natural gas as its fuel source. It operates on the principle of converting the chemical energy stored in natural gas into electrical energy. The equation (2.1) can be used to find heat content or energy value of fuels in mmBTU.

$$mmBTU = \frac{Hm^3 * GCV}{281.7385} \tag{2.1}$$

Considering a daily average load of 1172 kWh/day and a peak load of 180k, a 200kW gas generator

has been selected for the proposed system. The relationship between natural gas engine efficiency and electric load is influenced by specific operating conditions and the engine's design. Proper load management, control systems, and maintenance are essential to ensure that the engine operates at its optimal efficiency while meeting the variable demands of the electric load [8]. The gas engine efficiency load curve is shown in Figure 2.6.

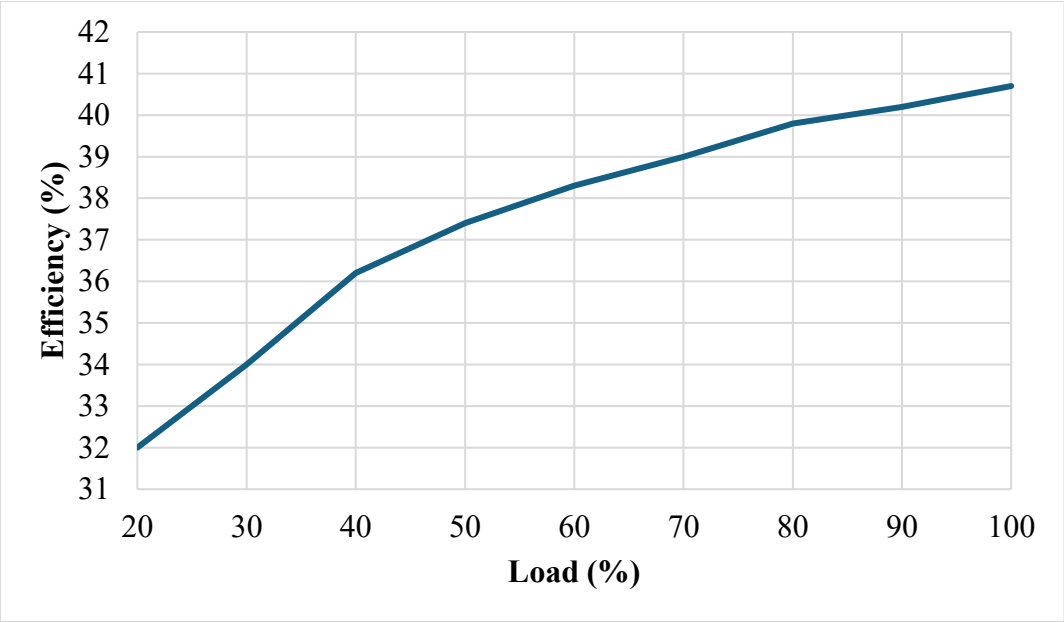

Figure 2.6. Gas engine efficiency curve

2.3.2 PV Panels

The PV panel selected for this project is of Longi Solar, model no. LR6-72PH-365M. It is monocrystalline solar panel having a maximum power rating of 365 watt and 18.80% efficiency. A solar cell is a PN junction diode in which current flows in the reverse direction. PV modules are constructed by combination of many solar cells. The diode current and voltage characteristics for a single solar panel is given by equations (2.2) and (2.3) [9].

$$I_d = I_o\{\exp[\frac{V_d}{V_T}]-1\} \tag{2.2}$$

$$V_T = \frac{KT}{q} * nl * N_{cell} \tag{2.3}$$

Where I_d and I_o represent diode current and diode saturation current respectively. V_d is diode voltage, 'K' is Boltzmann constant having a value of 1.380649×10^{-23} J·K^{-1}. T represents temperature of cell, *nl* represents ideality factor of diode and N_{cell} is the total number of cells connected in series in a PV module.

2.3.3 Battery Bank

The primary function of the battery bank within the proposed hybrid power system is to store surplus electrical energy generated by the solar PV system and to supply this stored energy to the electrical loads during periods when the PV system is not fully operational, such as at night or in the absence of sunlight. A 12V lead acid battery having current rating of 201Ah has been selected for the proposed hybrid power system. To ensure high lifetime of battery during cyclic applications, the depth of discharge for battery at 30% has been maintained.

2.3.4 DC to AC Converter (Inverter)

An inverter is an electrical device that converts direct current (DC) into alternating current (AC) at the desired amplitude and frequency, making it symmetrical. To meet the peak load of 180 kW, a 250-kW inverter, exceeding the peak load by at least 25%, has been chosen for the proposed system. Multilevel inverters are widely employed in high-voltage applications, and their performance surpasses that of conventional two-level inverters by exhibiting reduced harmonic distortion, lower electromagnetic interference, and higher DC link voltages.

2.4 Optimization of Proposed HPS using Homer Pro

For optimization of the proposed hybrid power system, a software tool called Hybrid Optimization Model for Multiple Energy Sources (HOMER Pro), developed by the National Renewable Energy Laboratory is utilized. It simulates every possible system configuration in a single execution and subsequently arranges these systems based on the selected optimization variable. The configuration of proposed HPS designed in Homer Pro is shown in Figure 2.7.

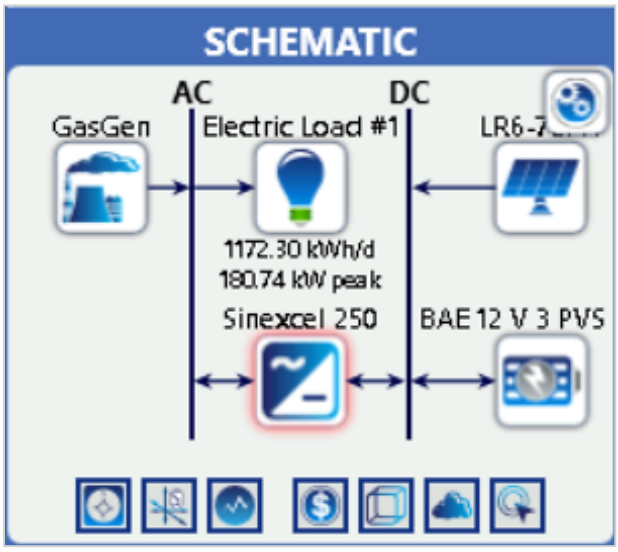

Figure 2.7. Configuration of proposed system in HOMER Pro

This configuration incorporates two separate buses: one for Alternating Current (AC) and the other for Direct Current (DC). A 840V DC bus is used and interfaced with a 12-volt, 201Ah lead-acid battery bank and 365-watt flat plate solar modules from Longi Solar. A derating factor of 85% is applied to account for the impact of dust and high temperatures. Gas genset and AC load are connected with AC bus. Sinexcel 250kW inverter is used to interlink AC bus with DC bus. The system is designed in such a way that there is no limitation on power generation through PV modules and PV modules will be used at maximum to optimize the overall system performance. HOMER Pro performs economic analysis by calculating the total lifecycle cost of a designed

system, considering factors such as capital costs, operating and maintenance (O&M) costs, fuel costs, replacement costs, and salvage value. It uses these costs to determine key metrics like Net Present Cost (NPC) and Levelized Cost of Energy (LCOE). The software simulates each system configuration to calculate energy production, fuel consumption, and unmet load, then uses these results to calculate the total costs over the project's lifetime. HOMER Pro optimizes the system by simulating and comparing thousands of possible configurations, ranking them based on NPC or other economic criteria, and selecting the most cost-effective solution. Additionally, it performs sensitivity analysis to evaluate how changes in variables like fuel prices or solar radiation affect the system's performance and cost. This ensures that the selected system remains reliable and economically viable over time.

The various system configurations evaluation and subsequently system sizing done by HOMER Pro is shown in Figure 2.8. As it is evident from simulation results in Figure 2.8 that HOMER Pro has provided different configurations by using different combination of available power sources and the most optimum configuration selected is combination of PV panels, battery bank and gas genset because the Net Present Cost (NPC) is $1.30M and Cost of Energy (COE) is $0.234 in this case, which is minimum among all configurations.

Export...

Optimization Results

Left Double Click on a particular system to see its detailed Simulation Resul

Architecture										
				LR6-72PH (kW)	GasGen (kW)	BAE 12 V	Sinexcel 250 (kW)	Dispatch	NPC ($)	COE ($)
				282	200	280	190	LF	$1.30M	$0.234
					200	140	66.8	CC	$1.85M	$0.335
					200			CC	$2.11M	$0.382
				582		1,260	201	CC	$2.12M	$0.383
				6.11	200		1.42	CC	$2.12M	$0.383

Figure 2.8. HOMER Pro optimization results for proposed HPS

In this configuration, PV modules will generate 282 kW power, so a total of 773 solar panels, along with 250 kW Sinexcel inverter and 280 12V batteries are required to meet the load demand of selected site. As selected DC bus has a voltage rating of 840V and 280 batteries are required to meet load demand so 4 battery strings having 70 batteries of 12V in each string will be used. According to Figure 2.9 below, the optimal system suggested by HOMER pro only uses gas generators for 15.5% of its total electricity and obtains 84.5% of its power from solar energy.

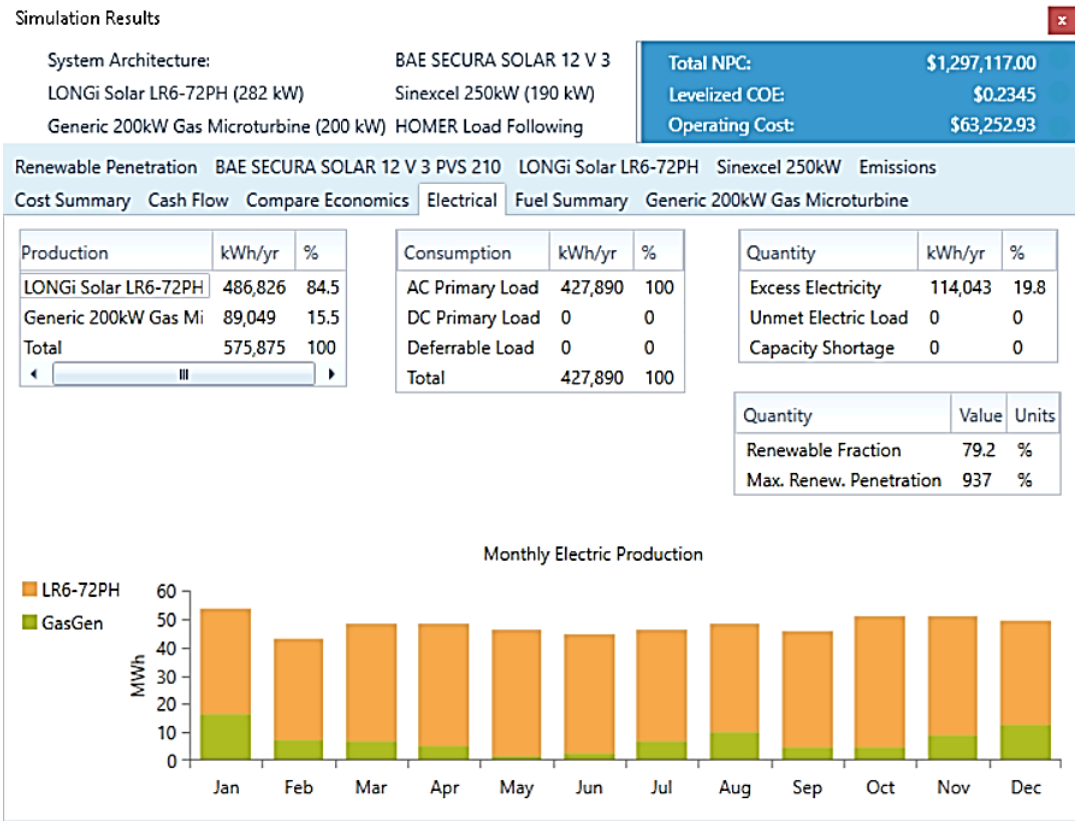

Figure 2.9. HOMER Pro simulation results for proposed HPS

HOMER Pro calculates the renewable energy fraction and total energy produced by both renewable and non-renewable sources through detailed simulations. It first models the energy production from renewable sources, such as solar or wind, based on input data like solar irradiance, system capacity, and efficiency, while also simulating non-renewable generation, such as gas or diesel generators, based on fuel consumption and load demand. The software matches energy

production to system load on an hourly basis and sums it to calculate the total energy produced annually in kWh/year for both renewable and non-renewable sources. The renewable energy fraction is then determined by dividing the total renewable energy produced by the total energy generated by all sources, providing insight into how much of the system's energy demand is met by renewables.

Also, the renewable energy fraction and total energy produced by both renewable and non-renewable sources represent average values calculated over a specific period. This average accounts for variations in energy production and load demand over time. HOMER Pro performs hourly simulations across the entire year, accounting for seasonal variations in renewable resource availability, such as solar irradiance or wind speed.

Table 2.1 shows information regarding rating and relative pricing of various components used in proposed HPS.

Table 2.1. Rating and cost of components used in proposed HPS

Component	**PV Panel**	**Inverter**	**Battery Bank**	**Gas Genset**
Rating per unit	0.365 kW	250kW	12V, 201Ah	200kW
No. of units required.	773	1	280	1
Total rating	282kW	250kW	840V, 804Ah	200kW
Cost per unit	$229	$38600	$385.32	$165300
Total cost	$176788	$38600	$107890	$165300

The area of one PV panel which is selected for this project is 1.937m2. Thus, to install 773 PV panels, a total of 1498m2 area is required. The total rooftop area available at selected site is calculated using google earth and it is equivalent to 2525m2 which is sufficient for installation of

required PV panels. Other than rooftop area, sufficient ground space is also available which can be utilized for future expansion considering the total load requirement.

HOMER Pro also performs cost analysis to find the best optimum system. Based on per unit price provided to HOMER Pro, it calculates total cost of the system and suggests the most optimum solution. The cost analysis done by HOMER Pro is shown in Figure 2.10.

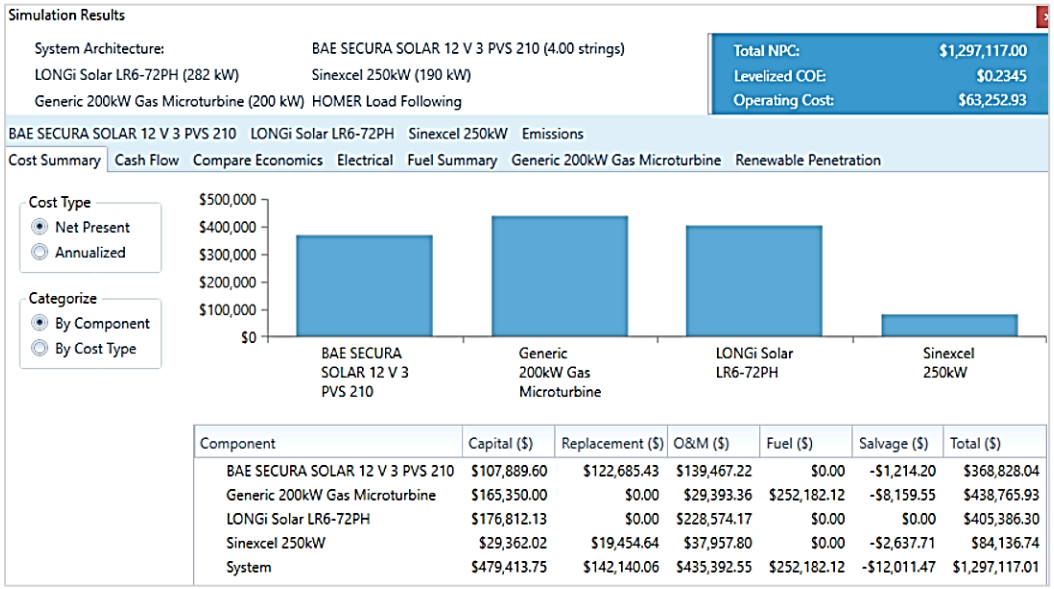

Component	Capital ($)	Replacement ($)	O&M ($)	Fuel ($)	Salvage ($)	Total ($)
BAE SECURA SOLAR 12 V 3 PVS 210	$107,889.60	$122,685.43	$139,467.22	$0.00	-$1,214.20	$368,828.04
Generic 200kW Gas Microturbine	$165,350.00	$0.00	$29,393.36	$252,182.12	-$8,159.55	$438,765.93
LONGi Solar LR6-72PH	$176,812.13	$0.00	$228,574.17	$0.00	$0.00	$405,386.30
Sinexcel 250kW	$29,362.02	$19,454.64	$37,957.80	$0.00	-$2,637.71	$84,136.74
System	$479,413.75	$142,140.06	$435,392.55	$252,182.12	-$12,011.47	$1,297,117.01

Figure 2.10. Cost summary of proposed HPS in HOMER Pro

Like cost analysis, cash flow analysis is also performed by HOMER Pro which is shown in Figure 2.11. Cash flow analysis considers capital cost, operating cost, fuel cost for gas genset, replacement cost and salvage cost. The cash flow analysis has been done for 25 years. A capital investment of $479,413.75 is required and there will be an operating cost of $33,679.52 and fuel cost of $19,507.39 per year. Replacement cost will also incur at during year 7,10,13 and 20 and during 25th year the salvage value of system will be equivalent to $50,140.

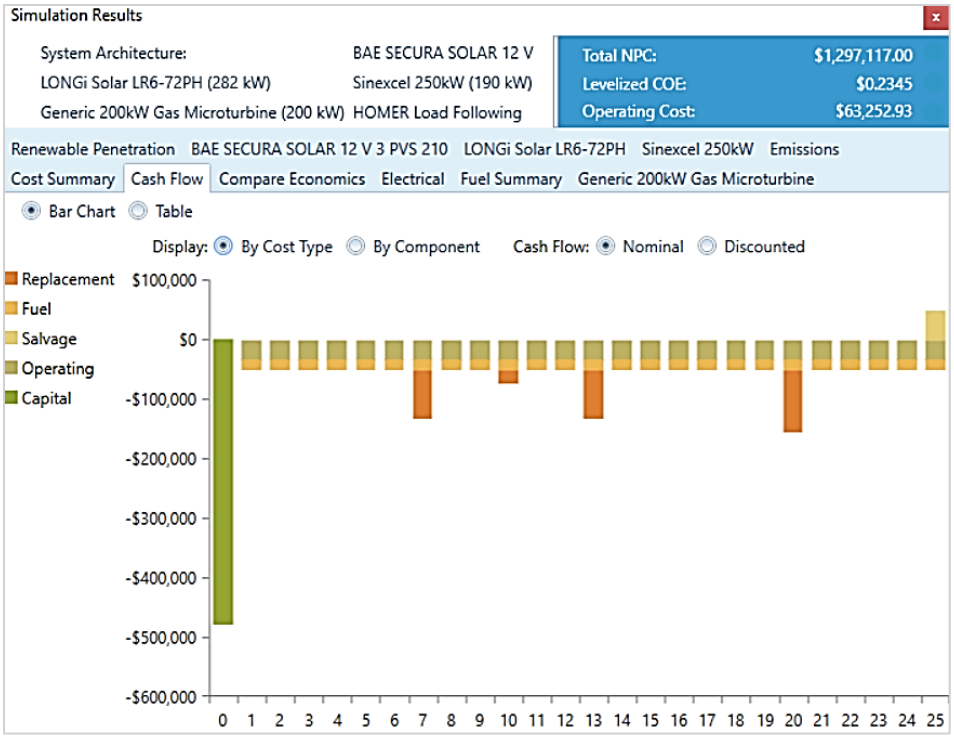

Figure 2.11. Cash flow analysis in HOMER Pro

2.5 Conclusion

Due to significant increase in prices of petroleum products over the recent years and to conserve the fossil fuels, it is critical to use of renewable energy sources for power generation specially in remote areas. But due to intermittent nature of renewable energy sources, hybrid power systems are the most appealing and feasible solution. In this paper a hybrid power system is designed for a remote natural gas pipeline facility which not only addresses the energy challenges faced by such facilities but also emphasizes that the adoption of hybrid power systems can lead to significant financial gains while aligning with broader energy sustainability goals. By reducing energy costs by $0.148 in comparison to already existing conventional practices, this study paves the way for more efficient, cost-effective, and environmentally responsible energy solutions in remote industrial settings.

References

[1] A. Raza, R. Gholami, G. Meiyu, V. Rasouli, A. A. Bhatti, and R. Rezaee, "A review on the natural gas potential of Pakistan for the transition to a low-carbon future," *Energy Sources, Part A: Recovery, Utilization, and Environmental Effects*, vol. 41, no. 9, pp. 1149–1159, Nov. 2018, doi: https://doi.org/10.1080/15567036.2018.1544993.

[2] S. Kanwal, M. T. Mehran, M. Hassan, M. Anwar, S. R. Naqvi, and A. H. Khoja, "An integrated future approach for the energy security of Pakistan: Replacement of fossil fuels with syngas for better environment and socio-economic development," *Renewable and Sustainable Energy Reviews*, vol. 156, p. 111978, Mar. 2022, doi: https://doi.org/10.1016/j.rser.2021.111978.

[3] "Access to electricity, rural (% of rural population) | Data," *data.worldbank.org*. https://data.worldbank.org/indicator/EG.ELC.ACCS.RU.ZS (accessed on 03 October 2023).

[4] D. Mazzeo, N. Matera, P. De Luca, C. Baglivo, P. M. Congedo, and G. Oliveti, "A literature review and statistical analysis of photovoltaic-wind hybrid renewable system research by considering the most relevant 550 articles: An upgradable matrix literature database," *Journal of Cleaner Production*, vol. 295, p. 126070, May 2021, doi: https://doi.org/10.1016/j.jclepro.2021.126070.

[5] S. Malik, M. Qasim, H. Saeed, Y. Chang, and F. Taghizadeh-Hesary, "Energy security in Pakistan: Perspectives and policy implications from a quantitative analysis," *Energy Policy*, vol. 144, p. 111552, Sep. 2020, doi: https://doi.org/10.1016/j.enpol.2020.111552.

[6] L. Ahsan and M. Iqbal, "Dynamic Modeling of an Optimal Hybrid Power System for a Captive Power Plant in Pakistan," *Jordan Journal of Electrical Engineering*, vol. 8, no. 2, p. 195, 2022, doi: https://doi.org/10.5455/jjee.204-1644676329.

[7] F. Hussain *et al.*, “Solar Irrigation Potential, Key Issues and Challenges in Pakistan,” *Water*, vol. 15, no. 9, p. 1727, Jan. 2023, doi: https://doi.org/10.3390/w15091727.

[8] L. Ahsan and M. Tariq Iqbal, “Design of an Optimal Hybrid Energy System for a Captive Power Plant in Pakistan,” *2021 IEEE 12th Annual Information Technology, Electronics and Mobile Communication Conference (IEMCON)*, Oct. 2021, doi: https://doi.org/10.1109/iemcon53756.2021.9623260.

[9] L. O. Aghenta and M. T. Iqbal, “Design and Dynamic Modelling of a Hybrid Power System for a House in Nigeria,” *International Journal of Photoenergy*, vol. 2019, pp. 1–13, Apr. 2019, doi: https://doi.org/10.1155/2019/6501785.

Chapter 3: Hybrid Power System Design and Dynamic Modeling for Enhanced Reliability in Remote Natural Gas Pipeline Control Stations

Preface

A version of this manuscript has been accepted and published in "Energies - An Open Access Journal from MDPI" in April 2024 (Energies ***2024****, 17, 1763. https://doi.org/10.3390/en17071763). As the primary author, I led the research efforts, including literature reviews, system design, modeling, and results analysis. I drafted the initial manuscript and revised it based on feedback from the co-authors and the peer review process. Dr. Mohsin Jamil, my research supervisor, and Dr. Ashraf Ali Khan, my research co-supervisor, provided research supervision and guidance, reviewed and corrected the manuscript, and contributed valuable research ideas throughout its development.*

Abstract

The most rapid and efficient method to transport natural gas from its source to its destination is through a pipeline network. The optimal functioning of control stations for natural gas pipelines depends on the use of electrical devices, including data loggers, communication devices, control systems, surveillance equipment, and more. Ensuring a reliable and consistent power supply proves to be challenging due to the remote locations of these control stations. This research article presents a case study detailing the design and dynamic modeling of a hybrid power system (HPS) to address the specific energy needs of a particular natural gas pipeline control station. The HOMER Pro 3.17.1 software is used to design an optimal HPS for the specified location. The designed system combines a photovoltaic (PV) system with natural gas generators as a backup to ensure a reliable and consistent power supply for the control station. Furthermore, it provides significant cost savings, reducing the cost of energy (COE) by USD 0.148 and the annual operating costs by USD 87,321, all while integrating a renewable energy fraction of 79.2%. Dynamic modeling of the designed system is performed in MATLAB/Simulink R2022a to analyze the system's response, including its power quality, harmonics, voltage transients, load impact, etc. The experimental results are validated using hardware in the loop (HIL) and OPAL-RT Technologies' real-time OP5707XG simulator.

3.1 Introduction

One of the most important necessities of modern living is energy. It plays a crucial role in enhancing a nation's economic development and raising the standard of living. As economic progress continues, the exploration and exploitation of oil and gas reserves progressively intensify alongside the consumption of these conventional sources [1]. The reliability of energy resources is pivotal for sustaining modern life, and a consistent energy supply is essential for fostering economic growth while promising solutions for addressing the depletion of traditional energy sources, including using clean energy devices [2,3]. The availability of energy at an affordable cost is a key determinant in fostering the prosperity of a nation [4].

In the present era, energy is pivotal in driving socio-economic advancement, with per capita energy consumption closely linked to a nation's development [5]. Energy can be derived from renewable resources such as solar, geothermal, biomass, hydro, and wind power or fossil fuel reserves like uranium, natural gas, coal, and oil [6]. Given its low carbon intensity and minimal environmental impact in production and consumption, natural gas is preferred over other fossil fuel sources such as oil and coal [7]. A substantial share of Pakistan's energy requirements is fulfilled by natural gas, making it a key contributor to electricity generation [8]. Figure 3.1 shows Pakistan's total energy supply (TES) from 1990 to 2021.

Due to challenges in storing natural gas, it must be promptly transported to its intended destination once extracted from the reservoir. Several methods exist for transporting natural gas from oil and gas fields to the end consumers [10]. Energy transportation refers to the transportation of various forms of energy from production sources to endusers. Main energy sources are typically distant from end consumers in remote and unpopulated areas. Therefore, an energy transportation system becomes essential for delivering energy to end-users. Due to its extremely low density,

economically transporting natural gas is challenging; hence, it undergoes compression before being transported. Weather conditions significantly impact the transportation of natural gas through pipelines. In regions where temperatures vary from -50 to +40 degrees Celsius annually, the physical properties of the pipeline metal are affected. Therefore, it is crucial to maintain an optimal temperature for efficient gas transportation through the main pipeline [11].

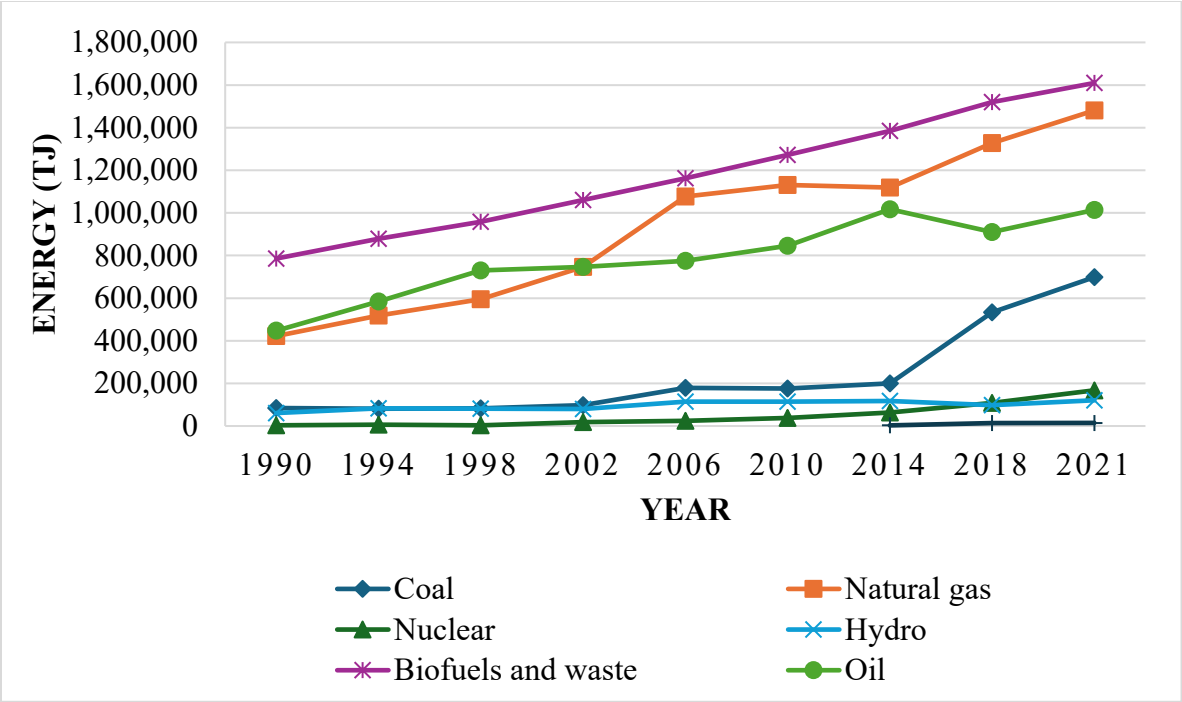

Figure 3.1. Total energy supply (TES) in Pakistan [9]

Natural gas energy may be transported from its source to its destination in several ways. Table 1 displays various methods of transporting natural gas from its source to its destination, along with the preferred transportation mode based on distance in kilometers (km) and capacity in billion cubic meters (bcm) per year [12].

Table 3.1. Modes of NG transportation: capacity–distance comparison.

Mode of transportation	Capacity (bcm)	Distance (Km)
LNG (Liquefied Natural Gas)	0.1 – 10.0	1000 – 10000
Gas to Liquid (GTL)	0.1 – 1.0	5000 – 10000
CNG (Compressed Natural Gas)	0.1 – 1.0	100 – 5000
Pipeline	0.1 – 10.0	100 – 1000
NGH (Natural Gas Hydrates)	0.1 – 1.0	100 – 5000
Gas to Wire (GTW)	0.1 – 1.0	100 – 5000

Various natural gas pipeline control stations oversee the operation and maintenance of high-pressure natural gas pipelines. The geographic distribution of these control stations poses operational challenges, especially in remote locations, where maintaining and operating high-pressure natural gas pipeline control stations can be difficult due to unreliable electricity supply and other logistical issues. At the same time, the smooth functioning of control stations depends on a range of electrically powered devices installed within these control stations [13].

Compared to rural and remote areas, metropolitan areas have a consistent and uninterrupted electricity supply throughout the year. Data from the World Bank for 2021 reveals that around 15.5% of the global population residing in remote and rural areas lack access to electricity [14]. In the current era, there is also an increasing concern about environmental issues, and society has an extensive dependence on fossil fuels [15]. Electricity production in Pakistan involves a mix of thermal power plants, with a primary focus on utilizing natural gas and coal, hydroelectric power stations, and nuclear power facilities, and there is an increasing emphasis on harnessing renewable energy sources like wind and solar power, particularly in regions with favorable conditions. The

percentage share of different energy sources used for power generation in Pakistan is shown in Figure 3.2.

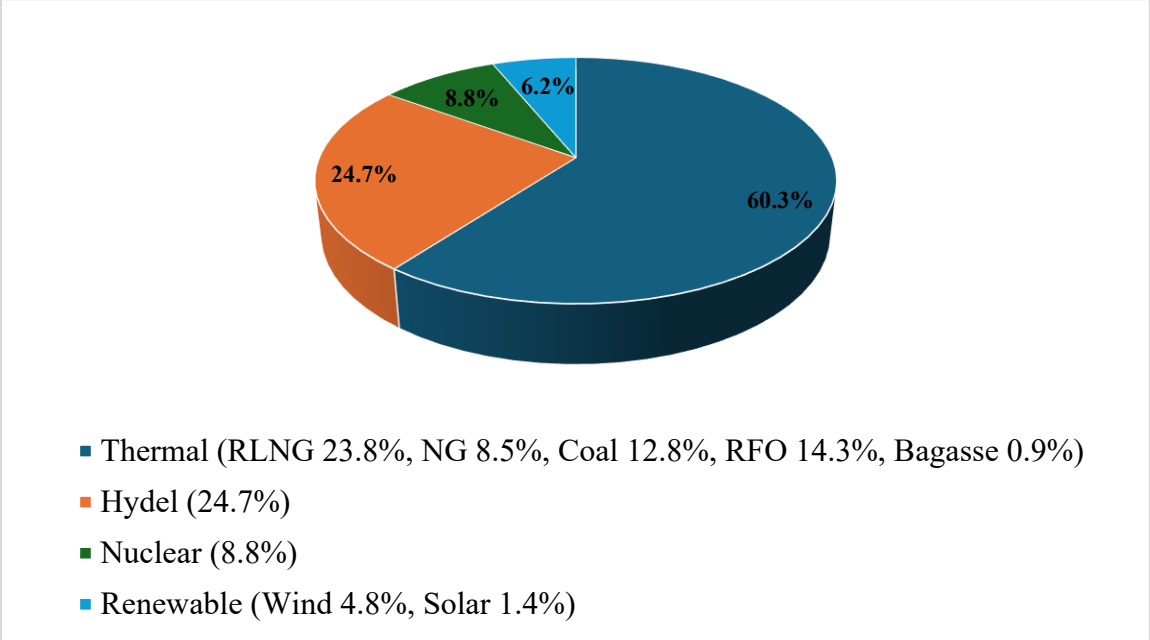

Figure 3.2. Sources of power generation in Pakistan [16].

The LNG price depends on the international market and is affected by various other global factors. By late 2021, the ultimate cost of LNG delivered to Pakistan had risen to nearly USD 16 per MMBtu, exceeding the average domestic gas price by more than fourfold [17]. Thus, a consistent and reliable supply of electric power from conventional fossil fuels is at risk due to increased fuel prices resulting from the ongoing conflicts and continued demands for environmental pollution reduction [18]. Likewise, the cost of energy in Pakistan is mainly affected by imported energy costs, transmission losses, economic conditions, and pricing policies. Figure 3.3 shows the forecast for the annual average cost of energy in Pakistan based on historical data.

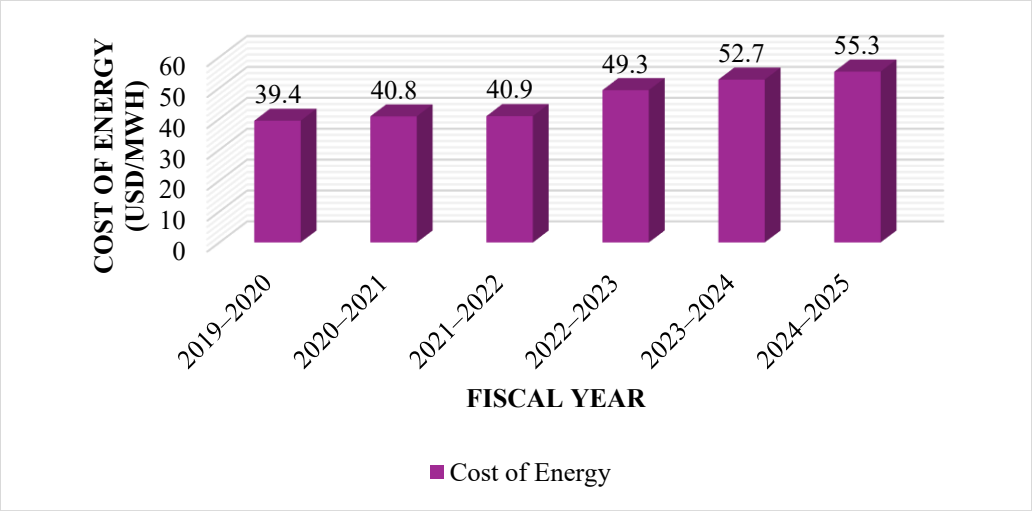

Figure 3.3. Cost of energy in Pakistan [19].

When Sui Northern Gas Pipelines Limited (SNGPL) commenced its operations following the discovery of substantial natural gas reserves in Pakistan, control stations were strategically established in remote areas to facilitate natural gas transportation across the country. These stations were initially designed to rely on the internal consumption of natural gas through natural gas generators for their electrical power needs, as reliable alternative power sources were not readily available in those areas. However, the continuous and dependable power supply demanded by these control stations became a critical requirement. Unfortunately, at their inception, little consideration was given to the future scenario when natural gas reserves might deplete.

With indigenous natural gas sources diminishing and a significant reliance on imported LNG, the internal consumption of natural gas for power generation at these control stations has become economically impractical due to the escalating LNG prices constituting both wastage and an economically inefficient practice. Therefore, exploring alternative methods, such as harnessing renewable energy sources for power generation at these control stations, is prudent. It is critical to switch to renewable energy sources, which are the most promising options because of their endless supply, low cost, and environmental friendliness. Because renewable energy sources are

intermittent, hybrid power systems that integrate both conventional and renewable energy sources are used to generate electricity [20]. HPSs are dependable, eco-friendly systems that efficiently reduce reliance on a single renewable resource. This is particularly significant in regions with scarce natural resources [21]. In most cases, a hybrid power system contains renewable energy sources (solar, wind, and hydro), conventional energy sources (diesel and/or natural gas generators and AC distribution systems), energy storage elements, power converters, and DC/AC loads.

Solar energy emerges as Pakistan's most viable renewable energy option, boasting a potential of about 5500 terawatt hours per year—which is over five times the nation's current electricity consumption. Pakistan has tremendous solar energy potential, with an average daily sun insolation of 5.30 kWh/m2, and the capacity to generate up to 10,000 GW. The distribution of solar insolation throughout Pakistan is shown in Figure 2.1 in Chapter 2, which provides clear evidence that ample solar energy is available for utilization [22].

Considering these facts, it is recommended to encourage the production of electricity using solar energy, especially in rural and remote areas where such control stations are located. Numerous researchers have explored the potential of employing PV systems for domestic and commercial structures, water pumps, reverse osmosis plants, and more. However, there is a notable absence of relevant research on implementing HPSs for such natural gas pipeline control stations located remotely. These stations require minimizing or ceasing the internal consumption of conventional fossil fuels to enhance the conservation of depleting resources, mitigate environmental impact, and reduce energy costs while ensuring a consistent and reliable power supply.

This research article addresses the challenges mentioned earlier by proposing the design of an optimal HPS. In particular, this research contributes to the existing research in the following ways:

- It designs and sizes the proposed HPS using HOMER Pro, which involves determining the

optimal capacity and configuration of components to meet the energy demands of a specific application. This process includes analyzing the load profile, assessing renewable resource availability, incorporating energy storage, determining the generator capacity, and implementing a control system.

- It carries out dynamic modeling of the proposed hybrid power system using MATLAB Simulink to analyze the system's response, voltage transients, load impact, and power quality under diverse conditions, which are specifically related to the control station under consideration.
- The experimental validation of the proposed hybrid power system (HPS) is carried out using hardware in the loop (HIL), and the real-time OPAL-RT Technologies' OP5707XG simulator (OPAL-RT, Montreal, QC, Canada) is used to confirm the systems' robustness and overall performance.

3.2 Site Selection

One of the most fundamental choices made during any project's establishment, expansion, or relocation is the site selection. The installation of a solar photovoltaic system component in large-scale hybrid power systems requires a significant long-term investment; therefore, choosing the right site is crucial to the system's success or failure. Hence, finding the best location with the ideal circumstances for solar photovoltaic system installation is one of the primary goals in the site selection process. The primary factors to consider when selecting a site for a solar photovoltaic system are solar irradiance; economic performance metrics, such as the return on investment (ROI), internal rate of return (IRR), and net present value (NPV); along with carbon emission reductions and policy support [23].

SNGPL is the biggest integrated natural gas provider in North Central Pakistan, serving over 7.22 million customers over a vast network spanning throughout Khyber Pakhtunkhwa (KPK), Punjab, and Azad Jammu and Kashmir (AJ&K). SNGPL's transmission network comprises 9239 km of high-pressure gas pipelines, while the distribution network comprises 142,998 km of low-pressure gas pipelines. Pipeline control stations play a crucial role in the compression and elevation of natural gas pressure, facilitating transportation from gas wells to end consumers. SNGPL operates eleven compressor stations to compress natural gas efficiently, ensuring its delivery to the doorsteps of end consumers. The overall operation of the company's business is shown in Figure 3.4.

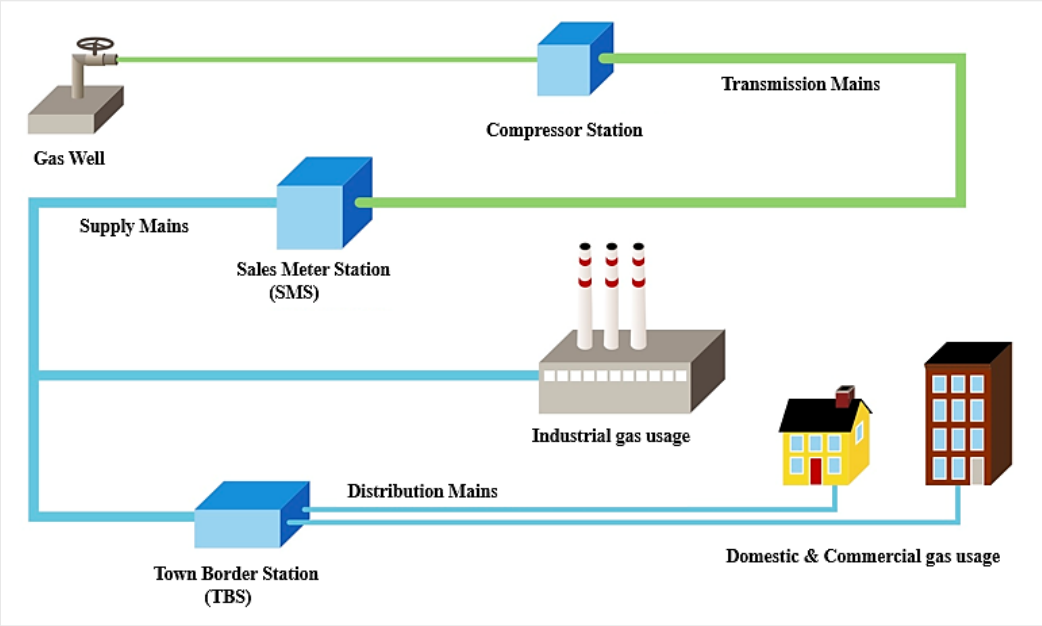

Figure 3.4. Schematic diagram of SNGPL's overall operation.

The site selected to be a part of this research is one of the natural gas compressor stations operated by Sui Northern Gas Pipelines Limited (SNGPL) in Pakistan. This selected site is located in a remote and sparsely populated area named Gali Jagir, Fateh Jhang (33.427522, 72.625862). An aerial view of the site on Google Maps is shown in Figure 1.3 in chapter 1 of thesis.

Figure 3.5 shows several viewpoints of the selected natural gas pipeline control station. The site covers a total area of 11 acres, with a designated 6-acre section for the compressor station and a 5-acre area for residential blocks. Ample space is present at the selected site, encompassing both rooftop and ground areas and providing opportunities for the installation of solar PV panels.

Figure 3.5. Real-life perspective of selected site.

3.2.1 Global Horizontal Irradiance (GHI)

Global horizontal irradiance (GHI), also known as solar global horizontal irradiance, is vital in assessing site viability. It is a measurement of the solar radiation intensity in a particular place. The solar global horizontal irradiance data for the selected site is obtained from the NASA Surface Meteorology and Solar Energy Database using the HOMER Pro software, as depicted in Figure 3.6. Solar energy remains consistently available at the chosen location year-round, with values varying between 3.19 kWh/m2/day and 7.43 kWh/m2/day, with an annual average of 5.19 kWh/m2/day. Similarly, the clearness index is another crucial factor considered during site feasibility assessment. It quantifies the atmosphere's clarity and is denoted by a unitless number ranging from 0 to 1. The clearness index for the selected site ranges between 0.552 and 0.689, as illustrated in Figure 3.6.

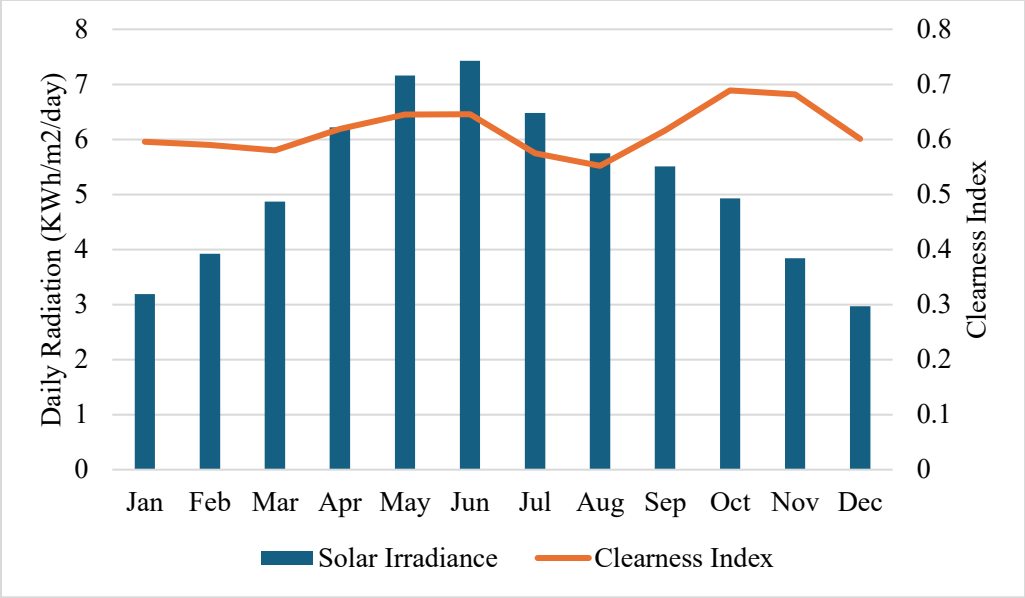

Figure 3.6. Solar global horizontal irradiance and clearness index of selected site.

Apart from various factors, such as atmospheric conditions, air pollution, and cloud cover, the angle at which sunlight strikes a solar cell affects how much solar energy reaches its surface. This angle, known as the altitude or elevation angle, represents the sun's vertical position relative to the horizontal plane and varies throughout the day as the sun moves across the sky. This angle is influenced by factors such as the observer's geographical location, the time of day, and the time of year [24]. The solar azimuth angle (z) represents the angle formed by the projection of sunlight onto a line extending either north or south. This angle is determined within the horizontal plane and can be measured using two different conventions, either clockwise or counterclockwise [25]. The solar elevation and the solar azimuth variation for the selected site throughout the year are obtained using an online tool named 'Solargis Prospect', as shown in Figure 3.7.

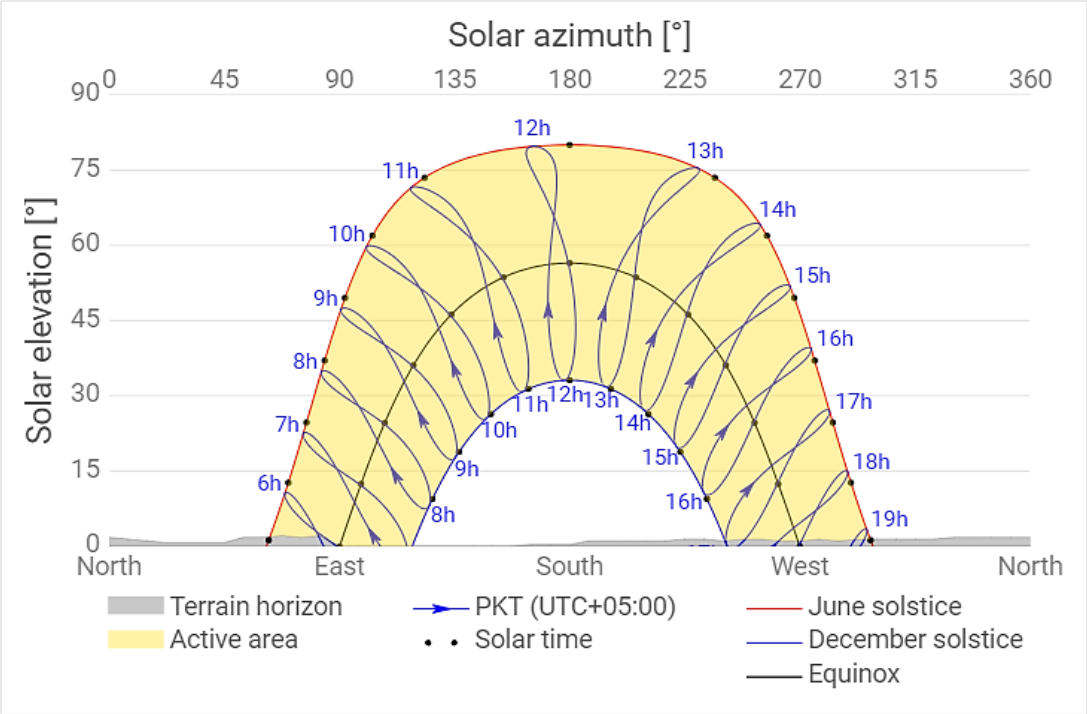

Figure 3.7. The solar azimuth and solar elevation for the selected site throughout the year [26].

3.2.2 Electrical Load Analysis

The overall electrical load is segmented into two primary categories: the gas compressor station load and the staff colony's residential load. The station load consists of air compressors, a discharge gas cooling system, control equipment for gas turbines, a fire suppression system, metering devices, etc. A breakdown of the total connected load is provided in Table 3.2.

Table 3.2. Detail of total connected load at selected site.

System Description		Number of Units	Rated Power of Unit Load Installed		Total Connected Load	
			HP.	KW.	HP.	KW
Discharge Gas Cooling (DGC) System	Fan Motors	4	25	18.65	100	74.6
	Fan Motors	2	40	29.84	80	59.68
	Pump Motors	0	0	0	30	22.38
Turbine Package	Lube Oil Tank Heater	0	0	0	0	0
	Evaporative Cooling Pump Motor	2	0.75	0.5595	1.5	1.119
Turbine Shed	Inlet Fan Motors	0	0	0	0	0
	Exhaust Fan Motor	0	0	0	0	0
Raw Water Pump	Pump Motor #1	2	15	11.19	30	22.38
Air system	Air Compressor Motors	2	15	11.19	30	22.38
Power House	Radiator Fan Motor	1	0.75	0.5595	0.75	0.5595
	Water Circulating Pump Motor	1	1	0.746	1	0.746
Auxiliary Load	Residential Load			75	0	75
Total Connected Load			**278.84 KW**			

3.2.3 Diversity Factor

In power distribution engineering, analyzing loads involves integrating the diversity factor to accommodate the probabilistic and temporal characteristics of multiple loads connected to a distribution feeder. The concept of 'load diversity' pertains to the idea that not all combined loads are simultaneously active at their maximum capacities.

Therefore, considering the temporal and probabilistic aspects of the loads allows for the sizing of power generation and distribution assets to be smaller than what would be required if all loads were activated simultaneously [27]. The diversity factor (DF) is given as follows:

$$D.F = \frac{\max(l_1(t)) + \max(l_2(t)) + ... + \max(l_N(t))}{Sup(l_1(t) + (l_2(t) + ... + (l_N(t))} \tag{3.1}$$

where the various connected loads are l_1, l_2, ..., l_N, and the numerator represents the cumulative non-simultaneous peak values of these loads, while the denominator employs the supremum function to denote the sum of the overall load. Therefore, the peak load for the selected is taken as 180.74 kW after accounting for the diversity factor, and the suggested HPS will be designed accordingly.

Figure 2.4 in Chapter 2 of the thesis displays the monthly power consumption and corresponding load profile for 2022 based on the total connected load.

3.3 Proposed Hybrid Power System (HPS)

The HPS suggested for the selected site incorporates a DC power source comprising a PV system, MPPT controller, battery bank, DC-DC buck converter, DC-AC inverter, LCL filter, AC power source, and natural gas generator. Therefore, this system incorporates AC and DC buses, configured to offer operational flexibility and facilitate maintenance, ensuring uninterrupted power supply. The proposed HPS is engineered with backup resources to ensure reliable and consistent power delivery for the smooth operation of natural gas control stations. Figure 3.8 shows the block diagram of the proposed hybrid power system.

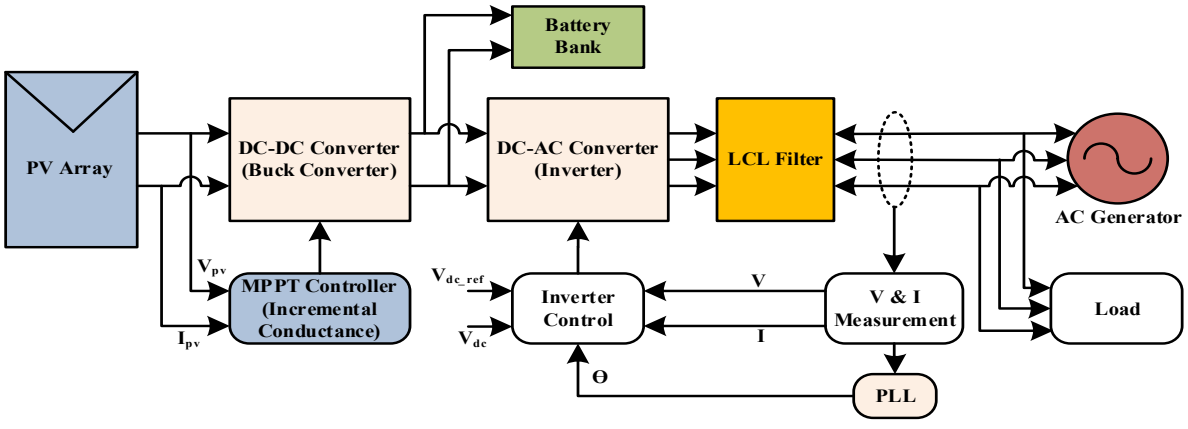

Figure 3.8. Schematic diagram of proposed hybrid power system.

3.3.1 Mathematical Modeling of Proposed HPS Components

- **Photovoltaic System:** A photovoltaic panel, also called a solar panel, transforms sunlight directly into electricity using the photovoltaic effect. This phenomenon involves the generation of an electric current and voltage in a material when exposed to sunlight. PV panels are made of multiple solar cells interconnected in a specific arrangement to achieve the desired voltage and current output. Figure 3.9 illustrates the equivalent circuit of the PV cell.

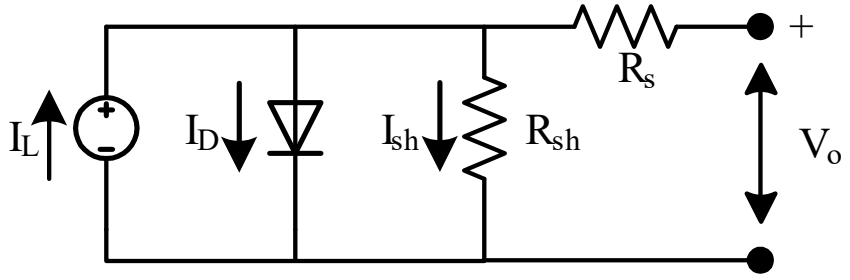

Figure 3.9.Equivalent circuit of a solar cell.

The diode represents the solar cell's nonlinear behavior, permitting a current in one direction while blocking reverse flow. Given that solar cells do not operate ideally, a shunt resistance (Rsh) and a series resistance (Rs) are included in the circuit. Shunt resistance represents unintended parallel paths for the current flow within the solar cell, caused by material imperfections. When no load is connected, it allows the current to bypass the load, mitigating the effects of leakage currents. This ensures stable voltage and current characteristics, minimizing losses and maintaining efficiency in the solar cell's operation. Meanwhile, series resistance accounts for internal resistance and interconnections between the solar cells within a module. The equations for the solar cell output current 'I' and light-generated current 'I_L' are

$$I = I_L - I_D - (\frac{V_o + IR_s}{R_{sh}}) \tag{3.2}$$

$$I_L = [I_{SC} + K_I(T_C - T_R)] \tag{3.3}$$

Here, 'I_D' is the diode current, 'ISC' is the short circuit current, 'K_I' specifies the solar cell's short circuit current temperature coefficient, and 'T_C' and 'T_R' represent the solar reference temperature and operating temperature. The equation for the diode current is given below.

$$I_D = I_o\{\exp[\frac{eV_b}{kT}] - 1\} \tag{3.4}$$

where 'Io' represents the diode's leakage or saturation current, and 'k' is the Boltzmann constant. So, the solar cell equation is derived as follows:

$$I = I_o\{\exp[\frac{eV_b}{kT}] - 1\} - I_L \tag{3.5}$$

A solar cell operates like a diode, with the current flowing in the opposite direction. Thus, the PV panel voltage, VPV, is

$$V_{PV} = V_{OC} \text{ x } N_S \tag{3.6}$$

where 'V_{OC}' represents the open-circuit voltage and *NS* is the number of cells connected in series. And the power generated by the solar panels is given as follows:

$$P_{pv} = \frac{V_{pv} \text{ x } I_{sc} \text{ x } G}{K_d} \tag{3.7}$$

Where K_d represents the derating factor.

- **Maximum Power Point Tracking (MPPT) Control:** The position of the sun and the direction of sun rays significantly impact the solar cells' ability to produce electricity, and any changes in these factors directly impact the electricity generated by the solar cells. The relationship between I–V (current-voltage) and P–V (power voltage) is also nonlinear in

the case of PV cells. As a result, the PV cells' output varies continuously. A PV module's output power is mostly affected by variations in the line and the load measured at its production without additional electrical control being needed [28]. The I–V and P–V curves of the PV module indicate that the PV module achieves its most optimized power output at a specific point, known as the maximum power point (MPP), since the power generated by the module on either side of the MPP is always less. Therefore, to enhance the conversion efficiency of the PV installation, it is important to track and ensure that PV modules operate at MPP.

An MPPT, or maximum power point tracker, is a DC-DC converter with an intelligent algorithm that tracks the output power of a PV array. Its role is to identify and maintain the optimum power output point for the PV cells, improving the overall efficiency of the solar installation process. Numerous techniques/algorithms exist for tracking the maximum power point (MPP), such as Hill Climbing, incremental conductance (INC), Perturb & Observe (P&O), and Neural Network Control. In this research article, the INC algorithm is used due to its superior performance in adapting to changing weather conditions, its accuracy in MPP tracking, and reliable robustness. Figure 3.10 illustrates the incremental conductance MPPT algorithm.

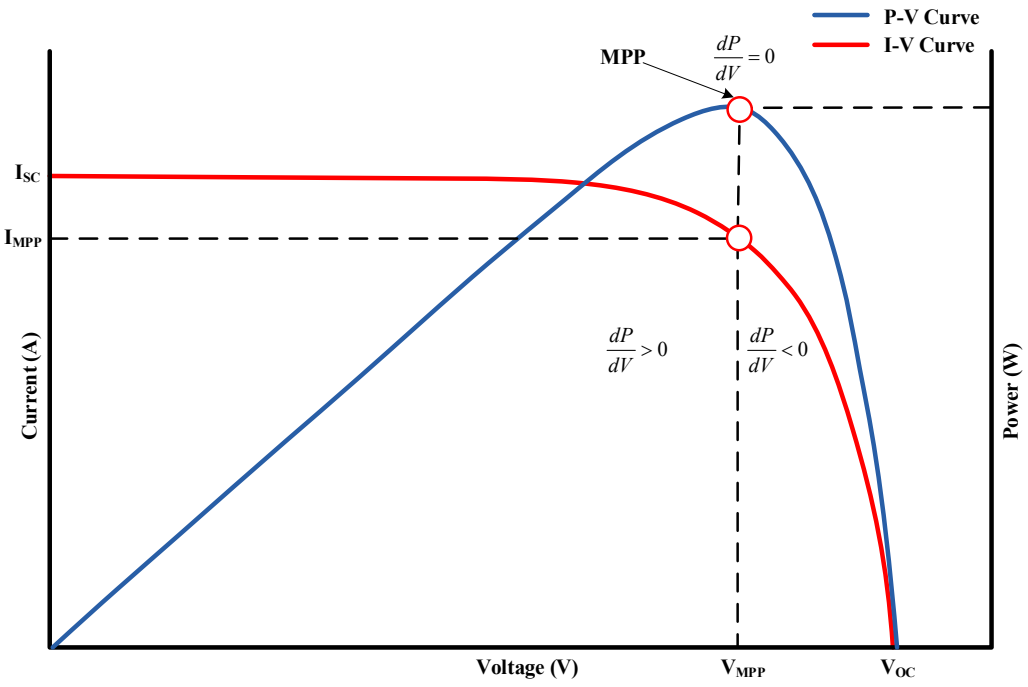

Figure 3.10. Incremental conductance MPPT algorithm.

The INC method relies on the fundamental idea that the PV module's P-V curve has a zero slope at MPP ($\frac{dP}{dV}=0$). The algorithm compares the incremental conductance ($\frac{dI}{dV}$) with the array conductivity ($\frac{I}{V}$) to determine the MPP. The following is the basic equation that powers INC's operations:

$$\frac{dP}{dV}=\frac{d(VI)}{dV}=I\frac{dV}{dV}+V\frac{dI}{dV}=I+V\frac{dI}{dV} \tag{3.8}$$

$$1 \text{ x } \frac{dP}{dV}=\frac{I}{V}+\frac{dI}{dV} \tag{3.9}$$

The incremental conductance is obtained by differentiating the PV module's output power with respect to voltage and equating it to zero. As $\frac{dP}{dV}=0$ at maximum power point (MPP), the important relationships that determine how the INC algorithm functions are listed below in Table 3.3.

Table 3.3. Maximum power point tracking conditions.

Condition	Constraint	Description
$\frac{dI}{dV} = -\frac{I}{V}$	If P = MPP	MPP Achieved
$\frac{dI}{dV} > \frac{I}{V}$	If P < MPP	Operating point is left to MPP
$\frac{dI}{dV} < \frac{I}{V}$	If P > MPP	Operating point is right to MPP

The I–V and P–V characteristics of the PV array used in this project under different temperature and solar GHI levels are shown in Figure 3.11.

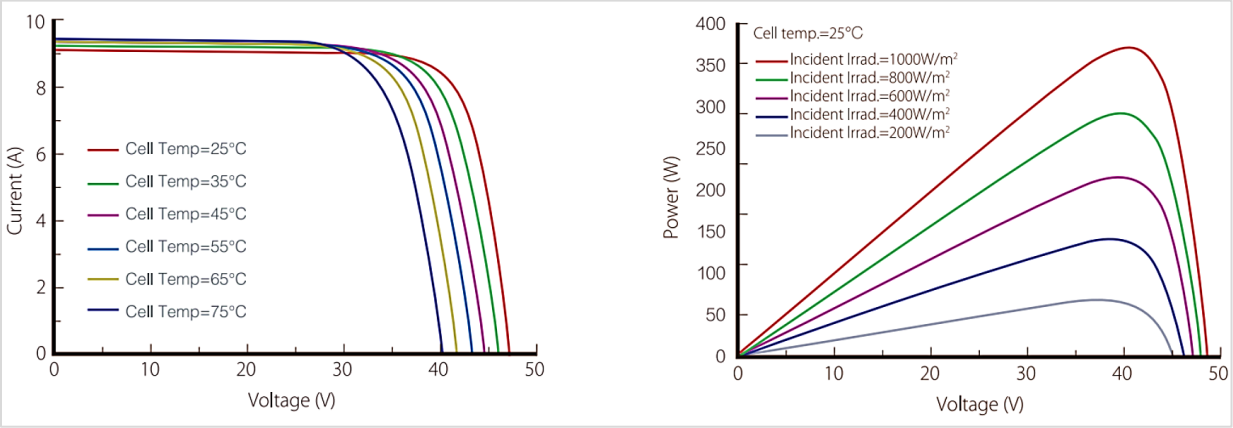

Figure 3.11. Current–voltage and power–voltage characteristics of PV panel used [29].

Several factors affect the solar PV module's performance, such as temperature and irradiance. The open-circuit voltage of a PV module changes with the cell temperature; as the temperature rises, the open-circuit voltage (Voc) decreases while the short-circuit current increases, consequently lowering the power output [30]. Solar panels operate most efficiently at approximately 25 °C (77 °F), as efficiency tends to decrease in both higher and lower temperature ranges. Similarly, temperature and irradiance influence the P–V curves of solar panels by affecting the voltage, current, and maximum power point of the panels. Higher temperatures typically lead to a decrease in the voltage and an increase in

the current, while higher irradiance levels result in a higher output power.

- **DC-DC Buck Converter:** The proposed HPS incorporates a DC-DC converter as an integral multistage power processing system component. The converter is critical in achieving the maximum power point (MPP) of PV modules, generating a DC voltage, and is designed to handle power variations. Together with the DC-AC inverter, the DC-DC converter constitutes the multistage system, providing flexibility in operating the PV voltage over a broad range. Additionally, this configuration eliminates the direct link between the AC output and PV modules, preventing the induction of double-line-frequency ripple in a PV voltage caused by AC power fluctuations. The DC-DC converter is a buck converter chosen for its high efficiency, uncomplicated configuration, and minimal voltage ripple. In this specific case, it plays an important role in maintaining the DC output voltage level by the inverter DC link, set at 360V DC. A buck converter steps down the voltage from its input (Vi) to produce a lower output voltage (Vo). The output voltage is controlled by regulating switch S's duty cycle (D) and can be implemented using an IGBT, MOSFET, or transistor, as illustrated in Figure 3.12.

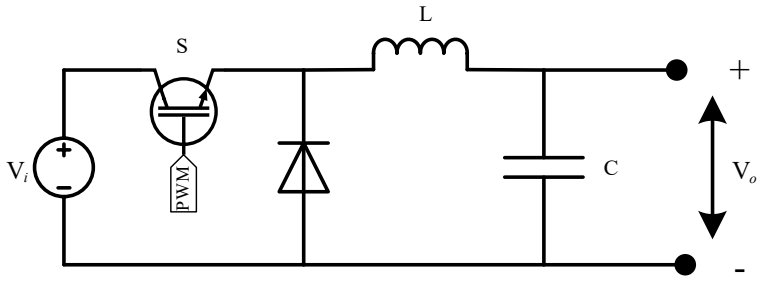

Figure 3.12. DC−DC buck converter.

The duty cycle (D) is a scalar quantity with a value ranging from 0 to 1. The following are the key equations that describe the functioning and design of a buck converter:

$$D = \frac{V_o}{V_{i(\max)} \text{ x } \eta} \tag{3.10}$$

$$\text{L} = \frac{V_o \text{ x } (V_i - V_o)}{\Delta I_L \text{x} f_s \text{ x } V_i} \tag{3.11}$$

where 'η' is the efficiency of an inductor, 'L' is the selected inductor value for the buck converter, f_s is the switching frequency of the converter, and ΔI_L is the inductor ripple current, which can be calculated as

$$\Delta I_L = (0.2 \text{ to } 0.4) \text{ x } I_{o(\max)} \tag{3.12}$$

Using the above expressions, the inductor value is calculated as 0.346 mH. Similarly, a capacitor is used in a buck converter, and its purpose is to reduce the ripples in the output voltage. Its value is calculated as 1.2 mF using the expression given below.

$$C = \frac{\Delta I_L}{8 \text{ x} f_s \text{ x } \Delta V_o} \tag{3.13}$$

- **DC-AC Inverter:** An inverter transforms direct (DC) electricity into symmetrical alternating (AC) electricity at the required voltage and frequency level using appropriate switching patterns and a control strategy. The buck converter provides a steady DC output, which is then supplied to the three-phase Voltage Source Inverter (VSI). The VSI transforms it into the desired AC voltage of 230 V (single phase). The sinusoidal pulse width modulation technique (SPWM) is selected from various PWM techniques to achieve suitable switching patterns and control strategies. This selection is based on its distinct advantages, such as simplicity, low Total Harmonic Distortion (THD), and better control schemes. By controlling the duty cycle of the SPWM pulses, the required output voltage waveform and a reduced THD can be achieved. The THD becomes an important factor to consider when dealing with nonlinear components, and most semiconductor devices, which

are at the cores of renewable energy systems, exhibit nonlinear behavior. Integrating sinusoidal pulse width modulation (SPWM) with an LCL filter is a powerful approach to reduce the Total Harmonic Distortion (THD). SPWM ensures precise control of the output voltage, while the LCL filter, with its inductors, capacitors, and resistors, effectively acts as a lowpass filter to suppress higher-order harmonics. This combination results in a cleaner and sinusoidal output waveform, making it particularly valuable in applications with low distortion, such as renewable energy systems and power electronics. The circuit diagram of the three-phase inverter is shown in Figure 3.13.

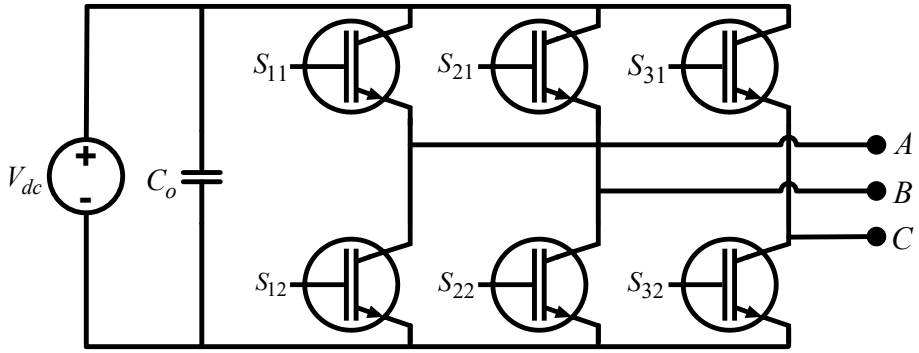

Figure 3.13. Three-phase multi-level inverter.

- **LCL Filter:** The LCL filter has been extensively applied in renewable energy systems due to its excellent high-frequency (HF) attenuation properties, compact size, and cost-effectiveness [31]. The LCL filter, shown in Figure 3.14, effectively attenuates harmonics, dampens resonance, enhances system performance, complies with grid standards, contributes to stability, offers flexibility in design, and ensures the reliability of renewable energy systems. It provides improved filtering compared to simpler LC filters, offering better damping of resonance peaks and enhancing the system's overall efficiency. Moreover, the use of lowrated inductors and capacitors in LCL filters makes it more cost-effective and affordable. Hence, the LCL filter addresses power quality challenges in the

context of renewable energy generation.

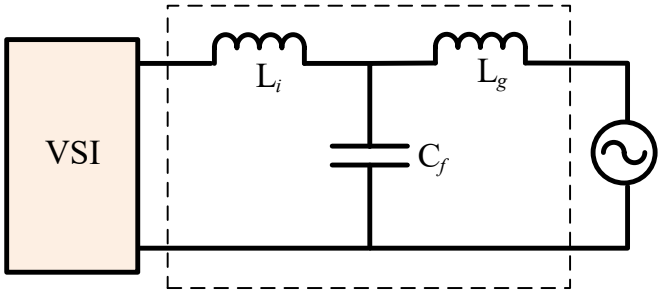

Figure 3.14. Configuration of LCL Filter.

The design process for an LCL filter begins by calculating the inductor on the inverter (L_i) side using the following equation:

$$L_i = \frac{V_{dc}}{6 \text{ x } f_s \text{ x } \Delta I_L} \tag{3.14}$$

where *'V_{dc}'* denotes the DC bus voltage and '*fs'* is the system frequency, while the inductor ripple current, 'ΔIL', is 10% of the maximum current and computed as

$$\Delta I_L = 0.1 \text{ x } \frac{P_{\text{nominal}} \text{ x } \sqrt{2}}{V} \tag{3.15}$$

Similarly, the value of the inductor on the generator side is calculated using the equation given below.

$$L_g = r \text{ x } L_i \tag{3.16}$$

where the value of '*r*' is the ratio of *Lg* and *Li*, and a value of r = 0.6 results in a 5% reduction in the power factor [32].

$$L_g = 0.6 \text{ x } L_i \tag{3.17}$$

Ultimately, the objective is to design the filter capacitor (Cf) to limit inverter output voltage oscillations to a maximum of 5%, ensuring the stable operation of the hybrid power system.

This involves calculating the capacitance using specific formulas.

$$C_f = 0.05 \text{ x } \frac{P_{\text{nominal}}}{\omega_g \text{ x } V^2_{ph-g}} \tag{3.18}$$

Similarly, it is important to analyze the resonance frequency (ω_{res}) of the filter. Equation (19) is used to calculate the resonance frequency in radians

$$\omega_{res} = \sqrt{\frac{L_i + L_g}{L_i \text{ x } L_g \text{ x } C_f}} \tag{3.19}$$

$$f_{res} = \frac{1}{2\pi}\sqrt{\frac{L_i + L_g}{L_i \text{ x } L_g \text{ x } C_f}} \tag{3.20}$$

In the last step, the value of the damping resistor (R_f), connected in series with the filter capacitor to prevent resonance issues, is determined using equation (21).

$$R_f = \frac{1}{3 \text{ x } C_f \text{ x } \omega_{res}} \tag{3.21}$$

Using the above-given equations, values of L_i, L_g, C_f, f_{res}, and R_f are calculated as 519μH, 312μH, *66* μF, 1.41MHz and 0.0573Ω respectively.

3.4 Optimization of Proposed HPS Using HOMER Pro

HPS optimization involves numerous factors, including system configurations, component sizing, project economics considering variable loads and component expenses, system lifespan, end-user energy expenditures, net present cost, annual operating costs, maintenance expenses, and the availability of renewable energy resources in the region. These factors are crucial for the overall design and functionality of the system and help decision makers pinpoint the most economically viable solutions customized to accommodate the specific electrical loads for which the hybrid system is being developed [33].

A ‘Hybrid Optimization Model for Multiple Energy Sources (HOMER Pro)’ is used to optimize

the proposed hybrid power system for cost-effective solutions. This software simulates systems integrating one or more power sources like photovoltaics and wind turbines. It facilitates the design of both grid-connected and off-grid systems in the most economically efficient way by considering the mentioned factors. It explores various configurations to pinpoint the most economically efficient combinations that meet the specified electrical load requirements. The optimization analysis of HOMER is pivotal in addressing important design considerations, such as identifying the most cost-effective technologies, evaluating the impact on project economics caused by variations in costs or loads, optimal component sizing, and assessing the adequacy of renewable energy resources.

After analyzing the total connected electrical load of the selected site using the data from Table 3.2, a corresponding load profile was generated and exported to the HOMER Pro software, which facilitated the sizing of a PV system and natural gas generator and optimized the design of the proposed hybrid power system. The simulation incorporated solar global horizontal irradiance (GHI) data for the selected site (Figure 3.6) and specific PV modules, batteries, and converters. Figure 3.15 illustrates the schematic diagram of HOMER Pro's optimized hybrid power system.

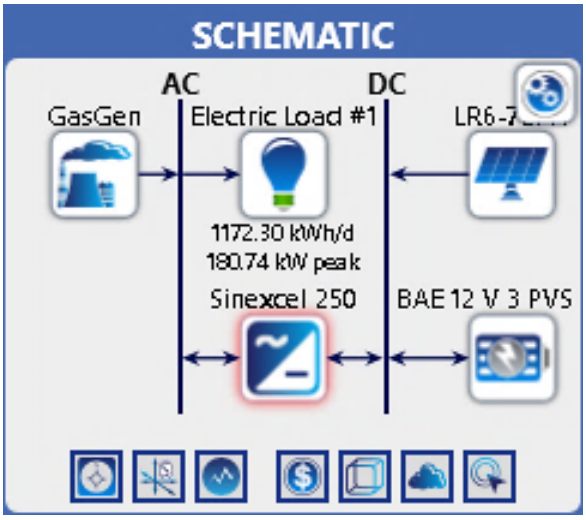

Figure 3.15. HOMER Pro-optimized HPS configuration.

The system is designed to enable unlimited power generation using PV modules, aiming to optimize the system's overall performance. HOMER Pro performed a total of 892 simulations, and the simulation results demonstrate that HOMER Pro presented different configurations using various combinations of available power sources. Table 3.4 presents the evaluation of optimized system configurations conducted by HOMER Pro. The optimal configuration selected includes PV panels, a converter, an energy storage system (ESS), which is a battery bank, and a natural gas genset, as it yields the least Net Present Cost (NPC) of USD 1.30 M and a cost of energy (COE) of USD 0.234, among all configurations. At the same time, the current actual cost of energy using only natural gas generators stands at USD 0.382. The optimal system also has the lowest annual operating cost of USD 63,253, which, in the present and actual cases, is USD 150,574, thus providing annual cost savings of USD 87,321.

Table 3.4. System optimization results in HOMER Pro.

System Architecture	PV (kW)	Gas Genset (kW)	ESS (No. of Batteries)	Converter (kW)	NPC (USD)	COE (USD)	Operating Cost (USD/Year)	Initial Capital (USD)
PV-Genset-ESS-Converter	282	200	280	190	1.30 M	0.234	63,253	479,414
Genset-ESS-Converter		200	140	66.8	1.85 M	0.335	125,403	229,611
Genset		200			2.11 M	0.382	150,574	165,350
PV-ESS-Converter	582		1260	201	2.12 M	0.383	95,462	881,476
PV-Genset-Converter	6.11	200		1.42	2.12 M	0.383	150,989	169,402

The optimized system, designed for a 25-year life cycle in HOMER Pro, is projected to have a net present cost (NPC) of USD 1.30 million. It would yield a levelized energy (COE) cost of USD 0.2345 per kWh and incur an annual operating cost of USD 63,252.93, as depicted in Table 4. The optimal system design achieves a 79.2% renewable energy fraction, significantly reducing the non-renewable fraction from 100% to just 20.8%. This addresses cost inefficiencies, as illustrated in Figure 3.16, which also depicts monthly electrical energy generation.

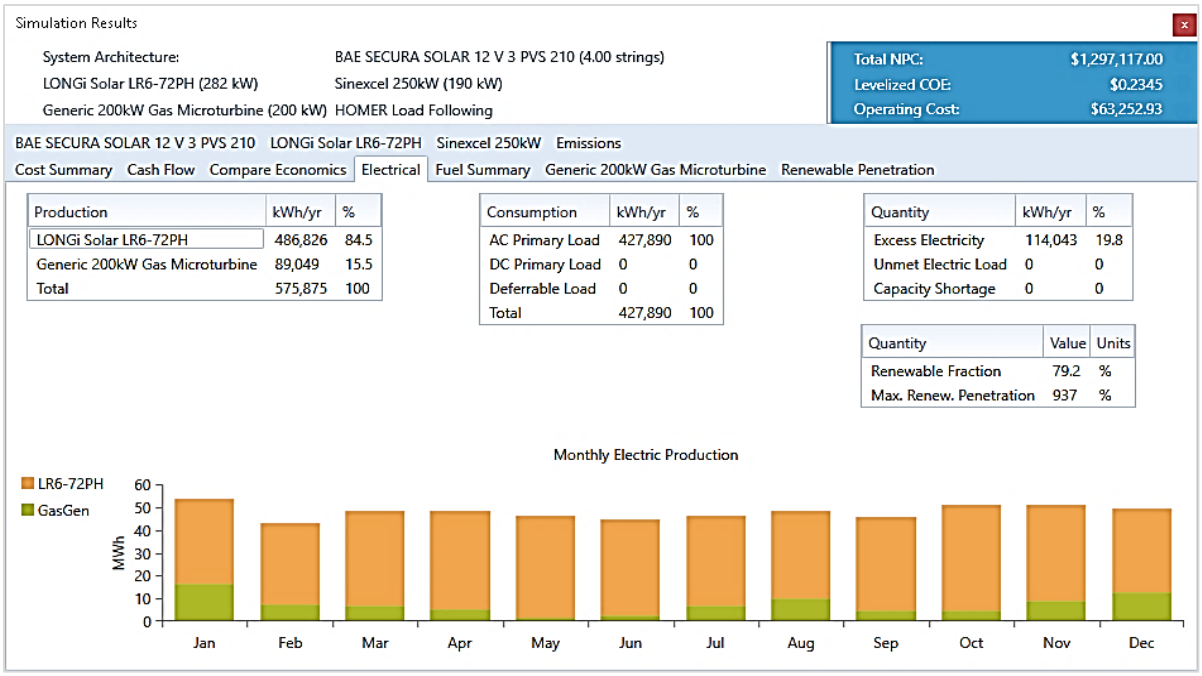

Figure 3.16. Electrical energy production results from optimal system.

The primary purpose of the natural gas generator is to serve as a backup power source when the primary PV system and battery bank cannot meet the load demands, primarily due to fluctuations in solar global horizontal irradiance (GHI) or during prolonged and severe weather conditions. The rest of this research paper focuses on dynamic modeling and analyzing the dynamic behavior of the proposed HPS using MATLAB.

3.5 Dynamic Modeling of Proposed HPS in MATLAB/SIMULINK

Dynamic modeling and simulation are necessary steps in analyzing the performance and behavior of any system. To examine the dynamic performance of the proposed hybrid power system, with a specific emphasis on power quality, voltage transients, and load impact, simulations are conducted using MATLAB/Simulink. Simulating a hybrid power system in MATLAB involves modeling key components like solar PV, generators, and batteries using Simulink and Simscape. Load profiles and renewable resource data are input to simulate real-world conditions. At the same time, control strategies manage the energy flow between renewable sources, conventional

generators, and storage to ensure balanced power delivery. Reliability and stability are tested by simulating different scenarios like load fluctuations and generator failures, and MATLAB's visualization tools track the system's performance over time.

To simulate the entire system for stable output, MATLAB ensures that energy from renewable sources and storage is optimally used to meet the load demand. The control algorithms balance generation and consumption, maintaining stability even when renewable input fluctuates or generators fail. By simulating the entire system under various conditions, the output is tested for consistency, ensuring the system can reliably meet the power needs of remote stations.

During this modeling process, careful consideration is given to the AM 1.5 spectrum, which is also known as Air Mass 1.5. It represents the average solar radiation reaching the earth's surface under standard conditions and accounts for the absorption and scattering of sunlight as it passes through the earth's atmosphere, providing a standardized reference for evaluating solar energy technologies. By incorporating the AM 1.5 spectrum into the simulation, the dynamic behavior of the hybrid power system can be accurately analyzed and optimized under realistic solar conditions. Hence, the initial value for irradiance is set at approximately 1000 watts per square meter (W/m2), reflecting standard solar radiation conditions. As for temperature, solar cell temperatures in the simulation may range from around 25 °C to 60 °C, representing typical operating conditions under sunlight exposure. The simulations cover a range of conditions tailored to the specific characteristics of the selected natural gas control station under discussion. The Simulink blocks used also incorporate the influence of real-time conditions, encompassing variations in solar irradiance, temperature, fluctuations in connected load, etc. Figure 3.17 displays the entire MATLAB/Simulink model, which is simulated to analyze the dynamic behavior of the proposed HPS.

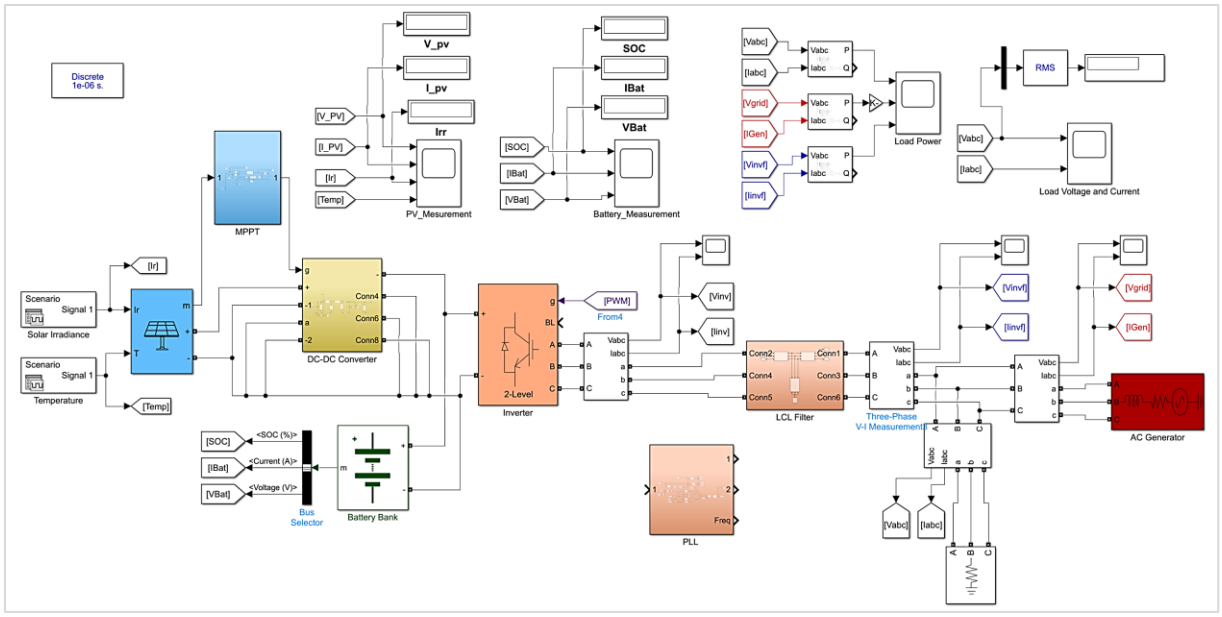

Figure 3.17. Dynamic model of proposed HPS in MATLAB/Simulink.

Figure 3.18 demonstrates how changes in the temperature and solar GHI affect the output voltage and current of the PV array, providing insight into the dynamic response of the PV component within the proposed HPS. Initially, the solar GHI value is set at 1000 W/m2 in accordance with the AM 1.5 spectrum, concurrently setting the temperature at 25 °C. This serves as the baseline condition. Subsequently, the solar GHI value is reduced from 1000 W/m2 to 400 W/m2, indicating a dip in GHI, and its impact on the PV output is observed. Likewise, the temperature gradually increases from 25 °C to 55 °C to evaluate its effect on the PV voltage and current. It is worth noting that higher temperatures typically lead to a decrease in voltage, while higher irradiance levels result in a greater output voltage from the PV array.

Figure 3.19 illustrates that the primary focus is prioritizing power flow from the PV system to the load, with any excess power being used to charge the battery bank. Initially, under a constant solar GHI and temperature in the simulation, the battery bank charges. However, in instances of a decreased solar GHI, the battery bank ceases charging and assumes a backup role, supplying power to the load.

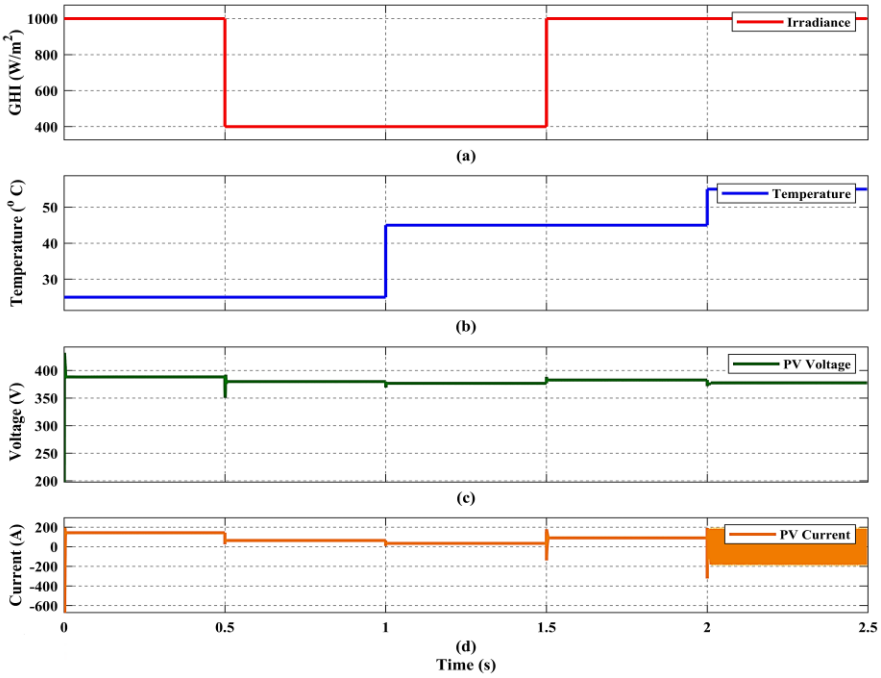

Figure 3.18. (a) Variable solar GHI. (b) Variable temperature. (c,d) PV panel output voltage and current due to varying input variables.

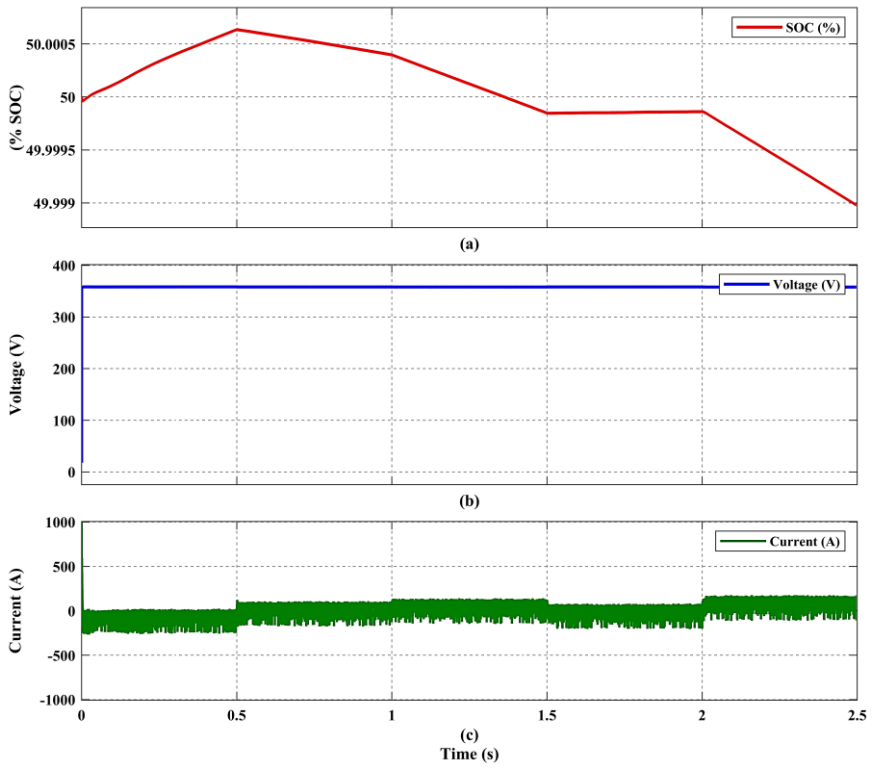

Figure 3.19. (a) Battery bank % state of charge. (b) Battery bank voltage. (c) Battery bank current

When the PV system output falls short of meeting the load requirement, the natural gas genset is used to supply the deficit, and any excess power is once again utilized to charge the battery bank. A phase-lock loop (PLL) is used to synchronize the natural gas genset and solar PV system, and it is sensitive to both frequency and phase. It operates as an electronic circuit incorporating a voltage or voltage-driven oscillator, continuously adapting to align with the frequency of an input signal. Hence, a stable three-phase output voltage and current are delivered to the connected load. Figure 3.20 shows the stable phase-to-ground voltage and current delivered to the connected load by the designed HPS.

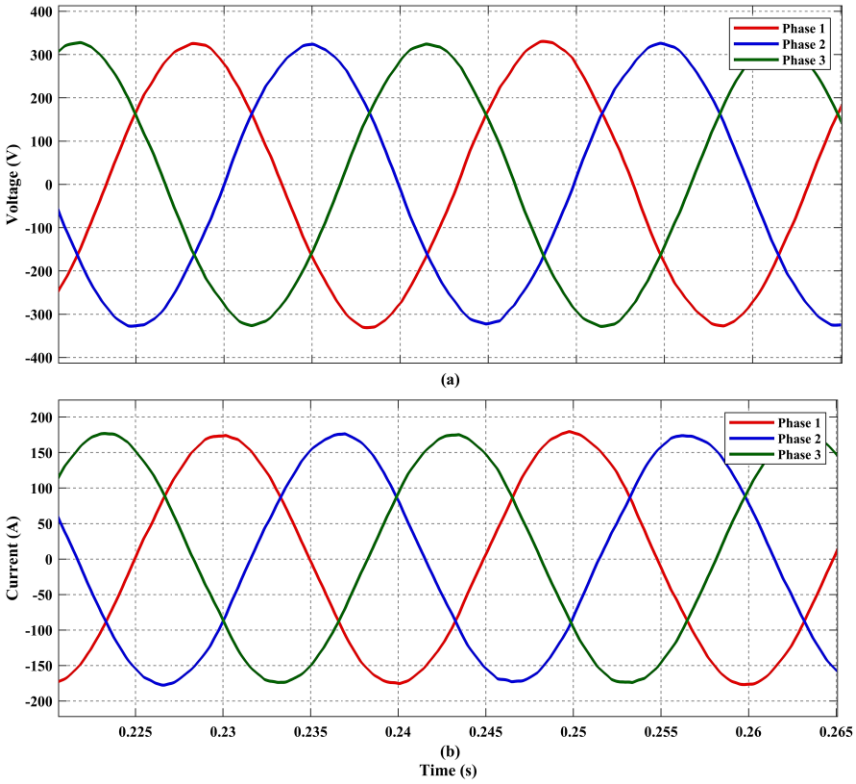

Figure 3.20. (a) Three-phase voltage (Vpeak) delivered to load. (b) Three-phase current delivered to load.

3.6 Experimental Results and Discussion

The real-time validation of a proposed hybrid power system is crucial for ensuring its reliability and efficiency in real-world applications. This validation process is facilitated by employing

Hardware-in-the-Loop (HIL) testing, which integrates physical hardware components with simulation models. OPAL-RT Technologies' high-performance realtime OP5707XG simulator plays a key role in this process by emulating real-world conditions and interactions. The OP5707XG is a comprehensive simulation system that operates on Virtex-7 FPGA platforms. As shown in Figure 3.21, it utilizes a combination of Intel processors to facilitate real-time computation to handle extensive models. Additionally, an FPGA is employed to achieve an ultra-fast loop time, enabling swift switching frequency in real-time simulations [34]. It enables closed-loop testing by continuously exchanging data between the simulation model and the hardware components, allowing engineers to evaluate the system's performance under various operating conditions and dynamic scenarios. Additionally, the simulator provides tools for fault injection, real-time visualization, and data analysis, empowering engineers to validate the system's designs and implement appropriate control strategies for optimal performance and reliability. This process confirms the robustness and proper functioning of the proposed system, as shown in Figure 3.8.

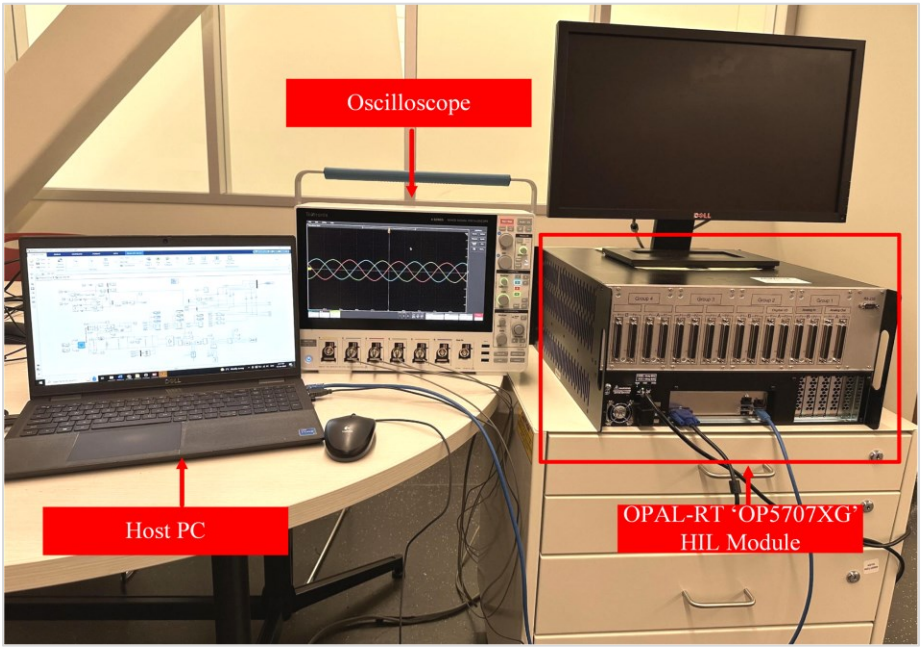

Figure 3.21. OPAL-RT real-time experimental setup.

The experimental results obtained from OPAL-RT Technologies' real-time OP5707XG simulator are displayed in Figures 3.22 and 3.23, which involve testing and validating a Simulink model. Running a Simulink model on OPAL-RT Technologies' OP5707XG simulator allows for the real-time validation of three-phase voltage and current waveforms. The results demonstrate the designed system's ability to maintain a stable three-phase power supply even amidst variations in the input parameters, such as the solar global horizontal irradiance, temperature, and changes in the output load. The stability exhibited by the system under diverse operating conditions underscores its robustness and suitability for powering a critical infrastructure, ensuring uninterrupted operation and reliability in energy supply. The results show that the load receives a steady three-phase voltage and current, validating the system's capability to supply reliable and consistent power to the selected control station for a natural gas pipeline as a case study.

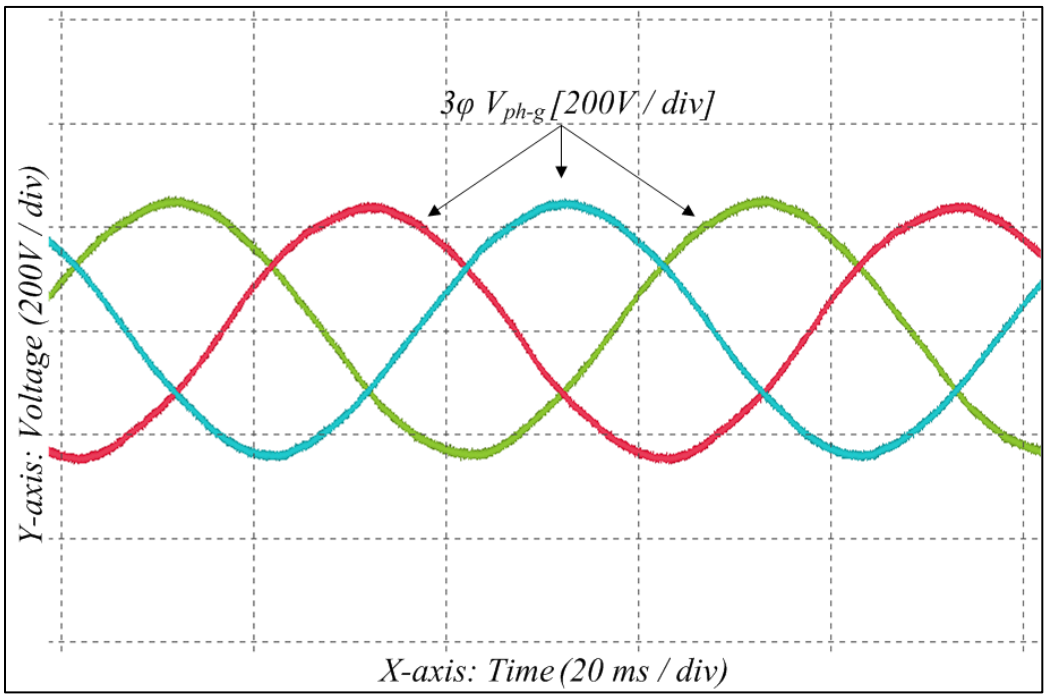

Figure 3.22. OPAL-RT experimental result for three-phase output voltage delivered to load.

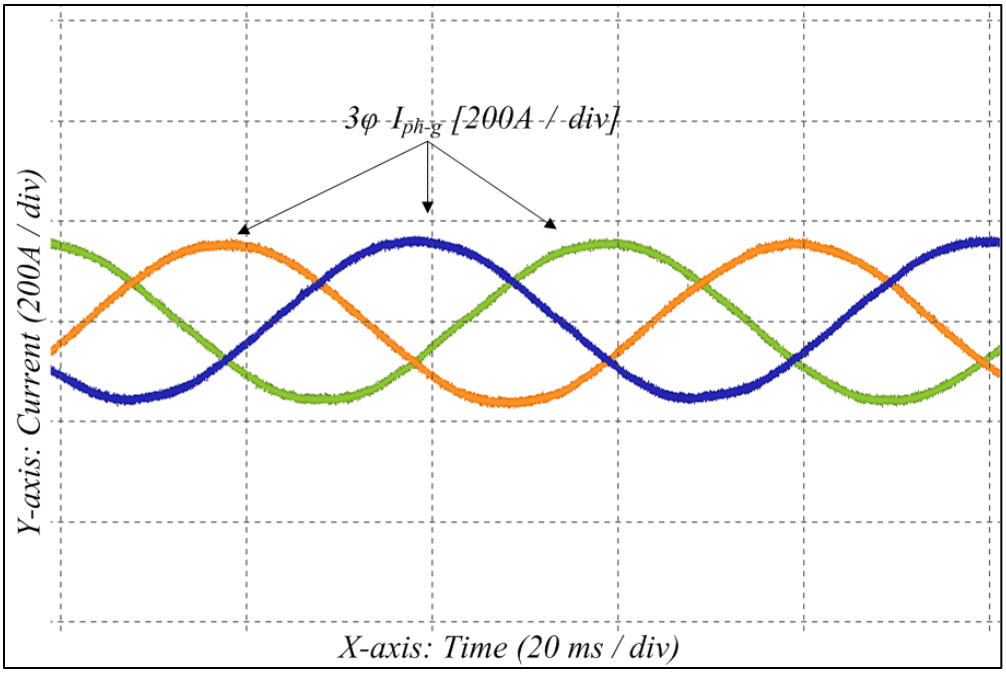

Figure 3.23. OPAL-RT experimental result for three-phase output current delivered to load.

3.7 Conclusions

In conclusion, this research article presents a novel approach to address the energy needs of remote natural gas pipeline control stations by designing and implementing a hybrid power system. This study underscores the importance of innovative energy solutions in remote locations and highlights the potential of hybrid power systems to provide a reliable and sustainable electricity supply for critical infrastructure. The proposed hybrid power system primarily comprises photovoltaic panels, a maximum power point tracking controller, a DC-AC inverter, a buck converter, a natural gas generator, a battery bank, and an electrical load. The optimal design is obtained using the HOMER Pro software, while the system's dynamic modeling is performed in the MATLAB/Simulink environment to evaluate its response. Subsequently, experimental validation is executed through Hardware-in-the-Loop simulation utilizing the real-time OPAL-RT Technologies' OP5707XG simulator. The main conclusions are as follows:

- Given the abundant solar global horizontal irradiance resource in Pakistan, solar photovoltaic systems play a predominant role in contributing to the hybrid power system's electricity supply. It addresses the unique energy demands of these facilities and underscores the financial benefits while aligning with broader energy sustainability goals.
- HOMER Pro performed a total of 892 simulations, and the designed optimal system features a 79.2% renewable energy fraction, reducing the non-renewable fraction from the prior 100% to only 20.8%, thereby addressing cost inefficiencies.
- The designed hybrid power system provides a cost of energy of USD 0.234, presenting noteworthy cost savings of USD 0.148 when compared to the current actual cost of energy, which stands at USD 0.382. Likewise, with an annual operating cost of USD 63,253, the system achieves significant savings of USD 87,321 compared to the current actual cost of USD 150,574.
- The dynamic modeling of an HPS coupled with experimental validation through Hardware-in-the-Loop and OPAL-RT Technologies' high-performance real-time OP5707XG simulator substantiates the comprehensive performance of the proposed system. This validation confirms the designed system's capability to supply reliable and consistent power and affirms the HPS's capability to fully satisfy the energy demands of control stations in remote areas, promising environmentally friendly and economical energy while contributing to the enhanced sustainability of energy infrastructure.

References

[1] Q. Li *et al.*, "Adsorption behavior and mechanism analysis of siloxane thickener for CO2 fracturing fluid on shallow shale soil," *Journal of Molecular Liquids*, vol. 376, pp. 121394–121394, Apr. 2023, doi: https://doi.org/10.1016/j.molliq.2023.121394.

[2] S. Ali *et al.*, "Evaluating Green Technology Strategies for the Sustainable Development of Solar Power Projects: Evidence from Pakistan," *Sustainability*, vol. 13, no. 23, p. 12997, Nov. 2021, doi: https://doi.org/10.3390/su132312997.

[3] F. Wang *et al.*, "Strategic design of cellulose nanofibers@zeolitic imidazolate frameworks derived mesoporous carbon-supported nanoscale CoFe2O4/CoFe hybrid composition as trifunctional electrocatalyst for Zn-air battery and self-powered overall water-splitting," *Journal of Power Sources*, vol. 521, pp. 230925–230925, Feb. 2022, doi: https://doi.org/10.1016/j.jpowsour.2021.230925.

[4] J. Anwar, "Analysis of energy security, environmental emission and fuel import costs under energy import reduction targets: A case of Pakistan," *Renewable and Sustainable Energy Reviews*, vol. 65, pp. 1065–1078, Nov. 2016, doi: https://doi.org/10.1016/j.rser.2016.07.037.

[5] E. Bergasse, W. Paczynski, M. Dabrowski, and L. De Wulf, "The Relationship between Energy and Socio-Economic Development in the Southern and Eastern Mediterranean," *SSRN Electronic Journal*, 2013, doi: https://doi.org/10.2139/ssrn.2233323.

[6] M. U. Etokakpan, S. A. Solarin, V. Yorucu, F. V. Bekun, and S. A. Sarkodie, "Modeling natural gas consumption, capital formation, globalization, CO2 emissions and economic growth nexus in Malaysia: Fresh evidence from combined cointegration and causality

analysis," *Energy Strategy Reviews*, vol. 31, p. 100526, Sep. 2020, doi: https://doi.org/10.1016/j.esr.2020.100526.

[7] T. Akhtar, A. U. Rehman, M. Jamil, and S. O. Gilani, "Impact of an Energy Monitoring System on the Energy Efficiency of an Automobile Factory: A Case Study," *Energies*, vol. 13, no. 10, p. 2577, May 2020, doi: https://doi.org/10.3390/en13102577.

[8] A. M. Shar, "Natural Gas Potential of Pakistan an Important Parameter in Mitigating Greenhouse Gas Emissions," *Pakistan Journal of Analytical & Environmental Chemistry*, vol. 21, no. 2, pp. 209–218, Dec. 2020, doi: https://doi.org/10.21743/pjaec/2020.12.23.

[9] IEA. Energy Statistics Data Browser—Data Tools. Available online: https://www.iea.org/data-and-statistics/data-tools/energystatistics-data browser?country=PAK&fuel=Energy%20supply&indicator=CoalProdByType (accessed on 31 March 2024).

[10] B. Guo, A. Ghalambor, "Natural Gas Engineering Handbook" Gulf Publishing Company: Houston, TX, USA, 2012; pp. 277–279.

[11] V. Fetisov *et al.*, "Development of the automated temperature control system of the main gas pipeline," *Scientific Reports*, vol. 13, no. 1, p. 3092, Feb. 2023, doi: https://doi.org/10.1038/s41598-023-29570-4.

[12] J. Gudmundsson, "Hydrate Non-Pipeline Technology For Transport Of Natural Gas La Technologie Du Transport Hors Pipe De Gas Naturel Sous Forme D'hydrates Resumé," 2003. Accessed: Aug. 01, 2024. [Online]. Available: https://citeseerx.ist.psu.edu/document?repid=rep1&type=pdf&doi=7203e7a462cb6198f0ece43b19b8ffa696dece14.

[13] L. Da Lio and A. Lazzaretto, "Remote Power Generation for Applications to Natural Gas

Grid: A Comprehensive Market Review of Techno-Energetic, Economic and Environmental Performance," *Energies*, vol. 15, no. 14, p. 5065, Jul. 2022, doi: https://doi.org/10.3390/en15145065.

[14] World Bank. Access to Electricity (% of Population)|Data. Worldbank.org. 2018. Available online: https://data.worldbank.org/indicator/eg.elc.accs.zs (accessed on 30 November 2023).

[15] H. A. Muqeet, H. M. Munir, H. Javed, M. Shahzad, M. Jamil, and J. M. Guerrero, "An Energy Management System of Campus Microgrids: State-of-the-Art and Future Challenges," *Energies*, vol. 14, no. 20, p. 6525, Oct. 2021, doi: https://doi.org/10.3390/en14206525.

[16] "Energy and Economy." Available: https://www.finance.gov.pk/survey/chapter_22/PES14-ENERGY.pdf

[17] "Rising LNG dependence in Pakistan is a recipe for high costs, financial instability, and energy insecurity," *ieefa.org*. https://ieefa.org/resources/rising-lng-dependence-pakistan-recipe-high-costs-financial-instability-and-energy.

[18] H. Javed, H. A. Muqeet, M. Shehzad, M. Jamil, A. A. Khan, and J. M. Guerrero, "Optimal Energy Management of a Campus Microgrid Considering Financial and Economic Analysis with Demand Response Strategies," Energies, vol. 14, no. 24, p. 8501, Dec. 2021, doi: https://doi.org/10.3390/en14248501.

[19] IEA. Annual Average Price of Electricity in Pakistan, 2019–2025—Charts—Data & Statistics. Available online: https://www.iea.org/data-and-statistics/charts/annual-average-price-of-electricity-in-pakistan-2019-2025 (accessed on 15 December 2023).

[20] L. Ahsan and M. Iqbal, "Dynamic Modeling of an Optimal Hybrid Power System for a

Captive Power Plant in Pakistan," *Jordan Journal of Electrical Engineering*, vol. 8, no. 2, p. 195, 2022, doi: https://doi.org/10.5455/jjee.204-1644676329.

[21] T. F. Agajie *et al.*, "A Comprehensive Review on Techno-Economic Analysis and Optimal Sizing of Hybrid Renewable Energy Sources with Energy Storage Systems," *Energies*, vol. 16, no. 2, p. 642, Jan. 2023, doi: https://doi.org/10.3390/en16020642.

[22] F. Hussain *et al.*, "Solar Irrigation Potential, Key Issues and Challenges in Pakistan," *Water*, vol. 15, no. 9, p. 1727, Jan. 2023, doi: https://doi.org/10.3390/w15091727.

[23] M. Deveci, U. Cali, and D. Pamucar, "Evaluation of criteria for site selection of solar photovoltaic (PV) projects using fuzzy logarithmic additive estimation of weight coefficients," *Energy Reports*, vol. 7, pp. 8805–8824, Nov. 2021, doi: https://doi.org/10.1016/j.egyr.2021.10.104.

[24] S. Herrería-Alonso, A. Suárez-González, M. Rodríguez-Pérez, R. F. Rodríguez-Rubio, and C. López-García, "A Solar Altitude Angle Model for Efficient Solar Energy Predictions," *Sensors*, vol. 20, no. 5, p. 1391, Mar. 2020, doi: https://doi.org/10.3390/s20051391.

[25] "Solar Azimuth Angle—An Overview|ScienceDirect Topics". Available online: https://www.sciencedirect.com/topics/engineering/solar-azimuth-angle (accessed on 2 January 2024).

[26] "apps.solargis.com. Solargis Prospect". Available online: https://apps.solargis.com/prospect/detail/scRwdD0kCL2vzMj1/info (accessed on 4 November 2023).

[27] G. T. Heydt, "Distribution Transformer Loading: Probabilistic Modeling and Diversity Factor," in *IEEE Transactions on Power Delivery*, vol. 38, no. 2, pp. 842-849, April 2023, doi: 10.1109/TPWRD.2022.3199999.

[28] R. Kahani, M. Jamil and M. T. Iqbal, "An Improved Perturb and Observed Maximum Power Point Tracking Algorithm for Photovoltaic Power Systems," in *Journal of Modern Power Systems and Clean Energy*, vol. 11, no. 4, pp. 1165-1175, July 2023, doi: 10.35833/MPCE.2022.000245.

[29] "Solaris. Longi Solar HiMO1 LR6-72PH-365M 365w Mono Solar Panel". Available online: https://www.solaris-shop.com/longisolar-himo1-lr6-72ph-365m-365w-mono-solar-panel/ (accessed on 27 March 2024).

[30] L. Martin, P. Vladislav, and K. Pavel, "Temperature changes of I-V characteristics of photovoltaic cells as a consequence of the Fermi energy level shift," *Research in Agricultural Engineering*, vol. 63, no. No. 1, pp. 10–15, Mar. 2017, doi: https://doi.org/10.17221/38/2015-rae.

[31] Y. Cai, Y. He, H. Zhou and J. Liu, "Design Method of LCL Filter for Grid-Connected Inverter Based on Particle Swarm Optimization and Screening Method," in *IEEE Transactions on Power Electronics*, vol. 36, no. 9, pp. 10097-10113, Sept. 2021, doi: 10.1109/TPEL.2021.3064701.

[32] A. Reznik, M. G. Simões, A. Al-Durra and S. M. Muyeen, "LCL Filter Design and Performance Analysis for Grid-Interconnected Systems," in *IEEE Transactions on Industry Applications*, vol. 50, no. 2, pp. 1225-1232, March-April 2014, doi: 10.1109/TIA.2013.2274612.

[33] L. O. Aghenta and M. T. Iqbal, "Design and Dynamic Modelling of a Hybrid Power

System for a House in Nigeria," *International Journal of Photoenergy*, vol. 2019, pp. 1–13, Apr. 2019, doi: https://doi.org/10.1155/2019/6501785.

[34] "Flagship Real-Time Digital Simulator|Simulation Tools|OP5707XG", OPAL-RT. Available online: https://www.opalrt.com/simulator-platform-op5707/ (accessed on 22 January 2024).

Chapter 4: Power Quality Improvement Using Nine-Level Cascaded H-Bridge Voltage Source Inverter for PV Applications

Preface

A version of this manuscript has been accepted and presented at the 12th IEEE International Conference on Smart Grid (ICSmart Grid 2024) Setubal, Portugal, and the full paper is published and available on IEEE Xplore database. As the primary author, I led the research efforts, including literature reviews, system design, modeling, and results analysis. I drafted the initial manuscript and revised it based on feedback from the co-authors and the peer review process. Dr. Mohsin Jamil, my research supervisor, provided research supervision and guidance, reviewed and corrected the manuscript, and contributed valuable research ideas throughout its development.

Abstract

Multilevel Inverters (MLI) are widely embraced in renewable energy applications such as photovoltaic (PV) solar systems and wind due to their compatibility with distributed generation. This article focuses on designing symmetrical cascaded H-Bridge Voltage Source Inverter (VSI) topologies, with up to nine levels, using Sinusoidal Pulse Width Modulation (SPWM). A comparison is made with a conventional two-level inverter under resistive and resistive-inductive load conditions. The simulation of multilevel inverter topologies is performed in the MATLAB/Simulink environment. As the number of voltage levels increases, the generated waveform gradually approximates a sinusoidal shape, which leads to a reduction in Total Harmonic Distortion (THD) and improved power quality. The experimental validation of the designed multilevel inverter is conducted using Hardware-in-the-Loop (HIL) testing.

4.1 Introduction

Fossil fuels have been the primary source of global energy demand for an extended duration. Nonetheless, their fast depletion and environmentally detrimental characteristics have prompted the emergence of renewable energy sources like wind, solar, biomass, and others. These renewable alternatives have gained popularity as they offer both environmental benefits and a limitless supply, making them a highly desirable solution. With a few exceptions, most existing renewable energy technologies produce direct current (DC) electricity. Electrical energy generation through photovoltaic technology has witnessed steady growth in the past few decades. Solar energy is the renewable energy source experiencing a surge in adoption due to its numerous benefits, including cleanliness, lack of pollution, lower maintenance cost, durability, and wide accessibility. Nevertheless, our power usage primarily relies on an alternating current (AC) supply system, while solar energy produces direct current (DC) output. Thus, to bridge this gap, a dependable conversion mechanism becomes necessary [1]. Power electronic converters regulate power flow and transform it into the appropriate DC or AC form as needed. Within solar photovoltaic (PV) systems, the relatively low output voltage produced by PV panels is elevated to a higher level through the implementation of a DC-DC boost converter. The elevated DC-link voltage is subsequently directed to an inverter, which produces the necessary alternating current (AC) voltage with the desired magnitude and frequency [2]. An inverter is an electronic device that converts DC power into AC power at the required voltage and frequency level making use of appropriate switching patterns and control strategy. A two-level inverter is a conventional power electronic device that generates an output voltage or current at two different (±) levels. In the past, a two-level conventional inverter was used to provide an output that was almost square and had both lower- and higher-order harmonics. Passive filters might be used to reduce these harmonics. However,

because the required inductors and capacitors are expensive and huge, it is not desirable to employ passive filters to remove the lower-order harmonics. This two-level conventional inverter has large switching losses, runs at a high switching frequency, and is limited in terms of its rating for high power and voltage applications. It also experiences significant stress, Electromagnetic interference (EMI), and harmonic distortion. By employing a new architecture of multi-level inverter, these issues can be solved.

In the evolving landscape of inverter development, the concept of multi-level inverter was initially introduced in 1975 by R. H. Baker and L. H. Bannister [3]. It is possible to increase the power rating of the inverter while lowering the device rating by adding a greater number of voltage levels. A multi-level inverter generates a continuous sinusoidal waveform by utilizing multiple DC voltage levels as its input. MLIs are becoming increasingly popular as an alternative to two-level inverters due to their numerous benefits. These advantages encompass reduced harmonic distortion, simplified filters, improved waveform capabilities resulting in sinusoidal outputs, and decreased voltage stress (dv/dt) on switches. Owing to their ability to ensure exceptional power quality, MLIs find extensive utility across diverse areas of electrical engineering. These areas include but are not limited to high voltage DC transmission, renewable energy conversion, distributed generation (DG) systems, uninterruptible power supplies, and more [4]. Multilevel Inverters (MLIs) are divided into two categories: Current Source Inverters (CSI) and Voltage-Source Inverters (VSI). Current source inverters can lead to a substantial fault current in case of a short circuit within the circuit, potentially causing damage to other connected equipment. As a result, multilevel voltage source inverters are favored due to their advantages [5].

4.2 System Overview

A photovoltaic system primarily consists of a PV array, DC-DC converter, and DC-AC inverter.

A typical structure of a two-stage single-phase PV system is shown in Figure 4.1. A photovoltaic (PV) panel operates by converting sunlight into electricity through the photovoltaic effect, which encompasses the generation of electric current and voltage within a material upon sunlight exposure. A PV panel consists of numerous solar cells that are interconnected in a particular configuration to attain the targeted voltage and current output.

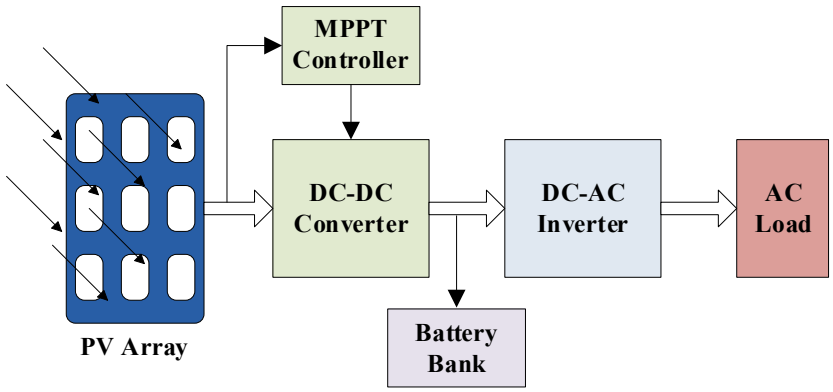

Figure 4.1. Single phase two-stage PV system

4.3 Multilevel Inverter Topologies

There are 3 main topologies for conventional multilevel inverters which are diode clamped/neutral point clamped (NPC), flying capacitor (FC), and cascade H-bridge (CHB) multilevel inverter as shown in Figure 4.2.

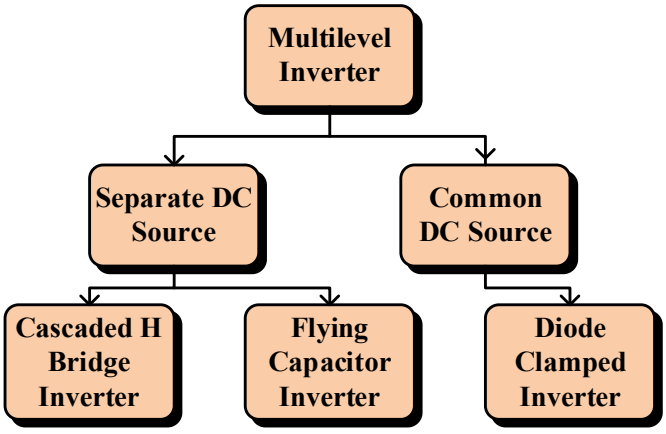

Figure 4.2. Classification of Multilevel Inverter Topologies

The NPC-MLI utilizes an array of diodes, with the quantity increasing as the desired output voltage level rises, resulting in higher costs. Similarly, in the FC-MLI, a higher output voltage level necessitates more storage capacitors. Conventional MLIs have found widespread use in various applications for generating specific output voltage levels, typically up to five levels. However, achieving a higher-level output voltage waveform entails an increase in the number of required components. Furthermore, to achieve capacitor voltage balancing in diode clamped and FC-MLIs, a sophisticated control algorithm is required [6].

The Cascaded H-Bridge Multi-Level Inverter (CHB-MLI) is the multilevel inverter topology that involves connecting multiple H-bridge cells in series, each with isolated DC voltage sources. The number of cascading cells required depends on the desired number of voltage levels or the acceptable percentage of voltage Total Harmonic Distortion (THD). Among the three conventional MLI types, the CHBMLI stands out with the fewest number of elements, resulting in lower overall cost. However, a notable drawback of the CHB-MLI is the necessity to add a new voltage source as the required level increases.

4.4 Cascaded H-Bridge Multilevel Inverter

Cascaded inverters utilize an isolated Direct Current (DC) source, which enables integration with diverse nonconventional energy sources like PV cells and fuel cells. In comparison to other multilevel inverter designs, they attain an equivalent number of voltage levels while utilizing a minimal number of components. Clamping diodes or voltagebalancing capacitors are unnecessary in cascaded inverters. Each level employs the same construction plan and packaging, facilitating optimization. Furthermore, due to the utilization of soft-switching techniques, cascaded inverters can significantly reduce switching losses and device stresses. A single H bridge inverter consisting of four semiconductor switches is shown in Figure 4.3.

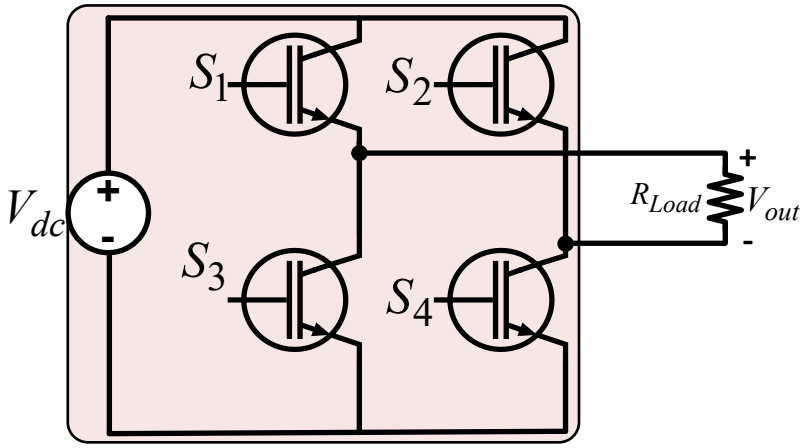

Figure 4.3. Single Phase Two and Three Level H-Bridge Inverter

This specific cell, consisting of one H bridge can produce an output voltage of two and three levels and is also known as a single-phase voltage source inverter. The cascaded H-bridge multilevel inverter (CHB- MLI) is formed by connecting a series of 'n' H-bridges or single-phase full-bridge inverters. Each of these H-bridge structures has its own distinct DC source. Cascaded Multilevel Inverters (MLI) can be configured to operate in symmetrical or asymmetrical configurations. In a symmetrical setup, the input DC source for each H-bridge has equal magnitude while in the case of an asymmetrical setup, the magnitude of input DC sources for H-bridges used is unequal. In the case of asymmetrical configuration, the input DC sources for H-bridges can be used either in 1:2 configuration or 1:3 configuration to generate different voltage levels and by combining different voltage levels more output levels can be generated as compared to symmetrical configuration [7]. The primary drawback of an asymmetrical configuration is that it compromises the modularity of the inverter, as the input DC sources have different magnitudes. Consequently, when the input DC source rating for H-bridge is increased, the power rating of the control switches in H-bridge must also be elevated. This necessitates several alterations in the design, which may not be appealing to industries that prioritize mass-scale production.

4.4.1 Symmetrical Cascaded H-Bridge MLI

In the symmetrical configuration of MLI, all the input DC sources have equal magnitude. The inverter's output is the sum of each H-bridge's output voltage, interconnected in a cascading arrangement. Hence, to generate an n-level output voltage from cascaded H-bridge VSI, the n-number of H-bridges with separate DC sources are connected in a series manner as shown in Figure 4.4. All Voltage Source Inverters (VSIs) can generate voltage levels of 0, +Vdc, and -Vdc. Hence, in a proportional relationship, if there are 'N_{sr}' counts of bifurcated DC sources, the number of levels in inverter output 'N_{lev}' is given as

$$N_{lev} = 2N_{sr} + 1 \tag{4.1}$$

The expressions for number of switches 'N_s', number of Direct Current (DC) sources 'N_{sr}' required, output voltage of inverter 'V_{out}' and peak voltage '$(V_{out})_{max}$' are given as

$$N_s = (N_{lev} * 2) - 2 \tag{4.2}$$

$$N_{sr} = \frac{(N_{lev} - 1)}{2} \tag{4.3}$$

$$V_{out} = V_{HB1} + V_{HB2} + V_{HB3} + ... + V_{HBn} \tag{4.4}$$

$$(V_{out})_{\max} = V_{dc} \sum_{k=1}^{N_{sr}} k = N_{sr}(V_{dc}) \tag{4.5}$$

As Symmetrical MLIs consist of multiple H-bridge inverters connected in a cascaded or series configuration, each H-bridge is responsible for generating a portion of the output voltage, and by combining the outputs of all the H-bridges, a high-quality symmetrical AC output voltage is achieved. According to the above-given expressions, the circuit diagrams for five-level, seven-level, and nine-level inverters are shown in Figure 4.4, Figure 4.5, and Figure 4.6 respectively.

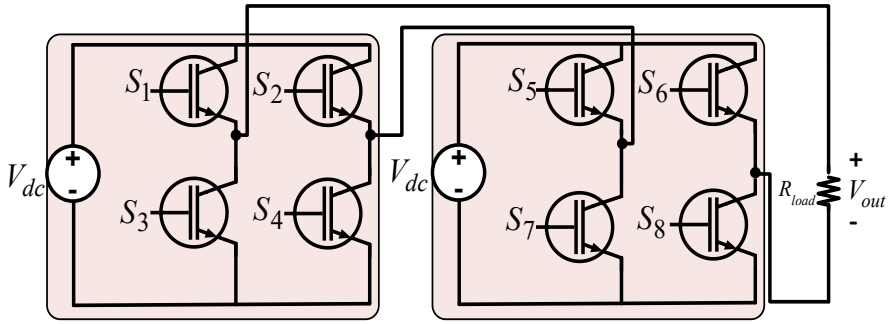

Figure 4.4. Single Phase Five Level CHB-MLI

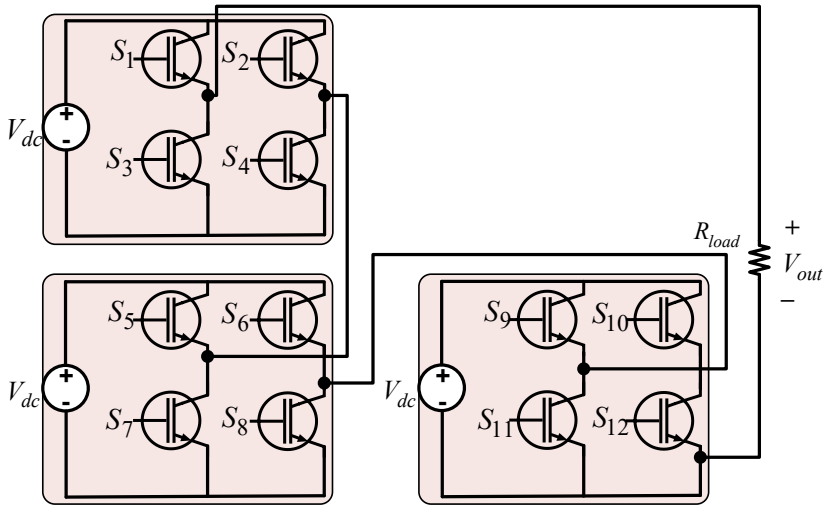

Figure 4.5. Single Phase Seven Level CHB-MLI

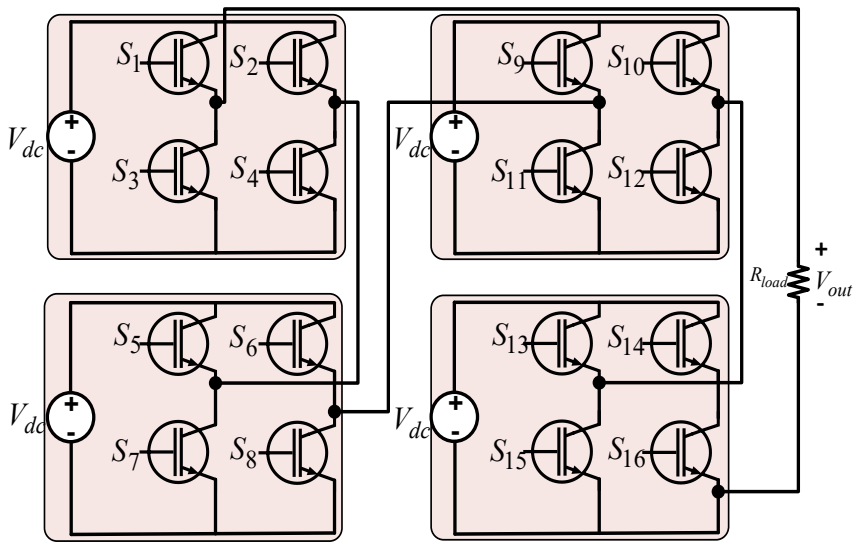

Figure 4.6. Single Phase Nine Level CHB-MLI

The selection of switches for a Multilevel Inverter (MLI) is a critical aspect of its design, and it depends on several factors including the desired output voltage levels, the power rating of the inverter, switching frequency, cost considerations, and the specific application requirements. The most used switches for multilevel inverters are Metal Oxide-Semiconductor Field-Effect Transistors (MOSFET) and Insulated Gate Bipolar Transistors (IGBT). Although an Insulated Gate Bipolar Transistor (IGBT) offers a high-power rating and can handle high voltage stress, its complex gate driver design renders it unsuitable for high-frequency operations. Conversely, a MOSFET is well-suited for high-frequency operation but falls short in terms of power rating when compared to an IGBT [8].

MOSFETs have bidirectional current conduction inherent to their design, while IGBTs require anti-parallel diodes to allow current flow in the reverse direction. Compared to diodes, MOSFETs exhibit lower conduction losses. Consequently, in a MOSFET-based configuration, the antiparallel diode operates solely during dead-time to prevent shoot-through currents. In contrast, in an IGBT-based system, the anti-parallel diode serves as the negative current path for the IGBT. Because of this difference, an inverter based on MOSFETs has a lower total conduction loss than one based on IGBTs. Recent advancements in GaN devices and SiC transistors have broadened the selection of transistors available for high voltage and high current applications. [9]. SiC and GaN MOSFETs available in the market typically have voltage ratings of 1700V and 650V, respectively. While it's feasible to increase the voltage rating by connecting multiple GaN MOSFETs and SiC in series, this method leads to increased complexity, power loss, costs, and decreased reliability. Despite GaN devices offering higher efficiency, the ability for higher switching frequencies and increased power density, commercially available GaN MOSFETs currently have a limitation of 60A. Consequently, using multiple switches in parallel becomes essential to accomplish a higher

current-handling capability [10]. In this research article, a conventional 2-level is compared with 5-level, 7-level, and 9-level symmetrical cascaded H-bridge inverter topologies for both resistive (R) loads and resistive-inductive (RL) loads. The analysis includes an examination of the Total Harmonic Distortion (THD) of the output voltage obtained.

4.5 Control And Modulation System

The control and modulation system for inverters plays a pivotal role in ensuring efficient and reliable operation. Different modulation techniques are used by the multilevel inverter to produce the required sinusoidal output. To obtain a regulated inverter output voltage, modulation is the process of adjusting the on and off time of inverter switches while keeping a constant input DC voltage. The control circuitry diagram for the multilevel inverters is shown in Figure 4.7.

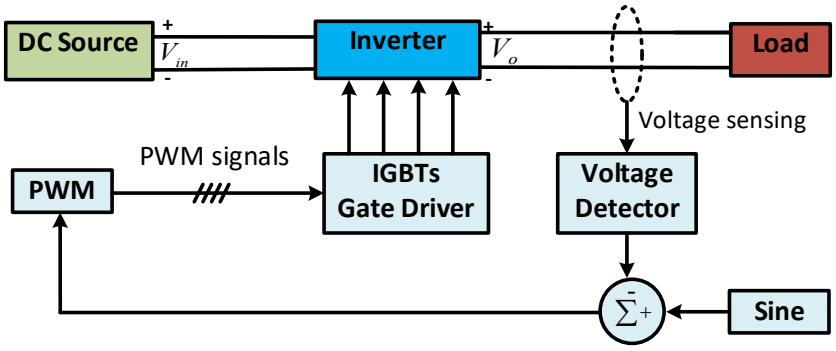

Figure 4.7. Control circuit block diagram of the MLI.

To obtain the desired output voltage level, a proper switching sequence is required which will switch on specific switches for a specific interval to achieve the desired voltage level. Besides the switching sequence, the pulse generator parameters for switches, which define the delay and pulse width for each switch are another important aspect of achieving the desired voltage level [11].

To obtain switching sequence and pulse generator parameters, various techniques are used. Pulse width modulation (PWM) is the most often utilized modulation technology for inverters. This method requires comparing the carrier signal and reference waveform. Sinusoidal Pulse Width

Modulation (SPWM) is extensively used for its numerous advantages, such as ease of understanding, straightforward implementation, lower switching losses, and reduced harmonic content in the output. In SPWM, two primary signals are utilized: the modulating signal and the carrier signal. Since the modulating signal is typically a pure sinusoidal waveform, it allows for the application of techniques like selective harmonic injection, dead band, and others to further enhance the performance [12].

$$mf = \frac{f_{\text{carrier}}}{f_{\text{modulation}}} \tag{4.6}$$

Where $f_{carrier}$ is carrier wave frequency and $f_{modulation}$ is the frequency of modulation wave.

In this technique, the modulating wave and the carrier wave are compared using a relational operator. This comparison creates a gating signal known as the parent signal. This general approach makes it possible to get the needed pulse. The working of the PWM modulation technique is shown in Figure 4.8.

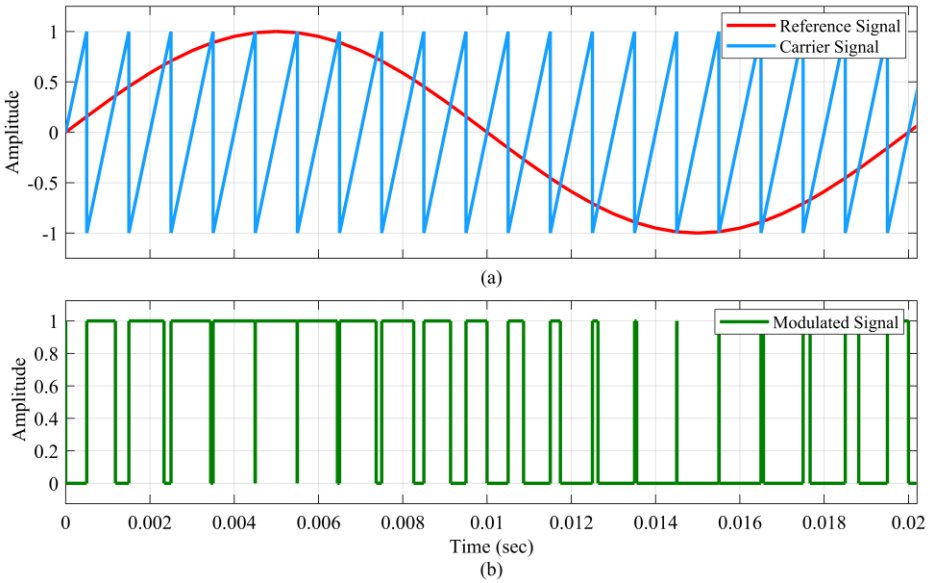

Figure 4.8. PWM Technique (a) Comparison of carrier signal and reference signal (b) Generated modulated signal.

At each instant in time, the instantaneous value of the reference sinusoidal signal is compared to the value of the carrier signal. The width (duration) of the pulses in the carrier signal is modulated based on the comparison between the carrier signal and the reference sinusoidal signal. When the instantaneous value of the carrier signal is higher than the reference value, the pulse is turned on. When the carrier signal value is lower, the pulse is turned off.

4.6 Simulation Results and Analysis

To affirm the theoretical analysis, all inverter configurations under discussion, coupled with SPWM control technique, are simulated using MATLAB/Simulink, validating the operational effectiveness of various multilevel inverters. Simulation studies are carried out using IGBT switches-based multilevel inverters to analyze the effect on the efficiency of inverters. The four inverter topologies including conventional TLI, 5-level, 7-level, and 9-level symmetric CHB MLIs are simulated with the same resistive (R) and resistive inductive (RL) load conditions to judge the performance of the inverter using THD analysis. Total Harmonic Distortion (THD) quantifies the level of distortion present in an electrical parameter, such as voltage or current, in relation to the ideal, desired output. It reflects the presence of different frequency components within the voltage or current waveform. Figure 4.9, Figure 4.10, Figure 4.11, and Figure 4.12 present simulation results for conventional TLI, 5-level, 7-level, and 9-level symmetrical CHB MLI respectively.

In their research, Mehlmann et al. [13] introduced a mathematical equation for theoretically computing voltage Total Harmonic Distortion (THD) without the requirement of complex Fourier Analysis. The resulting % THD value is presented by equation (10)

$$\%THD = \frac{1}{\sqrt{3}(N_{lev} - 1)m_i} \tag{4.7}$$

Table 4.1 summarizes the simulation results of % THD for four inverter topologies being examined.

Table 4.1. % THD analysis of Conventional TLI and CHB MLI

Parameter	Conventional 2-level inverter	5-level inverter	7-level inverter	9-level inverter
'R' load	37.38	27.92	21.59	17.75
'RL' load	47.85	29.04	21.67	18.21

It can be analyzed from the above-given table that the influence of resistive loads and resistive-inductive (RL) loads on inverter THD levels varies notably. Inverters linked to purely resistive loads usually display reduced THD because they avoid introducing phase shifts between voltage and current, thereby minimizing harmonic distortion. Conversely, RL loads, featuring an inductive element, tend to elevate THD levels due to the phase disparities between voltage and current. Ensuring the effective operation of inverters in practical applications when dealing with RL loads necessitates careful design and sizing, as well as the incorporation of filters or advanced control techniques to counteract THD effects.

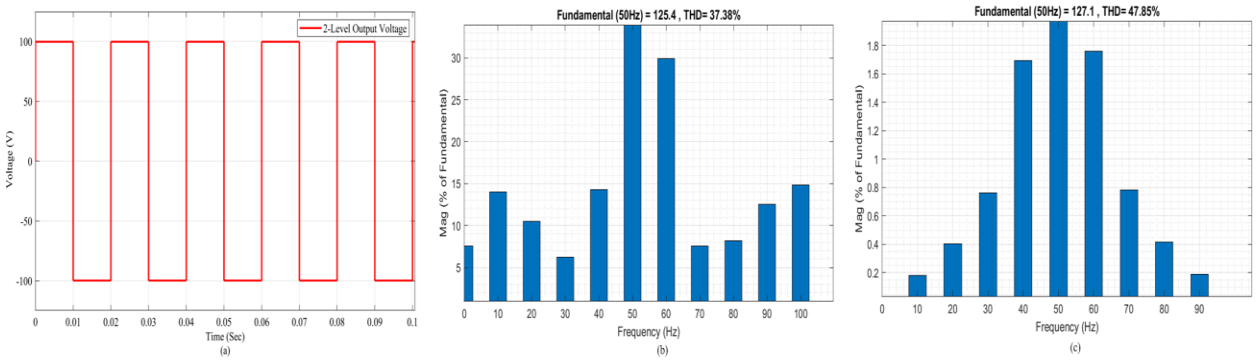

Figure 4.9. Simulation results for 2-level inverter (a) 2-level output voltage (b) % THD analysis for resistive load (c) % THD analysis for resistive inductive load.

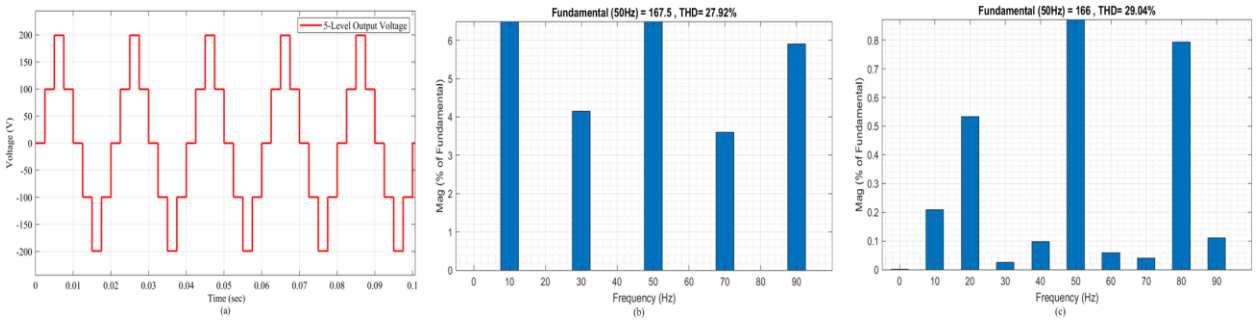

Figure 4.10. Simulation results for 5-level inverter (a) 5-level output voltage (b) % THD analysis for resistive load (c) % THD analysis for resistive inductive load.

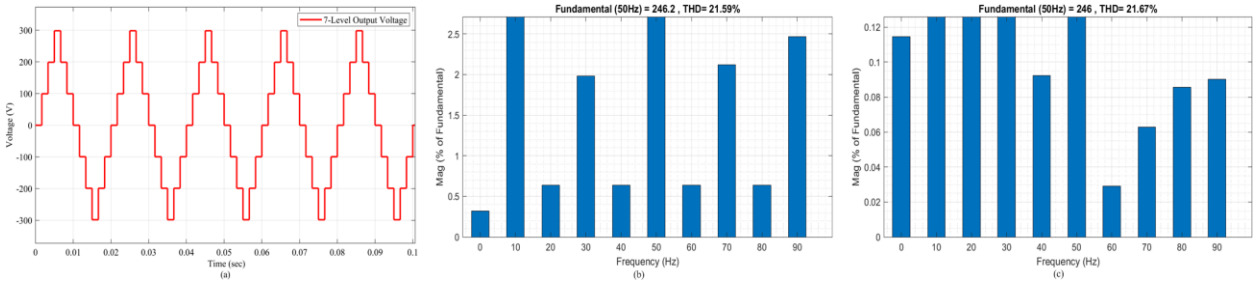

Figure 4.11. Simulation results for 7-level inverter (a) 7-level output voltage (b) % THD analysis for resistive load (c) % THD analysis for resistive inductive load.

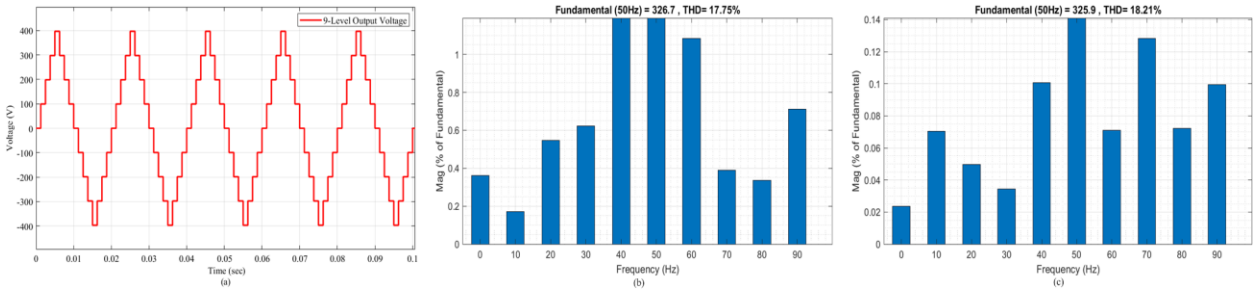

Figure 4.12. Simulation results for 9-level inverter (a) 9-level output voltage (b) % THD analysis for resistive load (c) % THD analysis for resistive inductive load.

It is evident that as the number of levels in MLI output voltage increases, THD decreases. Hence, MLIs outperform conventional inverters by delivering stepped voltage waveforms that mimic sinusoidal shapes, resulting in lower harmonic distortion and better voltage regulation. Their

capacity to generate higher output voltages, coupled with reduced switching losses and improved efficiency, proves advantageous for applications requiring stable power supply and efficient energy conversion.

4.7 Experimental Validation

To confirm the simulation results, real-time validation of a 9-level CHB inverter is performed. This validation utilizes Hardware-in-the-Loop (HIL) testing, which involves integration of MATLAB Simulink models with physical hardware. The process relies on OPAL-RT Technologies' OP5707XG simulator, operating on Virtex-7 FPGA platforms. In this system, as depicted in Figure 4.13, real-time computation is handled by Intel processors, while an FPGA ensures ultra-fast loop time, facilitating rapid switching frequency in simulations. This setup facilitates experimental testing through a continuous exchange of data between the simulation model and hardware components. [14].

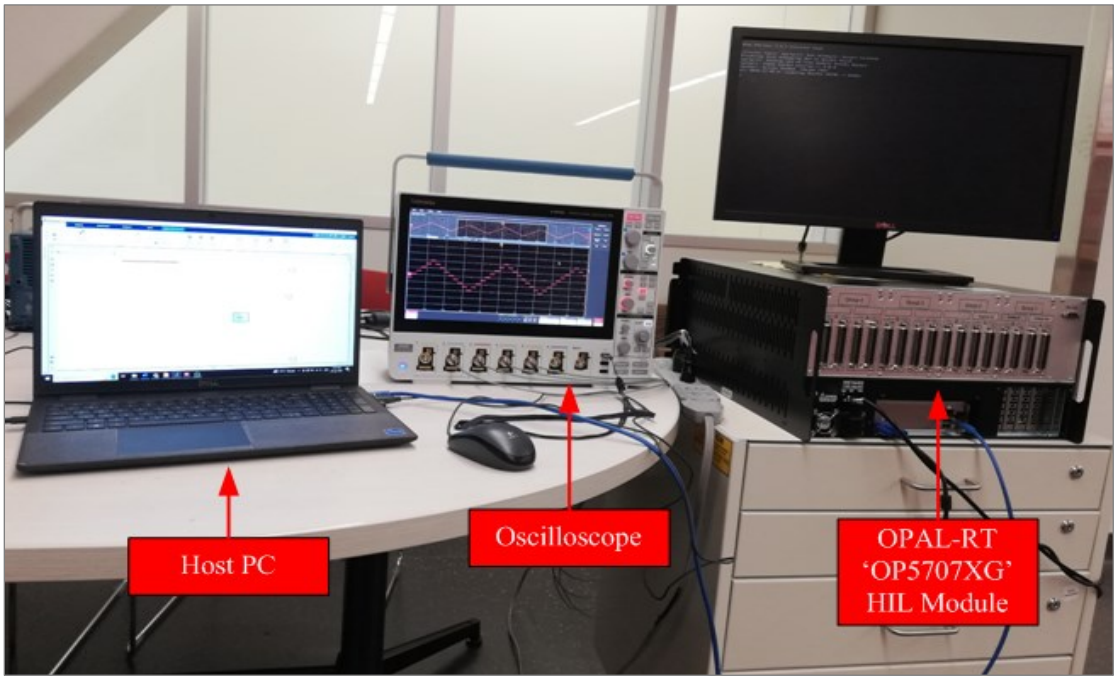

Figure 4.13.OPAL-RT Real-Time Experimental Setup

The experimental outcomes derived from OPAL-RT Technologies' real-time OP5707XG simulator are showcased in Figure 4.14.

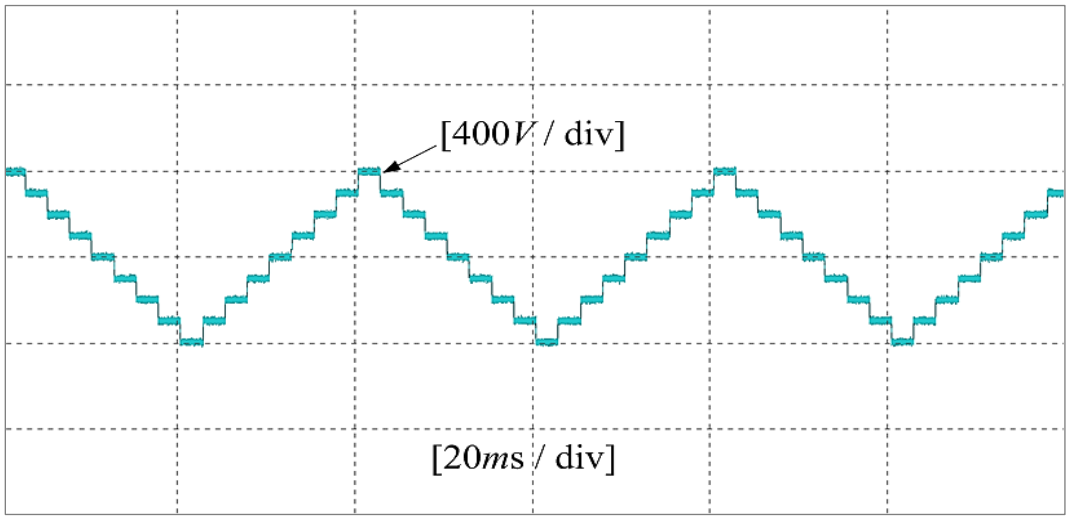

Figure 4.14. 9-level output voltage experimental result obtained from HIL

A steady output voltage of 400 volts from the 9-level inverter demonstrates its effectiveness in converting DC input into AC power at the desired level. This highlights its applicability in sectors requiring precise voltage control, like renewable energy, motor drives, and power grids. Furthermore, maintaining a consistent 400-volt output reflects the efficacy of the inverter's control algorithms, ensuring smooth operation and accurate voltage regulation across different loads, thereby boosting system performance and reliability.

4.8 Conclusion

In conclusion, this article has presented a comprehensive comparison of the design and analysis of a conventional two-level inverter with voltage source CHB MLIs up to nine levels. The investigation into multilevel inverter topologies highlighted their significance in addressing challenges associated with harmonic distortion, voltage quality, and energy efficiency. Through simulation studies and performance evaluations conducted based on THD using Fast Fourier

Transform (FFT) in MATLAB/Simulink, the viability and advantages of the multilevel inverter were established. Additionally, the experimental validation of nine-level CHB-MLI is performed using HIL and OPAL-RT real-time OP5707XG simulator. The results highlight the capability of Multilevel Inverters (MLI) to improve power conversion across a range of applications, including photovoltaic (PV) systems, renewable energy integration, and grid-connected systems.

References

[1] L. Wang, Q. H. Wu and W. Tang, "Novel Cascaded Switched-Diode Multilevel Inverter for Renewable Energy Integration," in *IEEE Transactions on Energy Conversion*, vol. 32, no. 4, pp. 574-1582, Dec. 2017, doi: 10.1109/TEC.2017.2710352.

[2] P. Manoj, A. Kirubakaran and V. T. Somasekhar, "An Asymmetrical Dual Quasi-Z-Source Based 7-Level Inverter for PV Applications," in *IEEE Transactions on Energy Conversion*, vol. 8, no. 2, pp. 1097- 1107, June 2023, doi: 10.1109/TEC.2022.3222498.

[3] Z. E. Abdulhamed, A. H. Esuri, N. A. Abodhir, M. N. A. Ghamudi and F. A. Azreeq, "Practical Implementation of a "Modified Hybrid Bridge Multi-level Inverter," *2022 IEEE 2nd International Maghreb Meeting of the Conference on Sciences and Techniques of Automatic Control and Computer Engineering (MI-STA)*, Sabratha, Libya, 2022, pp. 663- 667, doi: 10.1109/MI-STA54861.2022.9837639.

[4] C. Dhanamjayulu, S. R. Khasim, S. Padmanaban, G. Arunkumar, J. B. Holm-Nielsen and F. Blaabjerg, "Design and Implementation of Multilevel Inverters for Fuel Cell Energy Conversion System," in *IEEE Access*, vol. 8, pp. 183690-183707, 2020, doi: 10.1109/ACCESS.2020.3029153.

[5] E. Babaei, S. Laali and Z. Bayat, "A Single-Phase Cascaded Multilevel Inverter Based on a New Basic Unit With Reduced Number of Power Switches," in *IEEE Transactions on Industrial Electronics*, vol. 62, no. 2, pp. 922-929, Feb. 2015, doi: 10.1109/TIE.2014.2336601.

[6] M. A. Al-Hitmi, M. R. Hussan, A. Iqbal and S. Islam, "Symmetric and Asymmetric Multilevel Inverter Topologies With Reduced Device Count," in *IEEE Access*, vol. 11, pp. 5231-5245, 2023, doi: 10.1109/ACCESS.2022.3229087.

[7] C. Dhanamjayulu and S. Meikandasivam, "Implementation and Comparison of Symmetric and Asymmetric Multilevel Inverters for Dynamic Loads," in *IEEE Access*, vol. 6, pp. 738-746, 2018, doi: 10.1109/ACCESS.2017.2775203.

[8] C. -H. Hsieh, T. -J. Liang, S. -M. Chen and S. -W. Tsai, "Design and Implementation of a Novel Multilevel DC–AC Inverter," in *IEEE Transactions on Industry Applications*, vol. 52, no. 3, pp. 2436-2443, May-June 2016, doi: 10.1109/TIA.2016.2527622.

[9] Y. Wang, A. Poorfakhraei, N. Mehdi and A. Emadi, "Comparative Analysis of 2-Level and 3-Level Voltage Source Inverters in Traction Applications," *2021 IEEE Transportation Electrification Conference & Expo (ITEC)*, Chicago, IL, USA, 2021, pp. 614-619, doi: 10.1109/ITEC51675.2021.9490160.

[10] B. Wang, S. Dong, S. Jiang, C. He, J. Hu, H. Ye and X. Ding, "A Comparative Study on the Switching Performance of GaN and Si Power Devices for Bipolar Complementary Modulated Converter Legs," *Energies*. 2019; 12(6):1146. doi.org/10.3390/en12061146.

[11] A. A. Khan, M. Jamil, U. A. Khan, I. Khan, W. Eberle and S. Ahmed, "Novel Three and Four Switch Inverters With Wide Input and Output Voltage Range for Renewable Energy Systems," in *IEEE Journal of Emerging and Selected Topics in Power Electronics*, vol. 10, no. 6, pp. 7385-7396, Dec. 2022, doi: 10.1109/JESTPE.2022.3181071.

[12] S. N. Khan, A. A. Khan, M. Jamil, U. A. Khan, H. F. Ahmed and S. Ahmed, "Novel Three Phase Buck-Boost Inverter With Reduced Input Current Ripple and No Short-Circuit and Open Circuit Faults," in *IEEE Transactions on Power Electronics*, vol. 39, no. 5, pp. 5695-5706, May 2024, doi: 10.1109/TPEL.2024.3360309.

[13] R. Gautam, R. V. John and M. Kumar, "Cascaded H-Bridge Multilevel Inverter Based Solar PV Power Conversion System," *2022 IEEE Students Conference on Engineering and Systems (SCES),* Prayagraj, India, 2022, pp. 1-6, doi: 10.1109/SCES55490.2022.9887731.

[14] M. Waqas, M. Jamil, and A. A. Khan, "Hybrid Power System Design and Dynamic Modeling for Enhanced Reliability in Remote Natural Gas Pipeline Control Stations," *Energies*, vol. 17, no. 7, p. 1763, Jan. 2024, doi: https://doi.org/10.3390/en17071763

Chapter 5: Smart IoT SCADA System for Hybrid Power Monitoring in Remote Natural Gas Pipeline Control Stations

Preface

*A version of this manuscript has been published in "Electronics - An Open Access Journal from MDPI" in August 2024 (Electronics **2024**, 13, 3235. https://doi.org/ 10.3390/electronics13163235). As the primary author, I led the research efforts, including literature reviews, system design, modeling, and results analysis. I drafted the initial manuscript and revised it based on feedback from the co-authors and the peer review process. Dr. Mohsin Jamil, my research supervisor provided research supervision and guidance, reviewed and corrected the manuscript, and contributed valuable research ideas throughout its development.*

Abstract

A pipeline network is the most efficient and rapid way to transmit natural gas from source to destination. The smooth operation of natural gas pipeline control stations depends on electrical equipment such as data loggers, control systems, surveillance, and communication devices. Besides having a reliable and consistent power source, such control stations must also have cost-effective and intelligent monitoring and control systems. Distributed processes are monitored and controlled using supervisory control and data acquisition (SCADA) technology. This paper presents an Internet of Things (IoT)-based, open-source SCADA architecture designed to monitor a Hybrid Power System (HPS) at a remote natural gas pipeline control station, addressing the limitations of existing proprietary and non-configurable SCADA architectures. The proposed system comprises voltage and current sensors acting as Field Instrumentation Devices for required data collection, an ESP32-WROOM-32E microcontroller that functions as the Remote Terminal Unit (RTU) for processing sensor data, a Blynk IoT-based cloud server functioning as the Master Terminal Unit (MTU) for historical data storage and human–machine interactions (HMI), and a GSM SIM800L module and a local WiFi router for data communication between the RTU and MTU. Considering the remote locations of such control stations and the potential lack of 3G, 4G, or Wi-Fi networks, two configurations that use the GSM SIM800L and a local Wi-Fi router are proposed for hardware integration. The proposed system exhibited a low power consumption of 3.9 W and incurred an overall cost of 40.1 CAD, making it an extremely cost-effective solution for remote natural gas pipeline control stations.

5.1 Introduction

Global energy demand and consumption have increased in the current era, resulting in a widespread reliance on fossil fuels that are detrimental to humanity and the environment. This situation, combined with the growing and impending shortage of fossil fuels, has prompted the scientific community to seek alternative electricity generation methods through renewable energy sources [1]. Recently, there has been a substantial increase in the development and adoption of renewable energy sources (RESs). As energy specialists endeavor to utilize environmentally friendly and sustainable energy for society's benefit, renewable energy sources are progressively being incorporated into existing power networks. Notably, solar energy and wind energy have received significant attention [2,3].

Over time, Pakistan has increasingly depended on natural gas as its main energy source. Natural gas fulfills a substantial portion of Pakistan's energy needs, making it a major contributor to electric power generation. Because of the difficulties associated with storing natural gas, it must be quickly transmitted to its ultimate destination after being extracted from the gas wells. High-pressure natural gas pipelines are operated and maintained by several control stations. However, their dispersed strategic locations, particularly in remote areas, present operational hurdles due to challenges such as unreliable electricity supply and logistical constraints. Additionally, the efficient operation of these control stations relies on various electrically powered devices installed within them [4]. Therefore, an uninterrupted and reliable power supply and a monitoring system for such control stations have become necessary.

As renewable energy sources such as solar and wind are subject to intermittent conditions dictated by the environment, traditional energy generation methods are combined with renewable power sources to form a Hybrid Power System (HPS). Hybrid power systems typically require energy

storage systems to maintain stability in system operations and power supply. These storage systems play a crucial role in mitigating fluctuations in energy output, ensuring frequency regulation and facilitating load balancing, among other essential roles. Hybrid power systems typically combine conventional energy sources such as fossil fuels with one or more renewable sources such as wind and solar, alongside energy storage systems, power electronic converters such as inverters, and additional power system devices such as communication systems. These systems are often deployed across expansive geographical regions, including different situations, such as offshore locations and wetlands. Given their distributed nature, interconnecting these systems for power generation and supply poses several challenges. These include addressing power quality, controlling frequency, managing voltage tolerances, synchronizing the grid, facilitating data exchange and communication between components, and ensuring safety and security protocols [5]. Hence, modern systems must incorporate advanced digital and high-tech equipment that enable bidirectional communication between the supply and demand sides. They offer features such as real-time monitoring, communication, and control between generation and demand, which lowers energy consumption, improves efficiency, and enhances system resilience. This results in secure, adaptable, and intelligent operation [6].

To address these challenges and maintain smooth power system operations, a range of sensors, microprocessors, microcontrollers, pumps, actuators, valves, and other devices are typically interconnected throughout the entire HPS. They gather crucial data such as voltage, current, temperature, pressure, etc., enabling live monitoring and remote coordinated control. Supervisory Control and Data Acquisition (SCADA) serves as the ideal solution for these tasks. SCADA systems are the foundation of industrial automation. The automation pyramid, or automation hierarchy, is a conceptual model that organizes industrial automation systems into different levels,

from the physical devices on the plant floor to higher-level management systems. At the lower levels of the automation pyramid, SCADA is responsible for monitoring, controlling, and coordinating operations across all industrial devices. At the higher levels, SCADA serves as an interface for human supervision and Manufacturing Execution Systems (MES), facilitating decision making and the management of industrial processes [7].

SCADA is a widely recognized and proven technology used in various systems for remote monitoring, offering control and oversight capabilities for distant devices [8]. A SCADA system comprises of two parts: a hardware part for data collection, communication, operation, and control, and a software part for data storage, visualization, data processing, optimization, and alert management. A master terminal unit (MTU), remote terminal units (RTUs), and field instrumentation devices (FIDs) make up a SCADA system's hardware. An RTU is a microcontroller or programmable logic controller (PLC) that connects to FIDs such as sensors, transmitters, pumps, etc. RTUs and MTU exchange data over a communication network using a designated protocol. The MTU acts as the central unit of the SCADA system, processing data and displaying it on the human–machine interface (HMI) for the operator to easily monitor and operate. The HMI, which is a software component of SCADA, is a valuable feature that provides users or operators with an informative display for plant monitoring. Developers often utilize SCADA software that includes HMI design tools to build the SCADA user interface because of its convenience and rapid development capabilities [9].

Over the last three decades, SCADA technology has advanced to monitor and control distributed processes. Before SCADA, plant personnel used push buttons and selector switches for monitoring and controlling industrial processes, requiring many on-site workers. As industrial operations expanded and sites got increasingly remote, timers and relays were introduced to aid in supervision

and control, reducing the need for on-site personnel. Although timers and relays offered a reasonable level of automation, significant resources were still needed for management. To address the demand for greater process automation and the limitations of earlier monitoring and control systems, the first generation of SCADA systems, known as Monolithic SCADA, was developed in the 1970s as standalone units. The second generation, called Distributed SCADA, emerged in the 1980s and 1990s due to the development of Local Area Networks (LAN) and HMI software, along with advancements and miniaturization in computer systems. However, most communications then were proprietary, restricting access to third-party suppliers of a particular SCADA system [10]. Wide-area network (WAN) connectivity increased as SCADA systems adopted open-source architectures and non-proprietary communication protocols in the 1990s and 2000s. This resulted in the third generation, known as Networked SCADA. However, rapid advancements in computer technologies soon made these systems outdated. SCADA manufacturers responded by developing the fourth generation, known as IoT SCADA, which integrates classic SCADA with cloud services to improve monitoring and control. This enables real-time access to plant information from anywhere, across multiple platforms. The IoT concept involves connecting physical objects with sensors, embedded electronics, software, and networking to allow devices and operators to exchange data over a shared platform or the internet [11,12].

There are two methods for transitioning to an IoT-based SCADA system. The first method includes designing a new SCADA system from scratch using IoT or cloud technology. The second approach focuses on transitioning the current SCADA system to the cloud or integrating it with IoT-compatible components [13]. Despite the IoT technology having been available for some time, experts are still unable to agree on a common IoT architecture. Various scholars have suggested

distinct architectural designs, with the three-layer and five-layer models being the most common, as discussed extensively in [14]. Regardless of which architecture is implemented, reliable communication is crucial in IoT-based systems due to the widespread distribution of IoT devices. IoT technologies typically utilize the four layers of the basic TCP/IP model [15].

Research indicates that key design factors for IoT-based real-time applications such as SCADA include message encoding formats, communication protocols, and the chosen web-based or IoT platform. The TCP/IP model provides a framework for communication over the internet, with each layer performing specific tasks to ensure data is transmitted efficiently and accurately from one device to another. It comprises four layers, namely the Network Interface Layer, the Internet Layer, the Transport Layer, and the Application Layer. Consequently, selecting the appropriate protocol at each layer of the IoT protocol stack is crucial for a specific application. For instance, in the Application Layer, choices include MQTT, HTTP, and CoAP, while suitable protocols must also be chosen for the Internet, Transport, and Network Access Layer [16].

5.2 Literature Review

The site selection process is integral to designing a hybrid power system, playing a pivotal role in determining its performance and effectiveness. Key considerations include assessing the readiness of renewable resources, for instance, solar irradiation, wind speed, and hydro potential. Understanding the site-specific load profile is essential for appropriately sizing and configuring system components to meet energy demand. Environmental factors, including terrain, climate conditions, and regulatory requirements, also influence system design. Economic viability hinges on factors such as installation costs, potential energy savings, and payback periods, all of which are influenced by site selection. Ultimately, a well-chosen site maximizes energy generation

potential while minimizing environmental impact and operational costs, laying a strong foundation for the hybrid power system's success [17].

Research communities worldwide have significantly developed and enhanced SCADA systems for various applications. Sufficient research has been done to tackle the high costs and compatibility challenges of commercial SCADA systems by creating a range of open-source SCADA solutions that offer varying functionalities and price points.

A comprehensive literature survey reveals that SCADA systems are widely employed across various applications and sectors. In the industrial sector, SCADA systems are extensively used for monitoring and controlling manufacturing processes, ensuring efficiency and safety. The adoption of SCADA in these diverse applications highlights its versatility and critical importance in ensuring operational excellence and safety. Table 5.1 provides a brief overview of how SCADA systems are utilized across different applications and sectors.

Table 5.1. Overview of SCADA System Applications

Reference	**Design Parameter**
[5]	Design of low-cost SCADA system for distributed assets
[9]	Monitoring of Plant Leaf Temperature and Air and Soil Parameters
[18]	Monitoring and control of solar-powered water pumping system
[19]	Lightning damage detection on wind turbine blade
[20]	Remote control and monitoring of grid-connected inverters
[21]	Monitoring and control of reverse osmosis desalination system
[22]	Remote monitoring of PV system
[23]	Monitoring of HPS for Renewable Energy Laboratory
[24]	Secure cloud monitoring and control of high-power machines
[25]	A low-cost remote monitoring system for PV system
[26]	Local data logging and monitoring of the PV system for industrial plant
[27]	Monitoring and control of hybrid power systems
[28]	Remote control of motors and sensors deployed for oil and gas facilities

[29]	Monitoring of hybrid renewable systems in offshore and remote areas
[30]	Configuration and reconfiguration of an autonomous assembly system
[31]	Monitoring of power consumption using Fog computing
[32]	Vulnerability analysis of SCADA systems and security measures for a standard wastewater treatment plant.
[33]	A traffic control system
[34]	Detection of antenna and microphone problems in the telecommunication sector
[35]	Monitoring and control of renewable energy systems

A substantial amount of literature has been reviewed throughout this study, with pertinent findings summarized in the preceding section of this article. It has been noted that IoT-based remote monitoring and control systems have targeted a range of sectors and applications. These include electric power plants [5,12], plant monitoring [9,29], industrial applications [30], electric power distribution [23,31], education [24], wastewater treatment [32], traffic control [33], telecommunications [34], oil production [28], and so on.

As natural gas pipeline control stations are strategically placed in remote areas that often lack a reliable and consistent power supply, resulting in power generation through conventional fossil fuels or the internal use of natural gas. To conserve the depleting natural gas resource, minimizing or eliminating its internal use for power generation is essential, which can be achieved through using renewable energy sources. Therefore, a hybrid power system along with a cost-effective and efficient SCADA system is essential to ensure efficiency and safety. The SCADA system will collect data and remotely monitor and coordinate control from various field instrument devices spread across different locations, ensuring the optimal operation of these remote stations with a reliable power supply. To the best of the author's knowledge and based on the reviewed literature, there are currently no SCADA systems specifically designed for hybrid power monitoring at remote natural gas pipeline control stations that minimize internal natural gas consumption for

enhanced efficiency, use both GSM and Wi-Fi communication, are low-cost and power-efficient, and utilize IoT-based open-source platforms instead of proprietary vendor-specific network protocols. These facts inspired us to create an IoT-based SCADA system for such control stations. It is important to note that the research presented in this paper builds upon our previous work published in [4]. Our primary goals were to design a cost-effective solution for remote natural gas pipeline control stations that facilitates fast and easy development while being capable of measuring various parameters. Table 5.2 compares the proposed SCADA system with some prior research, emphasizing its distinct features and capabilities that are not present in other systems.

Table 5.2. Comparison of SCADA systems

Ref.	**SCADA System Features**						
	SCADA Platform	Open Source	GSM	Wi-Fi	Micro-Controller	Protocol	Total Cost ($)
[9]	Haiwell IoT Cloud	**X**	**X**	✓	Raspberry Pi Zero	TCP	**200**
[18]	Node-RED	✓	✓	**X**	Arduino Uno	MQTT	Not Mentioned
[21]	Node-RED	✓	**X**	✓	Arduino	Firmata	Not Mentioned
[22]	Node-RED	✓	**X**	✓	ESP32-E	MQTT	94.5
[26]	Emoncms	✓	**X**	Serial port Comm.	Arduino Mega 2586	MQTT	761.72
[27]	Node-Red	✓	**X**	✓	Arduino Mega2560	Firmata	93
[28]	Node-Red	✓	**X**	✓	Arduino Uno Arduino Mega	HTTP Firmata	Not Mentioned
[29]	Raspberry Pi (Raspbian OS)	✓	**X**	UART + WiFi	Arduino Uno Arduino Mega	TCP/IP	Not Mentioned

[35]	Wonderware Intouch + ThingSpeak	✓	**X**	✓	Arduino Mega2560	Not Mentioned	Not Mentioned
Proposed SCADA	Blynk	✓	✓	✓	ESP32-E	HTTP TCP/IP	40.1

This research introduces a cost-effective, energy-efficient, open-source SCADA system utilizing the latest IoT-based SCADA architecture. This proposed design integrates web services with traditional SCADA for enhanced supervisory control and monitoring. The proposed SCADA system employs robust, widely accessible components to perform the four fundamental functions of a commercial SCADA system: remote monitoring, data collection and presentation, networked data transmission, and supervisory control [12]. This study aims to design a SCADA system featuring the following elements:

- The proposed system is a cost-effective SCADA solution with a user-friendly HMI interface that can be accessed remotely, uses minimal power, and incorporates the most recent IoT architecture.
- The proposed system's scalability is enhanced by using Blynk, an open-source platform, along with commercially available components. This approach allows flexibility in selecting communication channels and the number of sensors.
- The proposed system's configuration is set up on a local host using the Blynk visual programming language, which is accessible via a web browser for convenient control.
- Web-based system offers intuitive dashboards and robust data analytics capabilities for live monitoring and control.
- Considering the remote locations of natural gas pipeline control stations and the potential lack of access to 3G, 4G, or Wi-Fi networks, the proposed SCADA system is designed and tested

using both GSM and Wi-Fi modules for communication. This approach enhances the system's adaptability, enabling users to remotely check the system status.

5.3 System Description

The proposed SCADA system, intended to be both cost-effective and open-source, employs the IoT SCADA architecture, recognized as the latest development in SCADA technology. SCADA enables the real-time exchange of data among central control and field devices associated with distributed operations.

Given the remote locations of natural gas pipeline control stations and the potential lack of access to 3G, 4G, or Wi-Fi networks, two configurations are considered for integrating the hardware components. In the first configuration, Field Instrumentation Devices (FIDs), such as voltage and current sensors used to measure various site parameters, interface with a Remote Terminal Unit (RTU). An ESP32 microcontroller serves as the RTU and is responsible for receiving, processing, and transmitting data collected from the FIDs. Considering the unavailability of 3G, 4G, or Wi-Fi networks in this configuration due to the remote location of natural gas pipeline control stations, the data collected by the ESP32 microcontroller in this configuration is transmitted to the Master Terminal Unit (MTU) via a GSM SIM800L module. The MTU plays a pivotal role in data acquisition, programming, visualization, and storage. In this configuration, the MTU is Blynk, a versatile software suite that facilitates the prototyping, deployment, and remote management of connected electronic devices at any scale. Blynk allows users to connect their hardware to the cloud and develop mobile and web applications for remote control. It provides real-time and historical data analysis capabilities, remote device control, alerts, and more. Blynk features an intuitive drag-and-drop interface for constructing custom dashboards and interfaces without necessitating coding skills, supporting a wide range of microcontrollers and single-board

computers [36]. A mobile device can be used as an HMI to monitor and analyze real-time data via TCP/IP communication protocol in this configuration.

In the second configuration, assuming the availability of 3G, 4G, or Wi-Fi networks, data collected by the ESP32 are transmitted via its integrated Wi-Fi module to the Master Terminal Unit (MTU). The MTU can be categorized into hardware and software components in this configuration. A DELL laptop (11th Generation Intel(R) Core(TM) i5) serves as the primary hardware for the MTU. As for the software component, the system utilizes Windows 10 Pro as an operating system alongside Blynk, an IoT-based platform. Communication between the RTU and MTU in this configuration is facilitated through the HTTP protocol. Figure 5.1 illustrates the configuration of the proposed SCADA system.

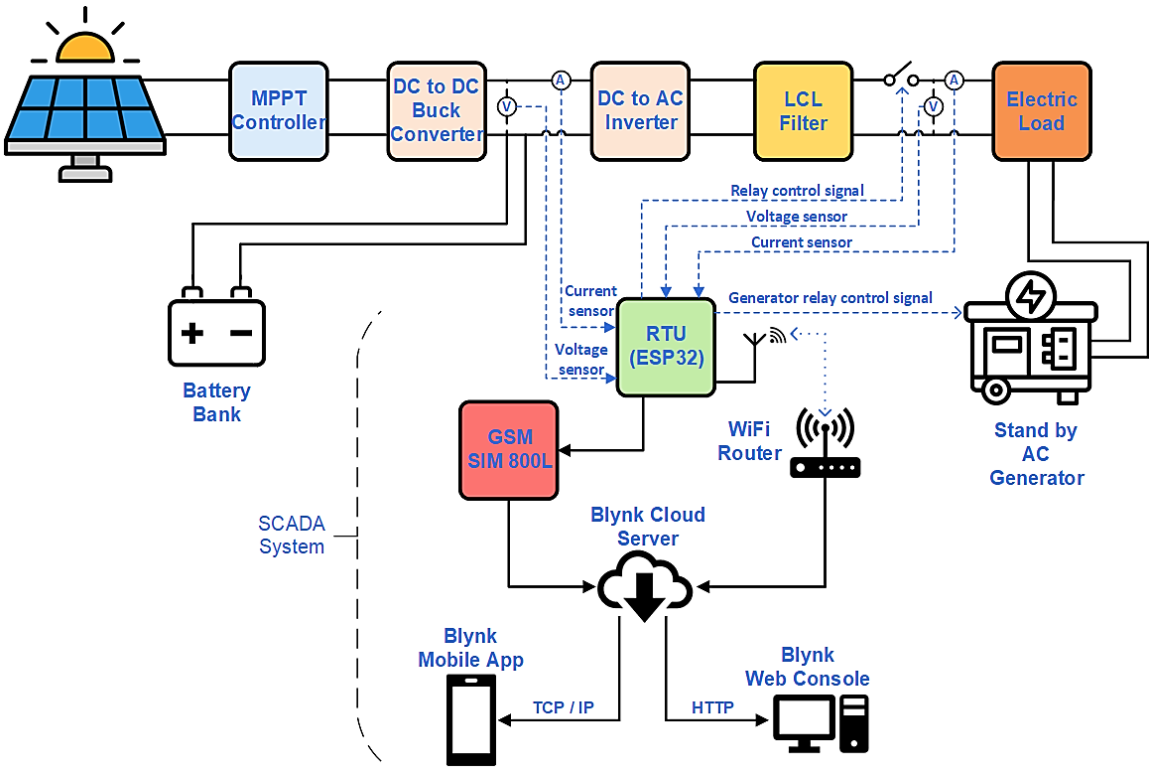

Figure 5.1. Proposed SCADA system schematic diagram.

5.3.1 Components of the Designed SCADA System

This research article section provides a brief overview of the cost-effective hardware components and software utilized to implement the proposed SCADA system architecture. The hardware components include voltage and current sensors to acquire site parameters; the versatile ESP32 microcontroller, which functions as an RTU for collecting, processing and transmitting FIDs data; an LCD; an SIM800L GSM module, which provides GSM functionality to the ESP32 microcontroller when 3G, 4G, or Wi-Fi networks are unavailable; the LM2596 voltage regulator, which serves as a buck converter to step down voltage; and a 5 V single-channel relay. The software components feature Blynk, an IoT-based platform that functions as an MTU and is employed to develop a user interface that can be accessed locally for the proposed SCADA system. The suggested SCADA system employs current and voltage sensors as FIDs to collect the necessary site data. The system utilizes ACS 712 Hall Effect Current Sensors and ZMPT101B Voltage Sensor as the analog sensors. The analog sensors operate at a signal voltage (VCC) of 5V, while the ESP32-WROOM-32E microcontroller operates between 0 V and 3.3 V. Due to the voltage difference, the current sensor cannot be connected directly to the ESP32-WROOM-32E's analog-to-digital converter (ADC) pins. To ensure compatibility, level shifting is achieved through a step-down resistor configuration, aligning the sensor's output with the 3.3 V input requirement of the ESP32-WROOM-32E, thus preserving measurement accuracy. The characteristics and usage of these sensors in this system are outlined below.

- **Hall Effect Current Sensor (ACS 712):** The ACS 712 Hall Effect Current Sensor, designed and manufactured by Allegro MicroSystems in Manchester, NH, USA, is a cost-effective, fully integrated linear current sensor IC utilizing Hall Effect technology. It features 2.1 kVRMS isolation and offers a current path with minimal resistance. Operating

with a low-noise analog signal pathway and powered by a 5V single supply, it offers an output sensitivity ranging from 66 to 185 mV/A with minimal magnetic hysteresis. In operation, the sensor detects the magnetic field generated by current flowing through its copper conductor, converting this field into a corresponding output voltage [37].

The ACS712 sensor comes in three different models, optimized for various current measurement ranges ±5 A, ±20 A, and ±30 A. For our research, we utilized the ACS712 current sensors rated at ±30 A to monitor the current in our designed PV system. This module outputs 2.5V when there is 0A current and 5V when there is 30A current. For the physical connections, a voltage divider circuit is used to adapt the 5V signal required by the Current Sensor to the 3.3V signal level supported by the pins of ESP32 microcontroller. Figure 5.2 illustrates the setup with step-down resistors connecting the sensor to the ESP32, and Equation (1) defines the formula for voltage division.

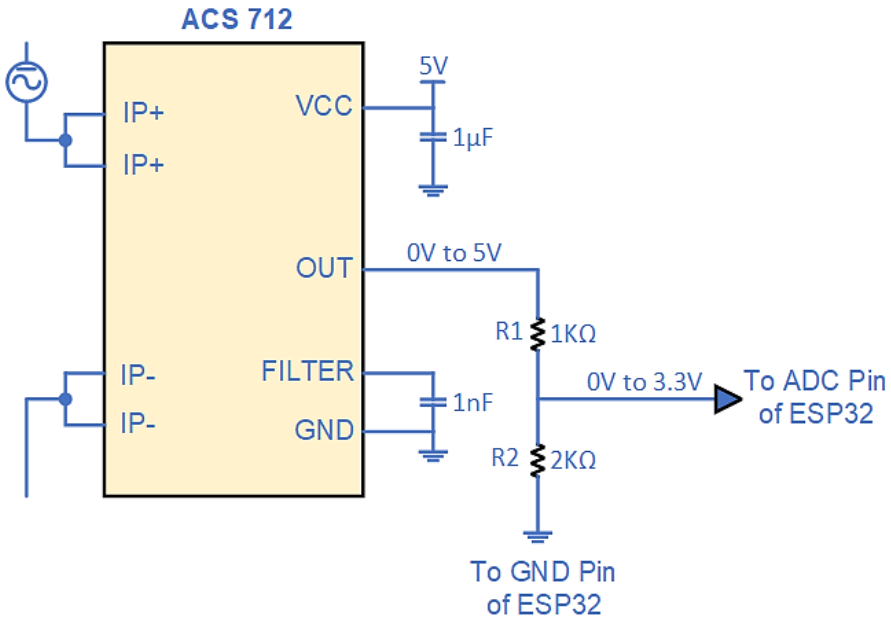

Figure 5.2. ESP32 voltage divider connection.

$$V_{ESP32} = \frac{R_2}{R_1 + R_2} \times VCC_{(ACS712)} \tag{5.1}$$

- **Voltage Sensor (ZMPT101B):** The Voltage Sensor ZMPT101B is a widely used module for measuring AC voltage, ideal for applications in power monitoring and energy management. It features a high-precision voltage transformer with a voltage ratio of 1:1 and an operational amplifier circuit, enabling accurate voltage measurements by amplifying the signal for analog-to-digital conversion [38].

  The sensor provides electrical isolation between the high-voltage AC side and the low-voltage DC side, ensuring safety and protecting microcontrollers from voltage spikes. The Voltage Sensor ZMPT101B provides an output signal ranging from 0-5V analog, operates within a voltage range of DC 5V-30V, and is capable of measuring up to 250V AC. It has a rated input current of 2mA and dimensions of 49.5mm in length and 19.4mm in width. The sensor functions effectively within an operating temperature range of -40°C to +70°C [39]. While the module is specifically designed for AC voltage and requires calibration for precise readings, its integration in microcontroller-based systems makes it suitable for smart meters, home automation, and industrial automation applications. Figure 5.3 shows the internal schematic diagram of ZMPT101B voltage sensor.

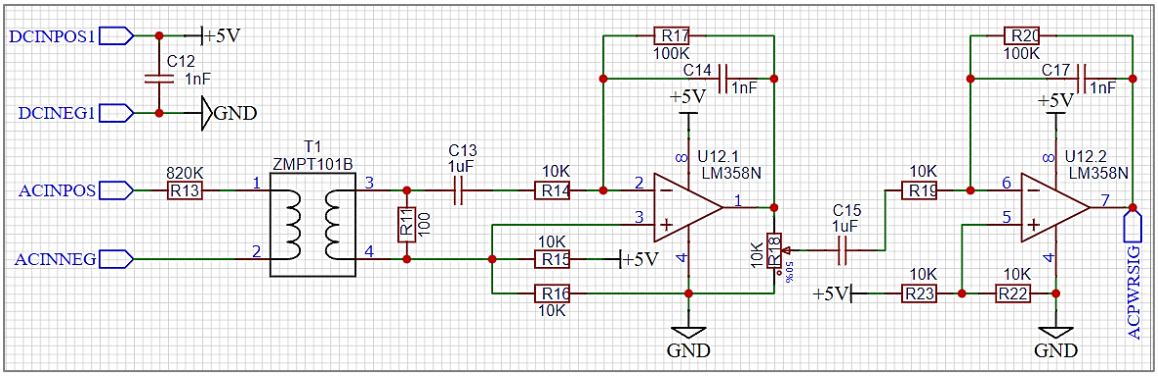

Figure 5.3. Internal schematic diagram of ZMPT101B voltage sensor.

- **ESP32-WROOM-32E Microcontroller (RTU):** The ESP32 series includes a range of microcontroller models such as ESP32-WROOM and ESP32-WROVER, developed by Espressif Systems. ESP32-WROOM-32E is a versatile and powerful microcontroller module from Espressif Systems, ideal for IoT applications featuring integrated Wi-Fi and Bluetooth capabilities [40]. The ESP32-WROOM-32E is a specific module within the ESP32 series, containing the ESP32-D0WD-V3 chip. It is designed for a wide range of applications, providing robust performance with its dual-core processor, integrated Wi-Fi, and Bluetooth. It features a dual-core Tensilica LX6 processor running up to 240 MHz, 520 KB of SRAM, 4 MB of flash memory, and supports both 2.4 GHz and 5 GHz Wi-Fi as well as Bluetooth v4.2.
- The ESP32-WROOM-32E features numerous input and output pins, along with ample processing power, allowing it to handle additional sensors and energy equipment. With 34 programmable GPIO pins, 18 ADC channels, 2 DAC channels, and numerous peripheral interfaces (SD card, SPI, I2C, UART, I2S, CAN, SDIO, GPIO, IR), it offers extensive connectivity options. Operating at 3.3 V, it boasts low power consumption, with deep sleep mode drawing only 10 µA. Security features include hardware encryption, secure boot, and

flash encryption. The module also includes a real-time clock, touch sensors, and built-in hall and temperature sensors, making it suitable for smart home devices, industrial automation, and wireless sensor networks. It can be programmed using various environments, such as Arduino IDE and ESP-IDF, supporting multiple languages, such as C and Python [41]. Figure 5.4 illustrates the pin layout of the ESP32 module with the ESP32-WROOM-32 chip.

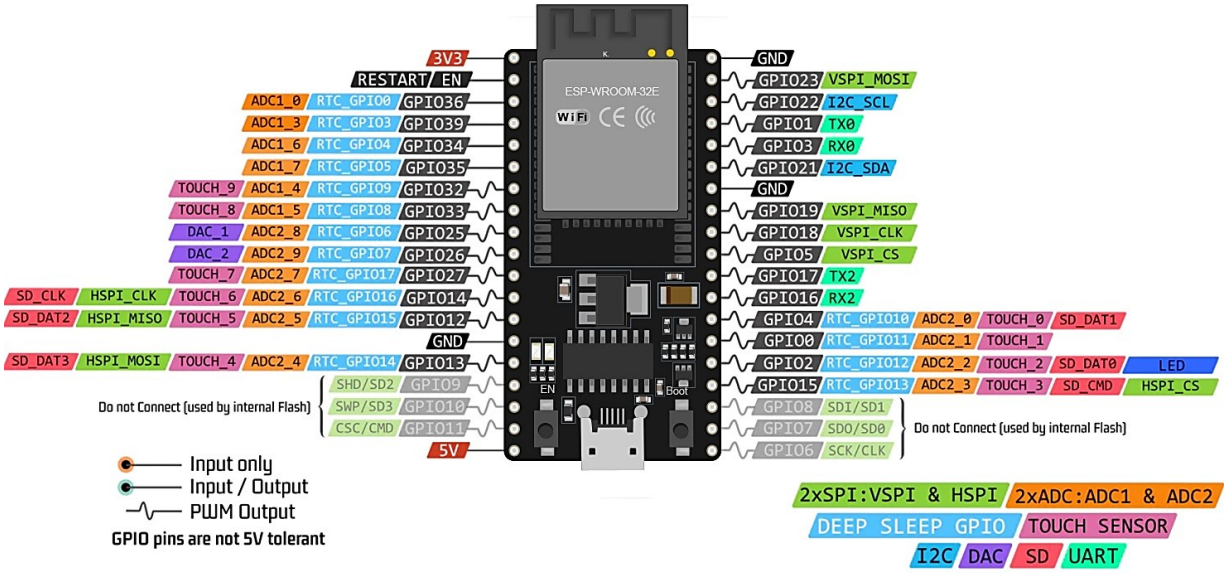

Figure 5.4. Pin layout of ESP32 module with the ESP32-WROOM-32 chip.

- **GSM SIM800L Module:** GSM, or Global System for Mobile Communications, is a widely adopted standard for 2G digital cellular networks, developed by the European Telecommunications Standards Institute (ETSI) in 1989. It employs digital transmission for voice and data services, enhancing call quality and enabling features such as SMS and internet access. Operating in various frequency bands (900 MHz and 1800 MHz in Europe, 850 MHz and 1900 MHz in North America), GSM uses SIM cards for user identification and facilitates easy switching between devices.

The SIM800L module is a compact and versatile GSM/GPRS module designed for embedded applications, enabling devices to connect to GSM networks for voice, SMS, and data services. It supports quad-band frequencies (850/900/1800/1900 MHz), ensuring global usability. Measuring about 25 mm x 23 mm, it is easy to integrate into various projects [42]. The module requires a 3.4 V to 4.4 V power supply and features low power consumption, typically drawing 1.1 mA in sleep mode. The SIM800L module functions within a temperature range of −40 to +85 °C and includes a microSIM card socket, UART interface, and IPX antenna connector. When powered, the module automatically searches for and connects to cellular networks, with an onboard LED indicating connection status. With features such as auto baud rate detection, power-saving mode, and an integrated LDO voltage regulator, the SIM800L supports GPRS multi-slot class 12/10, CS-1, CS-2, CS-3, and CS-4 coding schemes, and offers a maximum data rate of 85.6 kbps for uploading and downloading. These specifications make the SIM800L ideal for IoT applications, remote monitoring, and GSM-based communication projects due to its affordability and reliability [43].

- **LM2596 Buck Converter:** The LM2596 is a versatile and efficient step-down (buck) voltage regulator designed by Texas Instruments, ideal for converting a higher DC input voltage (4.5V to 40V) to a lower DC output voltage, adjustable between 1.23V and 37V. It can deliver up to 3A of continuous output current with high efficiency, typically around 80-90%, minimizing heat generation and power loss. Operating at a fixed switching frequency of 150 kHz, the LM2596 includes built-in thermal shutdown and current limit protection, ensuring reliable performance. With a low standby current, it enhances efficiency during idle periods. Due to its robust design and protective features, this regulator is widely used

in power supplies for electronic devices, battery chargers, distributed power systems, automotive, and industrial applications [44].

In our proposed system, the LM2596 effectively lowers the higher DC voltage generated by PV panels to a steady lower voltage, necessary for charging batteries or operating devices. By fine-tuning the output voltage to meet the needs of the charge controller and connected loads, the LM2596 improves the overall efficiency and dependability of the PV system. Its adjustable output voltage and current limits provide versatility in system setup and enhancement. In essence, the LM2596 buck converter is pivotal in ensuring the effectiveness and longevity of PV systems by efficiently managing voltage from solar panels.

- **Liquid Crystal Display (LCD):** Liquid Crystal Display (LCD) is a flat-panel display technology that utilizes liquid crystals sandwiched between polarized glass layers to create images or text. It operates using two main types: Passive Matrix LCDs, which are cost-effective with simpler electrode patterns but have slower response times and limited viewing angles, and Active Matrix LCDs (TFT-LCDs), featuring thin-film transistors (TFTs) per pixel for faster response times, better image quality, and wider viewing angles. Operating typically between 4.7V to 5.3V, LCDs have a low current consumption of about 1mA without backlight. They are commonly used in alphanumeric modules capable of displaying letters and numbers, with typical configurations featuring two rows of 16 characters each. Each character is composed of a 5×8 pixel matrix. LCDs can operate in both 8-bit and 4-bit modes, allowing flexible interfacing with microcontrollers. Additionally, they support custom character generation and are available with green and

blue backlight options, making them versatile for various applications in consumer electronics and industrial devices [45].

- **5V Single Channel Relay:** A 5V single-channel relay is an electromechanical switch triggered by a 5V DC signal, compatible with microcontrollers and digital circuits. It can handle loads up to 10A at 250V AC or 30V DC, making it ideal for controlling high-power devices in home automation, industrial systems, automotive electronics, and DIY projects. The relay features normally open (NO) and normally closed (NC) contacts, providing flexible switching options. It offers electrical isolation between the low-voltage control and high-voltage load circuits, enhancing safety and preventing interference. A 5V single-channel relay is a crucial component in electronic circuits, enabling the control of high-power devices with a low-power signal. Its ease of integration, safety features, and versatility make it widely used in home automation, industrial control, automotive electronics, and various DIY projects [46].
- **Master Terminal Unit (MTU):** In SCADA systems, the Master Terminal Unit (MTU) serves as the central hub for data collection, processing, monitoring, and controlling operations. It collects data from Remote Terminal Units (RTUs) and Programmable Logic Controllers (PLCs), processes and stores these data, and provides live monitoring and system control. The MTU manages communication between the central control room and remote sites, ensuring reliable and secure data transfer using various communication protocols. Additionally, it often includes or interfaces with human–machine interface (HMI) software, allowing operators to interact with the system via graphical displays and dashboards. The MTU's reliability, scalability, and real-time processing capabilities make

it essential for managing infrastructure in utilities, manufacturing, oil and gas, and transportation sectors.

The MTU can be categorized into hardware and software components. Our proposed SCADA system features two configurations. In the first configuration, Blynk, an IoT-based platform, is the MTU. The GSM SIM800L module facilitates communication between the RTU and MTU through the Blynk cloud server. Data transmission can occur either via text messages using 2G technology or through the TCP/IP communication protocol. A mobile device along with the Blynk app is used as HMI. In the case of the second configuration, A DELL laptop (11th Generation Intel(R) Core (TM) i5) serves as the primary hardware for the MTU. As for the software component, the system utilizes Windows 10 Pro as an operating system alongside Blynk, an IoT-based platform. Communication between the RTU and MTU in this configuration is facilitated through the HTTP protocol. In our proposed SCADA system, the MTU is Blynk, a versatile software that makes it easier to prototype, install, and remotely manage linked electronic devices of any size. Blynk enables users to link the hardware to the cloud and develop mobile and web applications for remote control. It offers real-time and historical data analysis, remote device control, alerts, and more. Featuring an intuitive drag-and-drop interface, Blynk allows for the development of custom dashboards and interfaces without requiring coding skills and supports a wide range of microcontrollers and single-board computers.

Designing an open-source SCADA system involves implementing robust security protocols to protect data and ensure system integrity, especially in remote locations [47]. The Blynk platform involves implementing robust security protocols to protect data and ensure system integrity, particularly in remote locations. Data are secured through

SSL/TLS encryption during transmission and end-to-end encryption to prevent unauthorized access. Secure authentication mechanisms and role-based access control ensure only authorized users can access the system. Network security is enhanced with firewalls, VPNs, and strong WiFi security measures such as WPA3 encryption. Regular firmware updates, secure boot, and code signing protect the device itself, while physical security measures prevent unauthorized access. Real-time monitoring, logging, and auditing help detect and address security breaches, while checksums, hashing, redundancy, and backups ensure data integrity. Secure remote updates and two-factor authentication for remote access further enhance the system's security, making it resilient against evolving threats [36].

5.4 Implementation Methodology

While deploying the proposed SCADA system, analog sensors act as FIDs and are connected to the previously designed hybrid power system for collecting the required data. The ESP32-WROOM-32E microcontroller acts as an RTU, receiving data from FIDs and transmitting it through the local set-up Wi-Fi network to Blynk, an IoT-based server designed for monitoring remotely and supervisory control. Current sensors for monitoring current levels are connected in series with these components. Voltage sensors for monitoring voltage levels in a hybrid power system are connected in parallel to the load and battery bank. Additionally, the relay is connected in series with the load to control the power supply, whether from the PV system or a standby AC generator operating on natural gas. All system components are properly grounded.

The SCADA system under consideration is deployed using two different approaches:

- An open-source IoT platform is built which features the ESP32-WROOM-32E microcontroller paired with a SIM800L GSM module. It interfaces with the Blynk app and

its cloud server through the TCP/IP protocol. This approach addresses scenarios where access to 3G, 4G, or Wi-Fi networks might be unavailable.

- An IoT-based open-source platform is designed using an ESP32-WROOM-32E microcontroller directly interfaced with the Blynk app and its cloud server through a local Wi-Fi router and HTTP protocol, providing a web console-based HMI.

To implement the proposed SCADA system, the process begins with designing a schematic diagram to illustrate the connections of the various hardware components. This design is created using EasyEDA software (V6.5.44). EasyEDA is a web-based software tool for electronic design automation (EDA). It allows users to design schematics, simulate circuits, and create PCB layouts in a user-friendly interface. The software supports importing and exporting various file formats, integrates with popular component libraries, and offers real-time collaboration features [48]. The next step involves soldering the hardware components such as the ESP32-WROOM-32E, GSM SIM800L, current sensors, voltage sensors, relay, buck converters, and LCD onto the zero PCB. The Blynk app, an open-source IoT platform, is configured for the software setup. Then, code is developed for the ESP32 to manage all SCADA system parameters. Finally, the ESP32 is programmed using Arduino IDE software (Version 2.3.2), and its functionality is tested and verified with the Arduino IDE serial monitor. Figure 5.5 shows the schematic diagram of the proposed SCADA system designed using EasyEDA software.

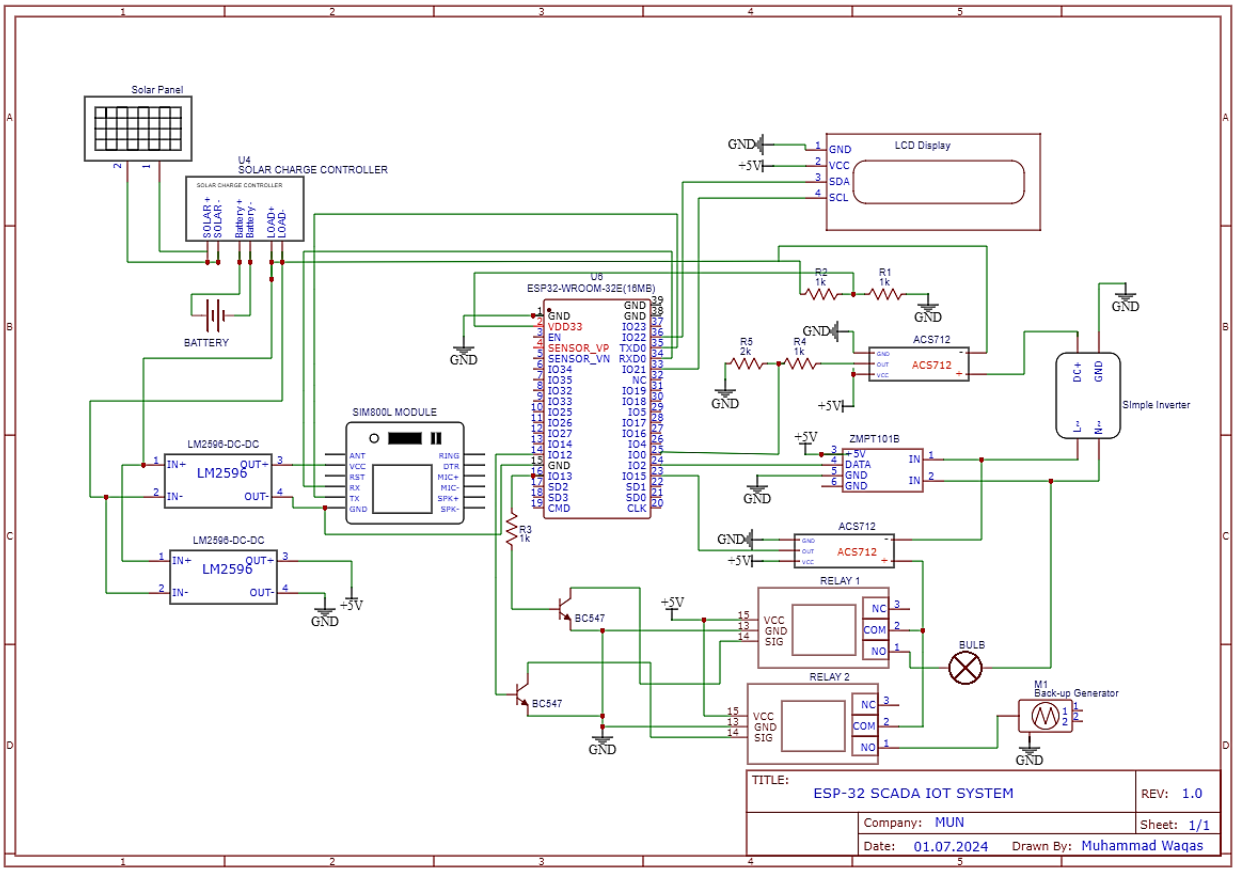

Figure 5.5. Proposed SCADA system schematic diagram.

As depicted in the schematic diagram, the solar panel connects to a solar charge controller, commonly referred to as an MPPT controller, which then connects to a 12-volt, 5-ampere battery. The output from the charge controller feeds into two LM2596 buck converters, which step down the higher voltage from the PV panel to a stable lower voltage (from 12V to 5V). Furthermore, a basic inverter is incorporated to convert DC to AC, which is crucial for the selected site, where the standard operating voltage is 220V AC. Table 5.3 illustrates the connections of current and voltage sensors, to the ESP32 microcontroller.

Table 5.3. ESP32-WROOM-32E interconnections with FIDs and other components.

Component No.	Description	Analog/Digital	ESP32-E Pin No.
1	ACS 712 Current Sensors	Analog	23, 25
2	ZMPT101 Voltage Sensor	Analog	24
3	GSM SIM800L	Digital	34,35
4	5V Relays	Digital	16, 14
5	LCD Display	Analog	21, 22

Algorithm 1 presents the pseudocode utilized in the ESP32-WROOM-32E and GSM SIM800L, programmed with Arduino IDE software (Version 2.3.2), to demonstrate the implementation methodology.

Algorithm 1: GSM, Voltage and Current Sensor Data Reading Algorithm

Start

1. Initialization
   1.1. Include necessary libraries (ZMPT101B, Arduino JSON, Software Serial, LiquidCrystal_I2C).
   1.2. Initialize the LCD and define the RX, TX, sensors, and relay pins.
   1.3. Initialize ‘software serial’ for communication with ESP-32.
   1.4. Initialize variables for storing sensor reading and calibration values.
   1.5. Set the sensitivity for the AC voltage sensor and set the pins for sensor inputs and relay output.
2. Setup Function
   2.1. Begin serial communication for debugging and ESP-32 communication.
   2.2. Initialize the LCD and set pin modes for the sensor and relay.
   2.3. Set the initial state of the relay to low; Print “initializing” on the LCD.
   2.4. Initialize the Wi-Fi connection and SIM800L.
3. Main Loop (Loop Function)
   3.1. Continuously check for incoming data from ESP-32:

3.1.2 If data is received, read the value; turn the relay ON or OFF based on the received value.

3.2. Read and process sensor data.

3.2.1 ‘take DC vol ()’-Read and calculate DC voltage; ‘take DC cur ()’-Read and calculate DC.

3.2.2 ‘take AC vol ()’-Read and calculate AC voltage; ‘take AC cur ()’-Read and calculate DC.

3.3. Check if AC voltage is below the threshold:

3.3.1 If AC voltage is below the threshold, turn ON the generator by setting the relay HIGH

3.3.2 Otherwise, turn OFF the generator by using the relay LOW.

3.3.3 Update the LCD with the latest sensor readings.

3.3.4 Send the sensor data to ESP-32 in JSON format.

4. Functions for sensor readings:

4.1. ‘takeDCvol( )’

4.1.1. Read analog value from the DC voltage pin; Calculate the DC voltage value of the serial monitor

4.2. ‘takeDCcur( )’

4.2.1. Read the analog value from the DC pin; Calculate the DC using the calibration formula.

4.2.2. Print the DC value to the serial monitor.

4.3. ‘takeACvol( )’

4.3.1. Use the ZMPT101B library to get the RMS voltage for AC.

4.3.2. Ensure the AC voltage is within a specific range; Print the AC voltage value to the serial monitor.

4.4. ‘takeACcur( )’

4.4.1. Calculate peak-to-peak voltage from the AC sensor.

4.4.2. Convert the peak-to-peak voltage to RMS voltage; Calculate the RMS current using the calibration formula; Print the AC value to the serial monitor.

5. LCD update function

5.1. ‘LCD update( )’

5.1.1. Clear the LCD.

5.1.2. Set the cursor positions and print DC and AC voltage and current on the LCD.

6. Data sending function:

6.1. ‘send data( )’

6.1.1. Create a JSON document and populate it with sensor data.

6.1.2. Serialize the JSON document to a string; Send the JSON string via Wi-Fi.

6.1.3. Send the JSON string via GSM using SIM800L.

6.1.4. Delay for 2 seconds before sending the next set of data.

7. Help function:

7.1. ‘getVPP1( )’

7.2. Measure the peak-to-peak voltage from the AC sensor.

7.3. Return the calculated peak to peak voltage.

End

The designed system can positively impact the environment by reducing reliance on fossil fuels through solar energy, minimizing greenhouse gas emissions, and decreasing the need for frequent site visits, which lowers vehicle emissions. Continuous monitoring enhances resource management and reduces the risk of environmental contamination. Overall, the deployment of this SCADA system can be environmentally sustainable with proper planning and adherence to environmental protection protocols.

5.5 Prototype Design and Setup of the Blynk IoT Platform

The design of hardware is crucial in research dealing with physical systems. It allows for testing, prototyping, and real-world validation, ensuring that the proposed system functions correctly and performs well. Additionally, it enables customization, improves hands-on skills, and provides a tangible proof of concept. This section provides an overview of the hardware setup for the proposed IoT-based open-source SCADA system, which uses a single 10-watt PV panel and a 12V battery exclusively for testing. Figure 5.5 illustrates the connection of the analog voltage and

current sensors to the ESP32-WROOM-32E microcontroller on a zero PCB, with step-down resistors arranged for the current sensor. The sensor inputs are wired to key points in the PV System to measure and acquire the necessary current and voltage ratings. Section 3 outlines the power supplies for each component. The designed circuit is powered by the DC voltage generated by the PV panel and stored in the 12V DC battery connected via the MPPT. A basic inverter is used to convert this DC power to AC power. ESP32-WROOM-32E WiFi module and the GSM SIM800L module are used to form the two previously described configurations of the proposed SCADA system. Figure 5.6 shows prototype design of the proposed SCADA system.

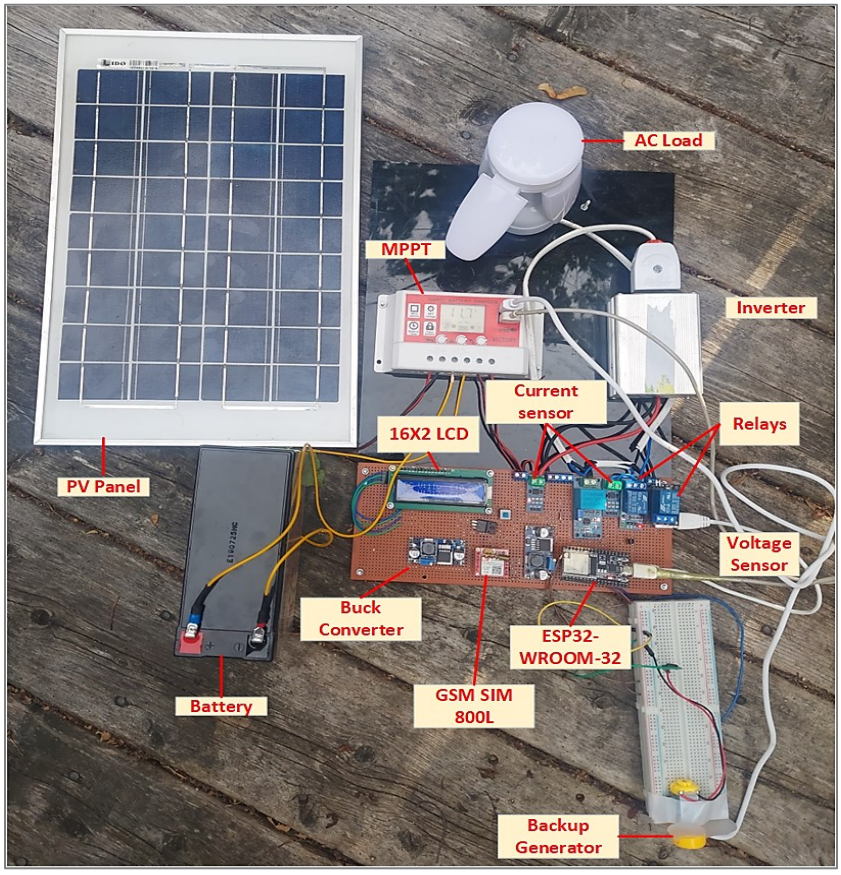

Figure 5.6. Prototype design of the proposed SCADA system.

For software part, Blynk, a versatile IoT platform that facilitates the development of mobile and web applications for controlling hardware remotely is used. It supports a wide range of

microcontrollers and single-board computers, making it highly adaptable for various IoT projects. The platform operates on a client-server model, where the Blynk app acts as the client running on a mobile device or web browser, and the Blynk cloud server serves as the backend infrastructure. For setting up Blynk IoT platform, users begin by creating an account and project within the Blynk app, specifying the hardware type (such as ESP32) and connection method (Wi-Fi or GSM). Setting up the Blynk app involves creating a user interface (UI) by dragging and dropping widgets, such as buttons, sliders, and graphs, onto a virtual canvas. These widgets are then linked to specific hardware components or sensors connected to the microcontroller via interfaces such as UART or Wi-Fi. The Blynk app communicates with the cloud server using the MQTT or HTTP protocols, allowing for seamless data exchange and control commands between the user interface and the hardware.

On the backend, the Blynk cloud server manages authentication, data storage, and communication between multiple Blynk apps and connected devices. It provides secure access to the IoT devices through tokens and APIs, ensuring data privacy and integrity. This setup enables real-time monitoring, control, and data logging from anywhere with an internet connection, making Blynk a powerful tool for IoT applications in research and beyond.

To ensure the system remains operational and effective over time, it is crucial to perform regular physical inspections of hardware components, such as the ESP32 microcontroller, sensors, and solar panels, to promptly identify and address any issues. Routine maintenance tasks include updating firmware to fix security vulnerabilities, conducting real-time monitoring with Blynk to detect anomalies, and periodically reviewing collected data for trends that may signal the need for maintenance. Preventive measures, such as cleaning, calibrating sensors, and keeping a stock of spare parts, are vital for minimizing downtime and maintaining system accuracy. Additionally,

setting up a replacement schedule for components with limited lifespans and utilizing technical support from the open-source community and manufacturers will further enhance the system's reliability.

5.6 Experimental Setup and Results

To assess the real-time performance of the designed open-source SCADA system, it has been set up to analyze solar PV parameters such as current and voltage of PV installation on the rooftop of the core science building at Memorial University of Newfoundland. The system description outlined in Section 3 served as the basis for the hardware connections. Figure 5.7 shows the experimental setup of the proposed SCADA system. The PV installation is shown in Figure 5.8. It consists of 12 solar panels with a combined surface area of 14 square meters and each solar panel can produce up to 130 W and 7.6 A at maximum. The system includes six maximum power point tracking (MPPT) controllers and a battery bank comprising four lead-acid batteries to maximize and sustain energy efficiency, as shown in Figure 5.9. For this test, the SCADA system was connected to two panels, providing a maximum output of 260 W and 15.2 A, to focus on the system’s data collection and control capabilities.

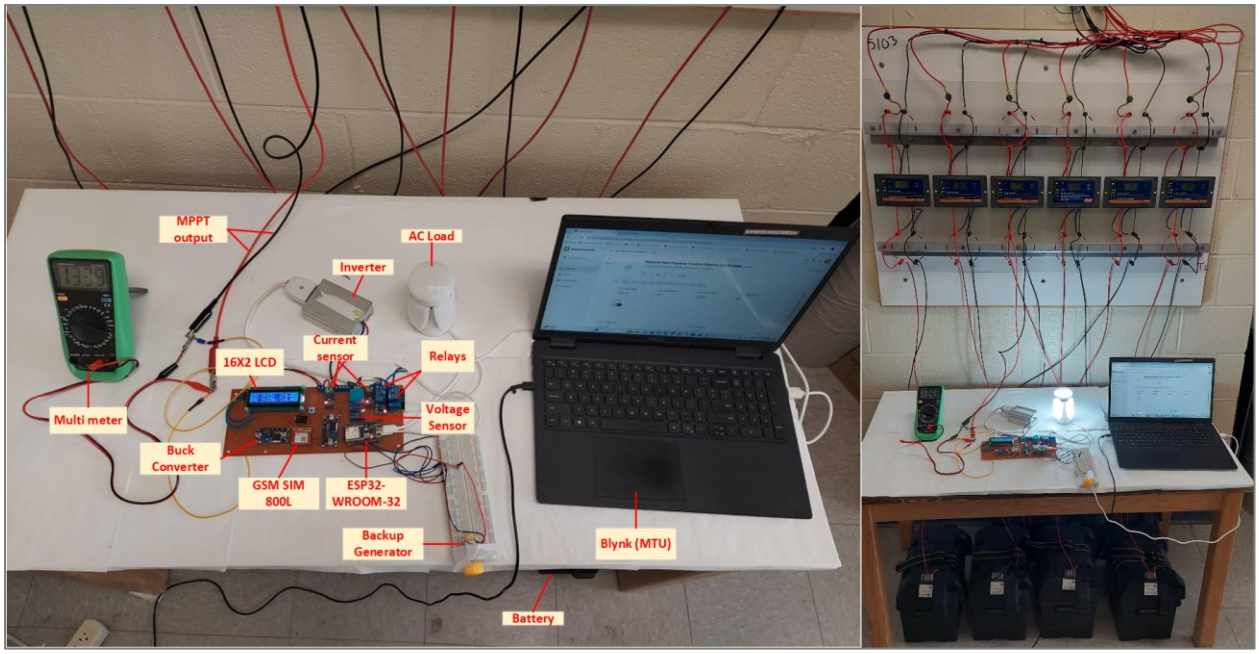

Figure 5.7.Designed SCADA system experimental setup.

Figure 5.8.PV panels setup at the rooftop of the MUN core science building.

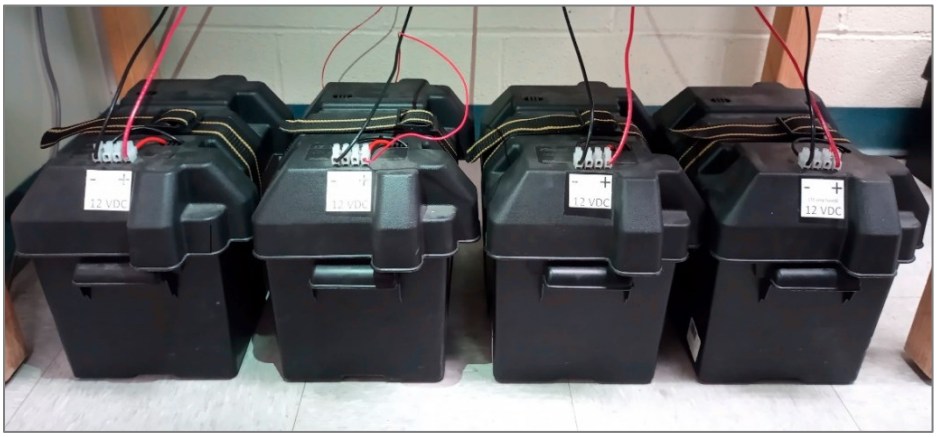

Figure 5.9. Battery bank

The voltage and current sensors gather data and transmit it to the analog pins of the ESP32 microcontroller, as depicted in the system's schematic diagram shown in Figure 5.3. The ESP32 then processes these analog signals, applying the necessary conversion factors to determine the actual voltage and current values. Using this data, the ESP32 manages load switching via a 5V single-channel relay. The processed information is subsequently transmitted to the Blynk cloud server using one of the two proposed configurations of the SCADA system. A digital multimeter was used at different points during the system testing phase to measure the required values. In both setups, the sensor data collected corresponded closely with the locally measured values from the multimeter, showing only slight differences. Moreover, during testing, an electric light bulb was used as a load to the battery, ensuring a substantial current to flow from the PV system through the MPPT for recharging the battery.

In the first configuration of proposed SCADA system, considering the possibility of no local Wi-Fi access, the GSM SIM800L module is employed to transmit data collected by the ESP32-WROOM-32E microcontroller from FIDs. The GSM SIM800L module connects to the internet using the cellular network, utilizing APN credentials provided by the SIM card carrier. The microcontroller and the SIM800L module are managed through AT commands communicated over a serial interface. Once an internet connection is established, the microcontroller firmware utilizes the Blynk library to transfer data to the Blynk cloud server via the TCP/IP protocol over the GSM network, ensuring reliable communication. The Blynk app then displays real-time data from the PV system, including DC and AC voltage readings and current measurements, offering a detailed overview of the system's performance. Figure 5.10 shows the DC and AC voltage and current parameters with AC load OFF and ON. Similarly, Figure 5.11 shows a graphical representation of

DC and AC voltage and current parameters recorded at different points and times within the PV system, as displayed on the Blynk mobile app.

Figure 5.10. Display of FID parameters on Blynk mobile app using GSM SIM800L module with load OFF and ON.

Figure 5.11. Graphical representation of FID parameters on Blynk mobile.

When there is no load connected to the power source, the terminal DC voltage reaches its maximum known as the open-circuit voltage (Voc), while the current remains zero due to the absence of a closed circuit for current flow. When no load is connected and in the "OFF" state, the system registers DC voltage at 13V and current at 0A, while AC voltage stands at 220V with a minimal current of 0A. as shown in Figure 5.12.

Figure 5.12. FID voltage and current display on the LCD when the load is off.

Once a load is connected, the terminal voltage decreases from its open-circuit level due to internal source resistance and voltage drop across the load. Simultaneously, current begins to flow through the circuit, its magnitude determined by the load's resistance and the applied voltage as per Ohm's Law. Upon connecting a load, the AC voltage decreases due to the inverter's internal impedance and wiring resistance. Figure 5.13 illustrates the display of FIDs parameters on an LCD screen when the load is on.

Moreover, to validate the supervisory control capabilities of our system, the Blynk app facilitates remote control of the load connected to the PV system. Through the app, users can toggle the connected load between "ON" and "OFF" states using virtual pins that correspond to specific digital pins on the microcontroller controlling relays or switches linked to the load. The microcontroller processes commands using the Serial2.write(val); command within the BLYNK_WRITE(V4) function, which receives input from the Blynk application and transmits it

to the relay to switch the load accordingly. This integration facilitates efficient remote monitoring and management of the PV system via the Blynk app, enhancing system usability and functionality.

Figure 5.13. FID voltage and current display on the LCD.

In the second configuration, the ESP32 collects data and transmits it through its integrated Wi-Fi module to the Master Terminal Unit (MTU) using a local WiFi router. The MTU in this setup comprises both hardware and software components. A DELL laptop equipped with an 11th Generation Intel(R) Core(TM) i5 processor serves as the primary hardware for the MTU. On the software side, the system runs Windows 10 Pro and utilizes Blynk, an IoT-based platform. Communication among the RTU and MTU is facilitated via the HTTP protocol. The system connects to the Blynk cloud server using HTTP over port 80, facilitated by the BlynkSimpleEsp32.h library. Network credentials are configured for WiFi access, and data communication with external hardware is managed through SoftwareSerial (Serial2). The primary functionality involves parsing JSON data received from Serial2, which includes measurements for DC voltage (DCvol), DC (DCcur), AC voltage (ACvol), and AC (ACcur). These values are processed, displayed on the serial monitor for debugging, and simultaneously updated on the Blynk web console using Blynk.virtualWrite() within the blynkupdate() function. The Blynk web interface presents live voltage and current measurements from various points in the PV system, allowing remote monitoring and control to detect operational irregularities. Figures 5.14 and

Figure 5.15 illustrate the Blynk console dashboard in both "OFF" and "ON" states, while Figure 5.16 depict real-time PV data monitoring on the Blynk console.

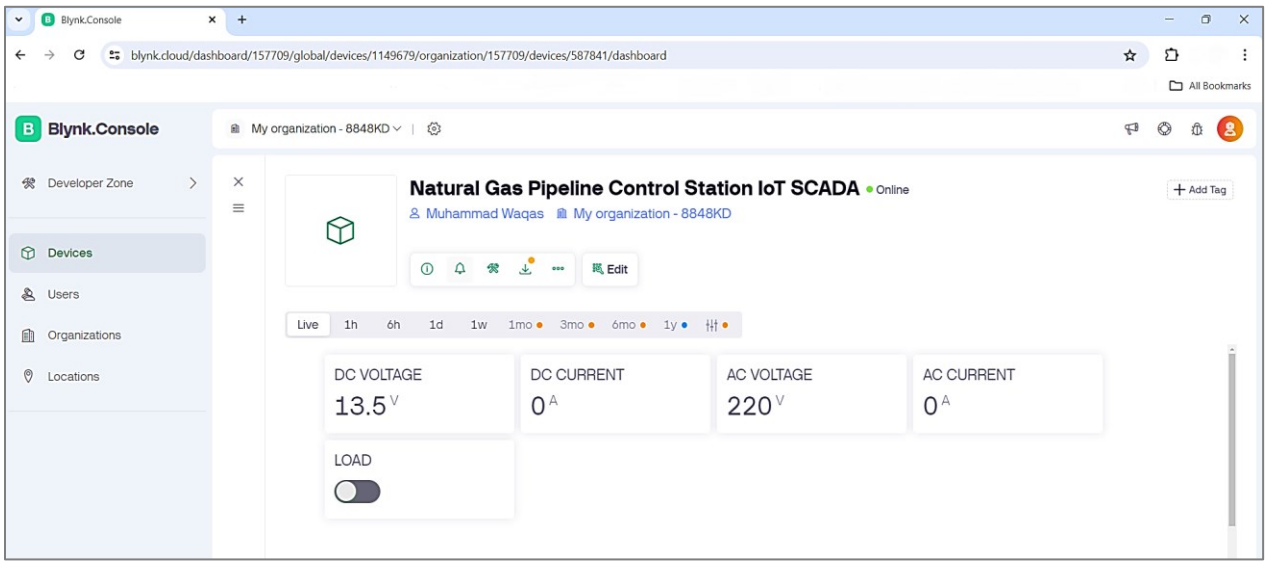

Figure 5.14. Blynk console dashboard when the load is OFF.

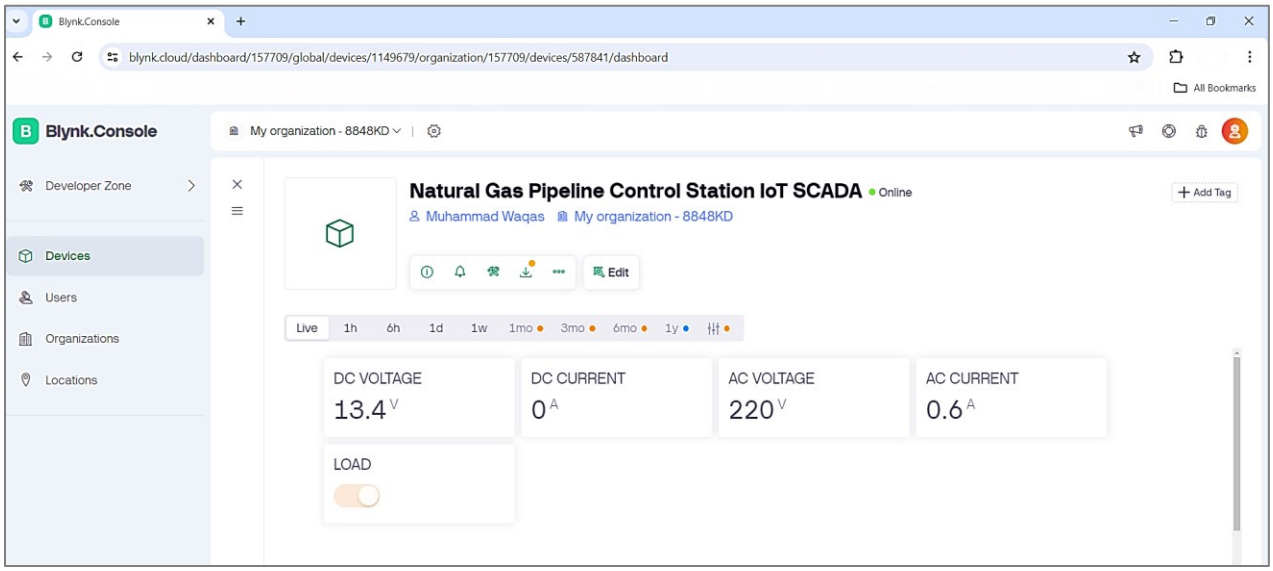

Figure 5.15. Blynk console dashboard when the load is ON.

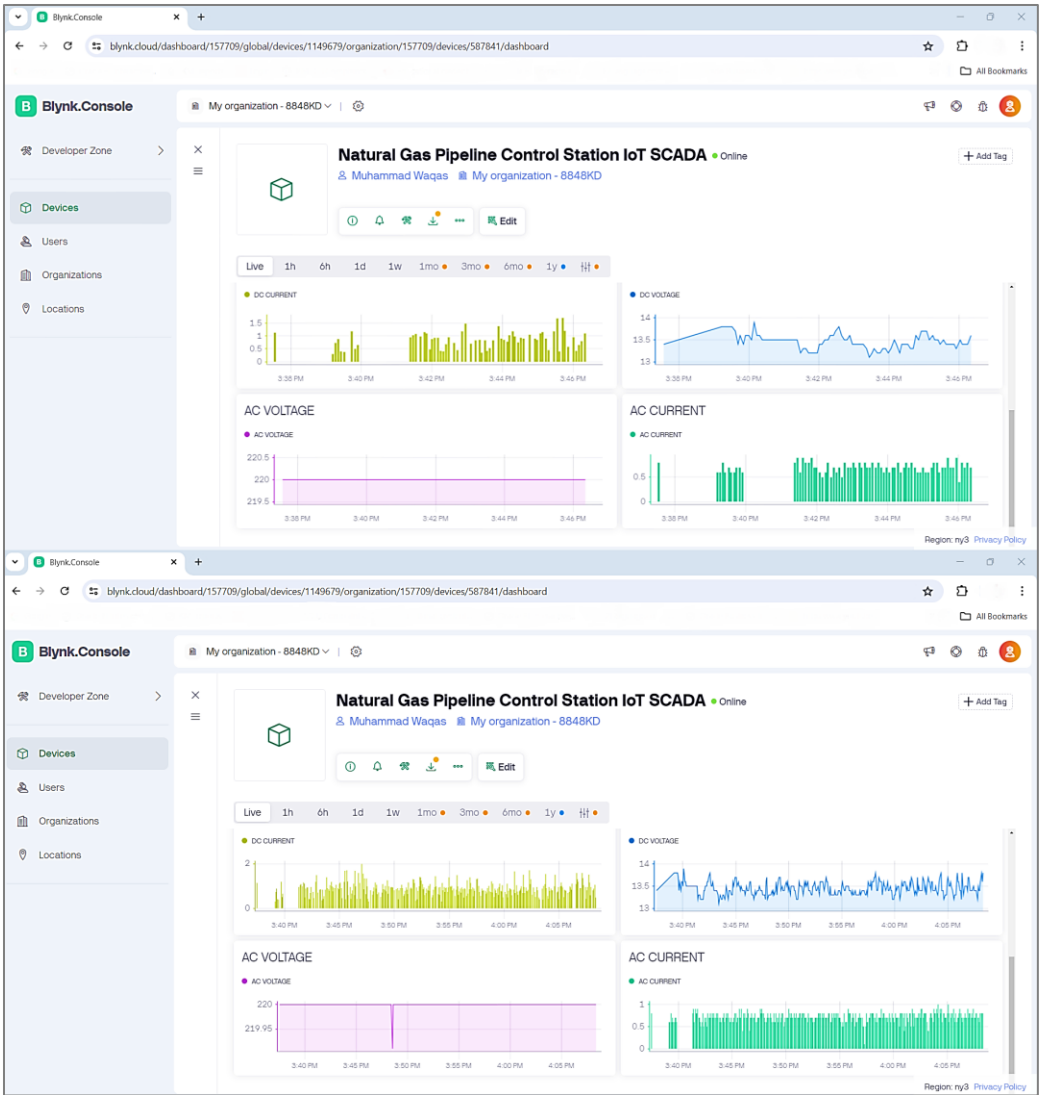

Figure 5.16. Real-time data monitoring on Blynk web console.

5.7 Discussion

This section describes the salient characteristics and advantages of the open-source, low-cost SCADA system designed for a remote natural gas pipeline control station in Pakistan.

- **System Architecture:** The proposed system is built on the fourth and latest IoT SCADA architecture, incorporating the four fundamental components of a SCADA system previously discussed. It features Field Instrumentation Devices (FIDs), an ESP32-E-based Remote Terminal Unit (RTU), a GSM SIM800L module, and a Master Terminal Unit

(MTU) set up on the Blynk IoT platform. The system utilizes both TCP/IP and HTTP communication protocols for two distinct configurations, enabling efficient data processing and facilitating human-machine interactions.

- **User-Friendly Interface:** The primary Blynk IoT server platform handles data processing and user interactions efficiently, requiring minimal customer training for ongoing use. This stands in contrast to typical commercial SCADA systems, where complex MTU platforms necessitate extensive training and experience to operate effectively.
- **Remote Monitoring, and Automated Control:** The required data is gathered locally through the RTU using FIDs and can be monitored and managed via a mobile app or web-based interface for efficient operation. Operators of the SCADA system can remotely deactivate the load as needed. Moreover, the load will be automatically deactivated when the voltage of the battery falls below a set value, ensuring battery safety.
- **System Versatility:** In both proposed configurations, the RTU wirelessly connects to the MTU using the GSM SIM800L module and the integrated Wi-Fi module, eliminating the restriction on the physical locations of the RTU and MTU.
- **System Availability and Reliability:** In the designed system, due to the use of open-source components and a locally installed, self-managed cloud server, system operators or administrators can easily ensure continuous reliability and availability. This stands in contrast to proprietary SCADA systems, where reliance on a single vendor may lead to delays in addressing customer concerns, as continuous on-site operator availability is often impractical.

- **Open-Source System:** The system utilizes the open-source Blynk software, accessible on any operating system without the need for licensing or annual fees, thereby eliminating ongoing operational expenses.
- **Energy-Efficient and Cost-Effective System:** All components utilized in the designed system are sourced from various manufacturers, making them easily accessible and cost-effective. Each component's power consumption and cost breakdown are detailed in Table 5.4, outlining the specifics of price and energy usage for transparency.

Table 5.4. Power rating and price of components used in the proposed SCADA system.

Sr. No.	Component	QTY	Power (Watt)	Total Price (CAD)
1	ACS 712 Current Sensors	2	0.128	4.84
2	ZMPT101B Voltage Sensor	1	0.025	1.38
3	GSM SIM800L	1	1.4	5
4	5V Relay	2	0.9	3.38
5	LCD Display	1	0.25	4.16
6	ESP32-WROOM-32E	1	0.528	7.76
7	LM2596	2	0.48	3.58
8	Miscellaneous (Zero PCB, jumper wires, resistors, etc.)	1	0.28	10

5.8 Conclusion

High-pressure natural gas pipeline control stations are strategically located in remote, challenging terrains and increasingly rely on traditional and renewable energy sources, such as solar PV systems and wind turbines, due to unreliable power supply for smooth operations. Ensuring a

reliable and consistent power supply along with a cost-efficient and advanced monitoring and control system is crucial for such control stations.

This research addresses the need for a low-power, cost-effective, and open-source SCADA system to enhance the efficient operation of remotely located natural gas pipeline control stations. The proposed solution utilizes an IoT-based SCADA architecture, the latest evolution in SCADA systems. The design includes the five essential elements of a SCADA system: Field Instrumentation Devices (voltage and current sensors), Remote Terminal Units (ESP32-WROOM-32E microcontroller), Master Terminal Units (Blynk IoT Server Platform), and SCADA Communication Channels (GSM SIM800L module and local Wi-Fi network). Two configurations were devised considering the potential lack of access to 3G, 4G, or Wi-Fi networks in such remote locations. The first configuration uses the GSM SIM800L module to communicate data from the RTU to the MTU (Blynk cloud server) via the TCP/IP protocol, while the second configuration employs the ESP32's integrated Wi-Fi module and a local Wi-Fi network using HTTP protocol.

The designed SCADA system's functionality was validated in a laboratory at the Core Science Building of Memorial University, NL, Canada. It successfully acquired and remotely monitored data from a 260 W, 12 V Solar PV System and performed necessary supervisory control activities. The SCADA system demonstrated capabilities in data acquisition, networked data communication, data presentation, remote monitoring, and supervisory control. The entire system operated with a low power consumption of 3.9 W, and incurred an overall cost of CAD 40.1, making it an extremely cost-effective solution for such critical applications.

Abbreviations:

The following abbreviations are used in this manuscript.

FIDs	Field Instrument Devices
GSM	Global System for Mobile Communications
HPS	Hybrid Power System
HTTP	Hypertext Transfer Protocol
IoT	Internet of Things
LCD	Liquid Crystal Display
MTU	Master Terminal Units
PV	Photo Voltaic
PLCs	Programmable Logic Controllers
RTU	Remote Terminal Unit
RESs	Renewable energy sources
SCADA	Supervisory Control and Data Acquisition
UI	User Interface

References

[1] C. Vargas Salgado, J. Águila-León, C.D. Chiñas-Palacios, E. Hurtado-Pérez. "Design and Deployment of a Web SCADA for an Experimental Microgrid", *Proceedings INNODOCT/20. International Conference on Innovation, Documentation and Education*. [online] doi: https://doi.org/10.4995/inn2020.2020.11878.

[2] D. Meng *et al.*, "Kriging-assisted hybrid reliability design and optimization of offshore wind turbine support structure based on a portfolio allocation strategy," *Ocean engineering*, vol. 295, pp. 116842–116842, Mar. 2024, doi: https://doi.org/10.1016/j.oceaneng.2024.116842.

[3] D. Meng, S. Yang, H. Yang, Jesus, J. Correia, and S.-P. Zhu, "Intelligent-inspired framework for fatigue reliability evaluation of offshore wind turbine support structures under hybrid uncertainty," *Ocean engineering*, vol. 307, pp. 118213–118213, Sep. 2024, doi: https://doi.org/10.1016/j.oceaneng.2024.118213.

[4] M. Waqas, M. Jamil, and A. A. Khan, "Hybrid Power System Design and Dynamic Modeling for Enhanced Reliability in Remote Natural Gas Pipeline Control Stations," *Energies*, vol. 17, no. 7, p. 1763, Jan. 2024, doi: https://doi.org/10.3390/en17071763.

[5] L. O. Aghenta and M. Tariq Iqbal, "Design and implementation of a low-cost, open source IoT-based SCADA system using ESP32 with OLED, ThingsBoard and MQTT protocol," *AIMS Electronics and Electrical Engineering*, vol. 4, no. 1, pp. 57–86, 2020, doi: https://doi.org/10.3934/electreng.2020.1.57.

[6] M. Kermani, B. Adelmanesh, E. Shirdare, C. A. Sima, D. L. Carnì, and L. Martirano, "Intelligent energy management based on SCADA system in a real Microgrid for smart building applications," *Renewable Energy*, vol. 171, pp. 1115–1127, Jun. 2021, doi: https://doi.org/10.1016/j.renene.2021.03.008.

[7] P. de Arquer Fernández, M. Á. Fernández Fernández, J. L. Carús Candás, and P. Arboleya Arboleya, “An IoT Open Source Platform for Photovoltaic Plants Supervision,” International Journal of Electrical Power & Energy Systems, vol. 125, p. 106540, Feb. 2021, doi: https://doi.org/10.1016/j.ijepes.2020.106540.

[8] M. J. A. Baig, M. T. Iqbal, M. Jamil, and J. Khan, “Blockchain-Based Peer-to-Peer Energy Trading System Using Open-Source Angular Framework and Hypertext Transfer Protocol,” *Electronics*, vol. 12, no. 2, p. 287, Jan. 2023, doi: https://doi.org/10.3390/electronics12020287.

[9] A. Soetedjo and E. Hendriarianti, “Development of an IoT-Based SCADA System for Monitoring of Plant Leaf Temperature and Air and Soil Parameters,” *Applied Sciences*, vol. 13, no. 20, p. 11294, Jan. 2023, doi: https://doi.org/10.3390/app132011294.

[10] *What is SCADA? (Supervisory Control and Data Acquisition) - RealPars*. [online] Available at: https://www.realpars.com/blog/scada.

[11] K. Medrano, D. Altuve, K. Belloso and C. Bran, "Development of SCADA using a RTU based on IoT Controller," *2018 IEEE International Conference on Automation/XXIII Congress of the Chilean Association of Automatic Control (ICA-ACCA)*, Concepcion, Chile, 2018, pp. 1-6, doi: 10.1109/ICA-ACCA.2018.8609700.

[12] L. O. Aghenta and M. T. Iqbal, "Development of an IoT Based Open Source SCADA System for PV System Monitoring," *2019 IEEE Canadian Conference of Electrical and Computer Engineering (CCECE)*, Edmonton, AB, Canada, 2019, pp. 1-4, doi: 10.1109/CCECE.2019.8861827.

[13] M. Yi, H. Mueller, L. Yu and J. Chuan, "Benchmarking Cloud-Based SCADA System," *2017 IEEE International Conference on Cloud Computing Technology and Science (CloudCom)*, Hong Kong, China, 2017, pp. 122-129, doi: 10.1109/CloudCom.2017.25.

[14] P. Sethi and S. R. Sarangi, "Internet of Things: Architectures, Protocols, and Applications," *Journal of Electrical and Computer Engineering*, vol. 2017, no. 9324035, pp. 1–25, Jan. 2017, doi: https://doi.org/10.1155/2017/9324035.

[15] N. Moustafa, B. Turnbull and K. -K. R. Choo, "An Ensemble Intrusion Detection Technique Based on Proposed Statistical Flow Features for Protecting Network Traffic of Internet of Things," in *IEEE Internet of Things Journal*, vol. 6, no. 3, pp. 4815-4830, June 2019, doi: 10.1109/JIOT.2018.2871719.

[16] T. Sultana and K. A. Wahid, "Choice of Application Layer Protocols for Next Generation Video Surveillance Using Internet of Video Things," in *IEEE Access*, vol. 7, pp. 41607-41624, 2019, doi: 10.1109/ACCESS.2019.2907525.

[17] M. Deveci, U. Cali, and D. Pamucar, "Evaluation of Criteria for Site Selection of Solar Photovoltaic (PV) Projects using Fuzzy Logarithmic Additive Estimation of Weight Coefficients," *Energy Reports*, vol. 7, pp. 8805–8824, Nov. 2021, doi: https://doi.org/10.1016/j.egyr.2021.10.104.

[18] O. Ahmed and M. T. Iqbal, "Remote Monitoring, Control and Data Visualization for a Solar Water Pumping System," *European journal of electrical engineering and computer science*, vol. 7, no. 5, pp. 71–77, Oct. 2023, doi: https://doi.org/10.24018/ejece.2023.7.5.552.

[19] T. Matsui, K. Yamamoto, S. Sumi and N. Triruttanapiruk, "Detection of Lightning Damage on Wind Turbine Blades Using the SCADA System," in *IEEE Transactions on Power Delivery*, vol. 36, no. 2, pp. 777-784, April 2021, doi: 10.1109/TPWRD.2020.2992796.

[20] A. B. Abdulsalam, H. A. J. Alsaadi and Z. Hamodat, "Control And Management of Solar PV Grid Using Scada System," *2022 International Congress on Human-Computer Interaction, Optimization and Robotic Applications (HORA)*, Ankara, Turkey, 2022, pp. 1-5, doi: 10.1109/HORA55278.2022.9799994.

[21] S. U. Uddin, M. J. A. Baig, and M. T. Iqbal, "Design and Implementation of an Open-Source SCADA System for a Community Solar-Powered Reverse Osmosis System," Sensors, vol. 22, no. 24, p. 9631, Jan. 2022, doi: https://doi.org/10.3390/s22249631.

[22] W. He, Mirza, and Mohammad Tariq Iqbal, "An Open-Source Supervisory Control and Data Acquisition Architecture for Photovoltaic System Monitoring Using ESP32, Banana Pi M4, and Node-RED," *Energies*, vol. 17, no. 10, pp. 2295–2295, May 2024, doi: https://doi.org/10.3390/en17102295.

[23] C. Vargas-Salgado, J. Aguila-Leon, C. Chiñas-Palacios, and E. Hurtado-Perez, "Low-cost web-based Supervisory Control and Data Acquisition system for a microgrid testbed: A case study in design and implementation for academic and research applications," *Heliyon*, vol. 5, no. 9, p. e02474, Sep. 2019, doi: https://doi.org/10.1016/j.heliyon.2019.e02474.

[24] F. A. Osman, M. Y. M. Hashem, and M. A. R. Eltokhy, "Secured cloud SCADA system implementation for industrial applications," *Multimedia Tools and Applications*, vol. 81, no. 7, pp. 9989–10005, Feb. 2022, doi: https://doi.org/10.1007/s11042-022-12130-9.

[25] L. O. Aghenta and M. T. Iqbal, "Low-Cost, Open Source IoT-Based SCADA System Design Using Thinger.IO and ESP32 Thing," *Electronics*, vol. 8, no. 8, p. 822, Jul. 2019, doi: https://doi.org/10.3390/electronics8080822.

[26] L. Ahsan, M.J.A. Baig and M.T. Iqbal, Low-Cost, Open-Source, Emoncms-Based SCADA System for a Large Grid-Connected PV System. *Sensors* **2022**, *22*, 6733. https://doi.org/10.3390/s22186733.

[27] S. Arash Omidi, M.J.A. Baig, and M.T. Iqbal, "Design and Implementation of Node-Red Based Open-Source SCADA Architecture for a Hybrid Power System," Energies, vol. 16, no. 5, pp. 2092–2092, Feb. 2023, doi: https://doi.org/10.3390/en16052092.

[28] C. A. Osaretin, M. Zamanlou, M. T. Iqbal and S. Butt, "Open Source IoT-Based SCADA System for Remote Oil Facilities Using Node-RED and Arduino Microcontrollers," *2020 11th IEEE Annual Information Technology, Electronics and Mobile Communication Conference (IEMCON)*, Vancouver, BC, Canada, 2020, pp. 0571-0575, doi: 10.1109/IEMCON51383.2020.9284826.

[29] A. J. Moshayedi, A. S. Roy, L. Liao and S. Li, "Raspberry Pi SCADA Zonal based System for Agricultural Plant Monitoring," *2019 6th International Conference on Information Science and Control Engineering (ICISCE)*, Shanghai, China, 2019, pp. 427-433, doi: 10.1109/ICISCE48695.2019.00092.

[30] H. Fazlollahtabar, "Internet of Things-based SCADA System for Configuring/Reconfiguring an Autonomous Assembly Process," *Robotica*, pp. 1–18, Jun. 2021, doi: https://doi.org/10.1017/s0263574721000758.

[31] R. J. Tom and S. Sankaranarayanan, "IoT based SCADA Integrated with Fog for Power Distribution Automation," *2017 12th Iberian Conference on Information Systems and Technologies (CISTI)*, Lisbon, Portugal, 2017, pp. 1-4, doi: 10.23919/CISTI.2017.7975732.

[32] M. Stanculescu, C. A. Badea, I. Marinescu, P. Andrei, O. Drosu and H. Andrei, "Vulnerability of SCADA and Security Solutions for a Waste Water Treatment Plant," *2019*

11th International Symposium on Advanced Topics in Electrical Engineering (ATEE), Bucharest, Romania, 2019, pp. 1-6, doi: 10.1109/ATEE.2019.8724889.

[33] N. I. M. Noor and N. N. M. Nasir, "Traffic Light Control System by Using Supervisory Control and Data Acquisition (SCADA), Programmable Logic Controller (PLC) Technology and Image Processing," *Journal of Electrical Power and Electronic Systems*, vol. 2, no. 2, Nov. 2020, Available: https://fazpublishing.com/jepes/index.php/jepes/article/view/35.

[34] K. Sasi Kumar, R. Anil Kumar, Mirza, K. Kumar, R. Kumar, and Y. Yasmeen, "Automation Control of Antenna and Microwave in Telecom Towers using SCADA," *International Journal for Modern Trends in Science and Technology*, vol. 8, no. 02, pp. 27–33, 2022, doi: https://doi.org/10.46501/IJMTST0802006.

[35] M. O. Qays *et al.*, "Monitoring of renewable energy systems by IoT-aided SCADA system," *Energy Science & Engineering*, vol. 10, no. 6, pp. 1874–1885, Mar. 2022, doi: https://doi.org/10.1002/ese3.1130.

[36] Blynk: a low-code IoT software platform for businesses and developers. Accessed: Jun. 15, 2024. [Online]. Available: https://blynk.io.

[37] Hall-Effect-Based Linear Current Sensor IC - ACS712 | Allegro MicroSystems. Accessed: Jun. 22, 2024. [Online]. Available: https://www.allegromicro.com/en/products/sense/current-sensor-ics/zero-to-fifty-amp-integrated-conductor-sensor-ics/acs712.

[38] L. H. Laisina, "Leak Current Detector In Low Voltage Network (Jtr) System Using Zmpt101b Sensor Based On The Internet Of Things (IoT)," *International Journal of Multidisciplinary Sciences and Arts*, vol. 2, no. 1, pp. 48–54, Jun. 2023, doi: https://doi.org/10.47709/ijmdsa.v2i1.2301.

[39] ZMPT101B AC Single Phase Voltage Sensor Module, VISHA WORLD. Accessed: Jun. 22, 2024. [Online]. Available: https://vishaworld.com/products/zmpt101b-ac-single-phase-voltage-sensor-module.

[40] C. N. Oton and M. T. Iqbal, "Low-Cost Open Source IoT-Based SCADA System for a BTS Site Using ESP32 and Arduino IoT Cloud," *2021 IEEE 12th Annual Ubiquitous Computing, Electronics & Mobile Communication Conference (UEMCON)*, New York, NY, USA, 2021, pp. 0681-0685, doi: 10.1109/UEMCON53757.2021.9666691.

[41] ESP32-DevKitC V4 Getting Started Guide - ESP32 - ESP-IDF Programming Guide v5.2.2 documentation. Accessed: Jun. 22, 2024. [Online]. Available: https://docs.espressif.com/projects/esp-idf/en/stable/esp32/hw-reference/esp32/get-started-devkitc.html

[42] P. Kanani and M. Padole, "Real-time Location Tracker for Critical Health Patient using Arduino, GPS Neo6m and GSM Sim800L in Health Care," *2020 4th International Conference on Intelligent Computing and Control Systems (ICICCS)*, Madurai, India, 2020, pp. 242-249, doi: 10.1109/ICICCS48265.2020.9121128.

[43] SIM800L-Datasheet.pdf. Accessed: Jun. 24, 2024. [Online]. Available: https://components101.com/sites/default/files/component_datasheet/SIM800L Datasheet.pdf.

[44] X. Fang and X. Li, “Design and Performance Analysis of Photovoltaic Power Generation Light Emitting Diode Device,” *Journal of Nanoelectronics and Optoelectronics*, vol. 19, no. 6, pp. 605–612, Jun. 2024, doi: https://doi.org/10.1166/jno.2024.3610.

[45] 16x2 LCD Module. Components101. Accessed: Jun. 24, 2024. [Online]. Available: https://components101.com/displays/16x2-lcd-pinout-datasheet.

[46] A. Hameed, A. Sultan, and M. F. Bonneya, “Design and Implementation a New Real Time Overcurrent Relay Based on Arduino,” *IOP Conference Series: Materials Science and Engineering*, 2020, doi: https://doi.org/10.1088/1757-899x/871/1/012005.

[47] M. Krichen, M. Lahami, O. Cheikhrouhou, R. Alroobaea, and A. J. Maâlej, “Security Testing of Internet of Things for Smart City Applications: A Formal Approach,” *Smart Infrastructure and Applications*, pp. 629–653, Jun. 2019, doi: https://doi.org/10.1007/978-3-030-13705-2_26.

[48] EasyEDA - Online PCB design & circuit simulator. Accessed: Jun. 25, 2024. [Online]. Available: https://easyeda.com/

Chapter 6: Conclusion and Future Work

6.1 Conclusion

In light of the significant rise in petroleum product prices and the urgent need to conserve fossil fuels, the utilization of renewable energy sources for power generation, especially in remote areas, has become imperative. However, due to their intermittent nature, hybrid power systems (HPS) have emerged as the most practical and effective solution. This thesis addresses the energy challenges of remote natural gas pipeline facilities by designing and implementing a hybrid power system, highlighting both financial benefits and alignment with broader energy sustainability goals.

The proposed hybrid power system comprises photovoltaic (PV) panels, a maximum power point tracking (MPPT) controller, a DC-AC inverter, a buck converter, a natural gas generator, a battery bank, and an electrical load. Using HOMER Pro software, 892 simulations were conducted to achieve an optimal design with a 79.2% renewable energy fraction, significantly reducing the non-renewable fraction from 100% to 20.8%. This addresses both cost inefficiencies and environmental concerns. Dynamic modeling in MATLAB/Simulink and experimental validation through Hardware-in-the-Loop (HIL) simulation with the OPAL-RT Technologies' OP5707XG simulator demonstrated the system's reliability and consistency in meeting the energy demands of remote control stations. The proposed system reduced energy costs to USD 0.234 per kWh, yielding significant savings of USD 0.148 per kWh compared to the current cost of USD 0.382 per kWh. Additionally, it achieved annual operating cost savings of USD 87,321, with total annual operating costs reduced to USD 63,253 from the current USD 150,574.

Inverters are indispensable components of hybrid power systems, enabling the effective integration and utilization of diverse energy sources. They play a crucial role in managing and converting

electrical power from various sources to provide a stable and reliable energy supply. This thesis also includes a comprehensive comparison of conventional two-level inverters with voltage source cascaded H-bridge multilevel inverters (CHB-MLI) up to nine levels. The study highlights the importance of multilevel inverter topologies in addressing challenges related to harmonic distortion, voltage quality, and energy efficiency. Multilevel inverters can eliminate the need for filters by generating smoother, near-sinusoidal waveforms through multiple voltage levels, which significantly reduces harmonic distortion. Unlike traditional inverters that rely on filters to clean up their output, multilevel inverters inherently produce high-quality AC power with minimal harmonics, making them more efficient and ideal for improving power quality in systems like photovoltaic installations. Simulations and performance evaluations using Fast Fourier Transform (FFT) in MATLAB/Simulink confirmed the advantages of multilevel inverters. Experimental validation with HIL and the OPAL-RT real-time OP5707XG simulator demonstrated the nine-level CHB-MLI's effectiveness in improving power conversion for applications such as PV systems, renewable energy integration, and grid-connected systems.

Furthermore, this research addresses the need for a reliable, cost-effective, and advanced monitoring and control system for high-pressure natural gas pipeline control stations in remote and challenging terrains. These stations increasingly depend on traditional and renewable energy sources, such as solar PV systems and wind turbines, due to unreliable power supplies. Ensuring a consistent power supply and an efficient monitoring and control system is crucial. The proposed IoT-based SCADA system incorporates the latest SCADA technologies, including Field Instrumentation Devices (voltage and current sensors), Remote Terminal Units (ESP32-WROOM-32E microcontroller), Master Terminal Units (Blynk IoT Server Platform), and SCADA Communication Channels (GSM SIM800L module and local Wi-Fi network). Two configurations

were devised to ensure robust data communication and control in remote locations.

The SCADA system's functionality was validated in a laboratory at the Core Science Building of Memorial University, NL, Canada. It successfully acquired and remotely monitored data from a 260 W, 12 V Solar PV System, performing necessary supervisory control activities. The system demonstrated effective data acquisition, networked data communication, data presentation, remote monitoring, and supervisory control, all with a low power consumption of 3.9 W and a total cost of 40.1 CAD, making it a highly cost-effective solution for critical applications.

In conclusion, the integration of hybrid power systems and advanced control technologies provides a promising approach to enhancing energy efficiency, reliability, and sustainability for remote natural gas pipeline control stations. This thesis not only offers a comprehensive solution to energy challenges but also paves the way for more efficient, cost-effective, and environmentally responsible energy solutions, significantly contributing to broader goals of energy sustainability and infrastructure resilience.

6.2 Research Contributions

The contribution of this research work to enhance the operational efficiency of remotely located natural gas pipeline control stations is summarised below:

- Evaluating the daily energy needs of remotely located natural gas pipeline control stations in Pakistan.
- Designing and sizing a hybrid power system in HOMER Pro to reduce reliance on fossil fuels by integrating renewable energy sources, minimizing natural gas consumption, and selecting reliable, compatible system components.
- Conducting an economic analysis of the designed hybrid power system compared to the existing power infrastructure at the selected site.

- Performing dynamic modeling of the hybrid power system under varying conditions to ensure real-life response and stability using hardware-in-the-loop OPAL-RT technology.
- Analyzing inverter designs and various multi-level inverter topologies to enhance power quality.
- Developing a cost-effective, low-power IoT-based SCADA system for monitoring the hybrid power system at natural gas pipeline control stations.

6.3 Future Work

The work presented in this thesis outlines the development of a hybrid power system for a remote natural gas pipeline control station, combining a photovoltaic system with a conventional generator. It demonstrates the system's potential for improving energy reliability and sustainability in remote applications. However, as energy technologies evolve, there are several opportunities to enhance the system's performance in terms of efficiency, reliability, and adaptability. The following future work suggestions build on the current design and incorporate advanced innovations to address emerging challenges and optimize performance in practical applications:

- This research was based on actual load data from the site. Implementing the designed system on-site to study real-time system dynamics will be a key next step.
- Further research into advanced energy storage technologies, such as lithium-ion and flow batteries, could increase storage capacity and efficiency. Additionally, integrating hydrogen-based energy storage or fuel cells as backup power could help reduce the system's carbon footprint and improve energy reliability during periods of low solar availability.
- The incorporation of a solar tracking system should be explored, as it can significantly enhance the photovoltaic system's efficiency by optimizing solar energy capture

throughout the day.

- The study of multilevel inverter topologies in this thesis emphasized their potential to mitigate challenges related to harmonic distortion, voltage quality, and energy efficiency. Implementing a multilevel inverter on-site would allow for an analysis of its real-world impact on system performance.
- A comprehensive hybrid design incorporating solar, wind, natural gas, and fuel cell technologies should be considered to increase the penetration of renewable energy at the site.
- Enhancing the security of the open-source SCADA system used in this design is critical. Implementing data encryption for communication channels would safeguard system integrity and prevent unauthorized access.

These areas of future research and development will further improve the system's efficiency, sustainability, and security, making it more robust and adaptable to real-world conditions.

6.4 List of Publications

Articles in Refereed Publications

- M. Waqas, M. Jamil, and A. A. Khan, "Hybrid Power System Design and Dynamic Modeling for Enhanced Reliability in Remote Natural Gas Pipeline Control Stations," *Energies*, vol. 17, no. 7, p. 1763, Jan. 2024, doi: https://doi.org/10.3390/en17071763.
- M. Waqas and M. Jamil, "Smart IoT SCADA System for Hybrid Power Monitoring in Remote Natural Gas Pipeline Control Stations," *Electronics,* vol. 13, no. 16, p. 3235, 2024, doi: https://doi.org/10.3390/electronics13163235.

Refereed Conference Publications

- M. Waqas and M. Jamil, "Power Quality Improvement Using Nine-Level Cascaded H-Bridge Voltage Source Inverter for PV Applications," *2024 12th International Conference on Smart Grid (icSmartGrid)*, Setubal, Portugal, 2024, pp. 429-434, doi: 10.1109/icSmartGrid61824.2024.10578256.

Regional Conference Publications

- M. Waqas, M. J. A. Baig, and M. Jamil, " Design and Analysis of a Hybrid Power System for a Remote Natural Gas Pipeline Control Station" *32nd Annual Newfoundland Electrical and Computer Engineering Conference (NECEC) 2023*, St. John's, NL, Canada.

Co-authorship Statement

I am the principal author of all the research papers used in the preparation of this thesis. My thesis supervisor, Dr. Mohsin Jamil, and my co-supervisor, Dr. Ashraf Ali Khan, are co-authors. As the principal author, I conducted the majority of the research, performed literature reviews, carried out the designs, hardware implementations, experimental setups, and result analysis for each manuscript. I also prepared the original manuscripts and revised them based on feedback from my supervisors and peer reviewers throughout the review process. Dr. Mohsin supervised the entire research project, reviewed and corrected each manuscript, provided research components, and contributed ideas throughout the research and manuscript preparation.